Assessment of the quality of Digital Terrain Models

Article *in* Official Publication - EuroSDR · January 2011

CITATIONS
27

READS
1,158

2 authors:

Joachim Höhle
Aalborg University
53 PUBLICATIONS **810** CITATIONS
SEE PROFILE

Marketa Potuckova
Charles University in Prague
35 PUBLICATIONS **197** CITATIONS
SEE PROFILE

European Spatial Data Research

December 2011

Assessment of the Quality of Digital Terrain Models

by Joachim Höhle and Marketa Potuckova

Official Publication Nº 60

Published by EuroSDR

Printed by Gopher, Amsterdam, The Netherlands

EUROPEAN SPATIAL DATA RESEARCH

PRESIDENT 2010 – 2012:
Jean-Philippe Lagrange, France

VICE-PRESIDENT 2009 – 2013:
Dieter Fritsch, Germany

SECRETARY-GENERAL:
Joep Crompvoets, Belgium

DELEGATES BY MEMBER COUNTRY:

Austria: Michael Franzen
Belgium: Ingrid Vanden Berghe; Jean Theatre
Croatia: Željko Hećimović; Ivan Landek
Cyprus: Christos Zenonos; Michael Savvides
Denmark: Thorben Hansen; Lars Bodum
Finland: Jurkka Tuokko
France: Jean-Philippe Lagrange; Xavier Briottet
Germany: Hansjörg Kutterer; Klement Aringer; Dieter Fritsch
Ireland: Colin Bray; Ned Dwyer
Italy: Fabio Crosilla
Netherlands: Jantien Stoter; Aart-jan Klijnjan
Norway: Jon Arne Trollvik; Ivar Maalen-Johansen
Spain: Antonio Arozarena; Emilio Domenech
Sweden: Anders Olsson; Anders Östman
Switzerland: Francois Golay; André Streilein-Hurni
United Kingdom: Malcolm Havercroft; Jeremy Morley

COMMISSION CHAIRPERSONS:

Sensors, Primary Data Acquisition and Georeferencing: Michael Cramer, Germany
Image Analysis and Information Extraction: Norbert Pfeifer, Austria
Production Systems and Processes: André Streilein-Hurni, Switzerland
Data Specifications: Ulf Sandgren, Sweden
Network Services: Lars Bernard, Germany

OFFICE OF PUBLICATIONS:

Bundesamt für Kartographie und Geodäsie (BKG)
Publications Officer: Andreas Busch
Richard-Strauss-Allee 11
60598 Frankfurt
Germany
Tel.: + 49 69 6333 312
Fax: + 49 69 6333 441

CONTACT DETAILS:

Web: www.eurosdr.net
President: president@eurosdr.net
Secretary-General: secretary@eurosdr.net
Secretariat: admin@eurosdr.net

EuroSDR Secretariat
Public Management Institute
K.U. Leuven
Faculty of Social Sciences
Parkstraat 45 Bus 3609
3000 Leuven
Belgium
Tel.: +32 16 3231803

The official publications of EuroSDR are peer-reviewed.

Joachim Höhle and Marketa Potuckova:
„Assessment of the Quality of Digital Terrain Models“ 9

PREFACE 11

1. OVERVIEW ON METHODS OF DERIVING DTMs 12

1.1 DTM definition 12
1.2 Methods of data acquisition for DTMs 13

1.2.1 Aerial photogrammetry 14

1.2.1.1. Stereophotogrammetry 14
1.2.1.2. Image matching 15
1.2.1.3. DTM derivation by means of photogrammetry 17
1.2.1.4. Accuracy of a DTM derived by photogrammetry 18

1.2.2 Airborne laser scanning 19
1.2.3 Interferometric SAR 23
1.2.4 Spaceborne imaging systems 25
1.2.5 Summary of methods for DTM data collection 25

1.3 Filtering of raw data 26

1.3.1 Progressive densification 27
1.3.2 Surface-based filters 27
1.3.3 Segmentation-based filters 28
1.3.4 Morphological filters 28

1.4 Completion of DTMs by interpolation 29
1.5 References 30

2. METHODS OF CHECKING AND IMPROVING THE QUALITY OF DTMs 33

2.1 What means DTM quality? 33
2.2 Checking of the accuracy 34

2.2.1 Absolute and relative accuracy 34
2.2.2 DEM terrain types 34
2.2.3 Reference values for checking of the accuracy 35

2.2.3.1. Measuring by land surveying 35
2.2.3.2. Measurement by aerial photogrammetry 35
2.2.3.3. Existing objects in topographic data bases 36

2.2.4 Accuracy measures 36
2.2.5 Some details 48
2.2.6 Completeness of the DTM 52
2.2.7 Metadata 54

2.3 Improving the quality of DTMs 54
2.3.1 Improvement of the accuracy 54
2.3.2 Improvement of the completeness 56
2.4 Visualization of the quality 56
2.5 Tools for the checking, completion and visualization 59
2.5.1 Photogrammetric stereo workstations 59
2.5.2 Editing stations 59
2.5.3 Software packages 59
2.6 Tools for the calculation accuracy measures 61
2.6.1 Use of statistical functions in MS EXCEL 61
2.6.2 Use of the statistical computing environment "R" 62
2.7 References 65
3. PHOTOGRAMMETRIC METHODS FOR AUTOMATED DTM CHECKING 66
3.1 Method of two overlapping orthoimages 66
3.2 Method of back-projection 70
3.3 Other DTM checking methods in the EuroSDR test 71
3.4 Discussion on methods for DTM checking and improving based on images 71
3.5 References 72
4. EXISTING SPECIFICATIONS, STANDARDS, AND RECENT DEM PROJECTS 74
4.1 Specifications and standards 74
4.1.1 Specification of the Danish National Survey and Cadastre (KMS) 74
4.1.2 German Standards 75
4.1.3 European standards, directives, and guidelines 75
4.1.4 Standards in USA 76
4.1.5 International standards 77
4.2 Assessment of quality in recent projects 78
4.2.1 Danish DEMs 78
4.2.2 EuroSDR project "Automated checking and improving of DEMs" 80
4.2.3 Tests of the German Society of Photogrammetry and Remote Sensing (DGPF Test) 81
4.2.4 Elevation Model of the Netherlands (AHN-2) 82
4.2.5 Elevation Model of Sweden 82
4.2.6 EuroDEM 83
4.3 References 83
5. SUMMARY AND OUTLOOK 85

Assessment of the Quality of Digital Terrain Models

by

Joachim Höhle and Marketa Potuckova

Preface

This book deals with the assessment of the quality of Digital Terrain Models. It is based on the European Spatial Data Research (EuroSDR) project "Checking and improving of Digital Terrain Models" and several e-learning courses, which were organized by the Educational Service of EuroSDR. Other EuroSDR projects as well as discussions during the annual EuroSDR meetings have also been inspiring when writing this book. It is the wish of the authors that National Mapping Agencies and other people involved in quality assurance and quality control of Digital Terrain Models will benefit from this book.

Joachim Höhle and Marketa Potuckova

5th November 2011

1. Overview on methods of deriving DTMs

Quality of digital terrain models (DTMs) depends on methods of data collection, the calibration of the used systems and data processing. This introductory chapter summarizes basic procedures of DTM derivation from imagery and airborne laser scanning that must be considered when dealing with DTM quality assessment. First, the terms digital terrain model and digital surface model are defined. A short explanation of different data acquisition methods is given afterwards. Principles of several algorithms for filtering raw data follow. A brief description of interpolation methods for completion of the models closes this overview.

1.1 DTM definition

The terms Digital Elevation Model, Digital Terrain Model and Digital Surface Model are used when dealing with a digital representation of the earth surface and objects on it. Although the definitions can slightly differ in literature, for the purpose of this book these terms are understood as follows:

Digital Elevation Model (DEM): a generic term for a digital and mathematical representation of a topographic surface expressed as regularly or irregularly spaced point elevation values

Digital Terrain Model (DTM): a digital model of a topographic surface represented as regularly or irregularly spaced point elevation values corresponding to bare earth (avoiding vegetation and manmade objects)

Digital Surface model (DSM): a digital model of a topographic surface represented as regularly or irregularly spaced point elevation values including the top surface of vegetation, buildings and other features elevated above bare earth.

The terms DEM and DTM are often used as synonyms. Nevertheless, according to some literature a gridded DTM includes also elevations of significant topographic features, mass points and breaklines that improve accuracy, level of detail and morphological quality of the model (El-Sheimy et al., 2005 cited in Pfeifer & Mandlburger, 2009). When processing laser scanning data, a normalized DSM is sometimes required and it is calculated as nDSM = DSM – DTM. Figure 1.1 explains the difference between DSM and DTM.

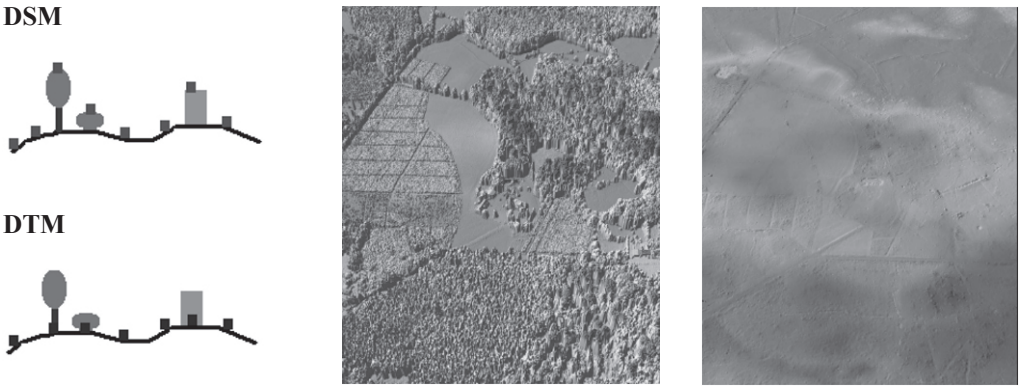

Figure 1.1. DSM versus DTM. From left to right: examples of gridded DSM and DTM. Source: TopoSys.

A DEM represented by original measurements from automated photogrammetric procedures or airborne laser scanning in general has a form of irregularly distributed points (point clouds). These points can be connected to non-overlapping triangles (e.g. by means of Delaunay triangulation), a so-called Triangulated Irregular Network (TIN). Another form of DEM is a regular, usually squared, grid interpolated from original points or measured manually exactly at grid positions. Grid interpolation may be connected with reducing the number of original points that is needed with respect to data storage, analysis, and visualisation. The data structure is an important parameter characterizing a DEM. Its connection to DEM quality is discussed in the chapter 2.

1.2 Methods of data acquisition for DTMs

The data acquisition method for DTM derivation is always driven by an application and its requirements for accuracy and point density (compare Table 1.1). In the scope of this book there are considered mainly nationwide DTMs supporting orthoimage production or larger area projects such as designing construction work or hydrological modelling. Therefore terrestrial measurement techniques of high spatial accuracy (1-2 cm and better) by means of GNSS or total stations are not discussed in this chapter. These methods are considered as supplementary for measurement of control and check points used for image orientation and quality assessment (see chapter 2.2.3.1).

Table 1.1. Examples of DEM applications and requirements on accuracy and point density

Application	Type of DEM	Vertical accuracy	Point spacing	Format	Suitable acquisition method
Design of roads, engineering	DTM	< 0.5 m	1- 5 m	TIN	ALS & PHM
Hydrology (flood risk modelling)	DTM	< 0.2 m	1- 5 m	TIN/grid	ALS & PHM
Urban modelling	DSM	< 0.15 m	< 1 m	TIN/grid	ALS & PHM
Orthoimages	DTM	> 0.5 m	5 - 50 m	grid	PHM & InSAR
True orthoimages	DSM	< 0.5 m	1 - 5 m	TIN	ALS & PHM

ALS – airborne laser scanning, PHM - photogrammetry

Aerial photogrammetry, airborne laser scanning and airborne interferometric SAR (InSAR) currently represent technologies suitable for data acquisition for DEM generation over larger areas (e.g. nationwide coverage). In the following paragraphs basic principles, latest developments, accuracy and advantages of each method are described. Supplementary literature is given for a detailed study.

1.2.1 Aerial photogrammetry

Principles of stereophotogrammetry have been known for over 100 years and measurement in stereopairs of aerial photographs has been used as a mapping technique since the twenties of the last century. Currently, digital photogrammetric workstations are the main processing devices. Together with software packages for (semi)automated image orientation, DTM derivation and orthoimage production they comprise equipment for a comfortable stereo vision (see Figure 2.19) for manual measurement in stereomodels. In some countries, digital images are still obtained by digitizing analogue photographs in precise photogrammetric scanners. Nevertheless, production and utilization of large-format digital cameras have increased considerably during the last decade. Higher radiometric resolution giving a possibility of better recognition of objects in shadows, higher spectral resolution (in addition to conventional panchromatic, red, green and blue bands, images in a near infrared band are acquired at the same time) and high spatial resolution (pixel size down to 5.2μm) are the main advantages of digital cameras in comparison to analogue ones. A less favourable image format influencing the accuracy in elevation of measured points is discussed later in the chapter 1.2.1.4.

1.2.1.1. Stereophotogrammetry

A spatial position of a point of interest is determined by space intersection of two rays, each connecting a corresponding point in a left and right image with its perspective centre as depicted in Figure 1.2. Coordinates X, Y, Z of the point P are calculated by means of collinearity equations. Measurement of image coordinates x´, y´ of the point P in both images must be carried out. Parameters of inner orientation (camera constant, coordinates of a principal point, lens distortions) are determined by the camera calibration. Parameters of exterior orientation (X_0, Y_0, Z_0 coordinates of a perspective centre and rotations ω, φ, κ with respect to the reference coordinate system) are usually calculated by means of aerotriangulation using

ground control points (GCPs) or measured directly by GNSS/IMU or determined by combination of both methods (aerotriangulation with GNSS/IMU). More information about orientation procedures can be found in photogrammetric textbooks (e.g. Kraus, 2007).

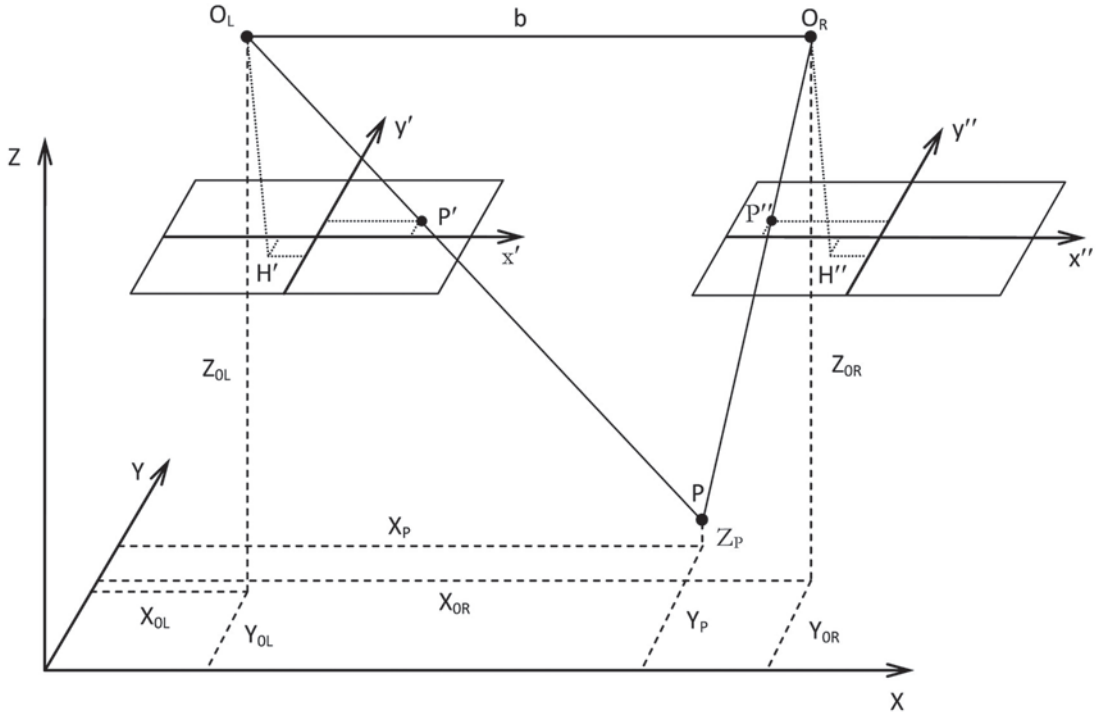

Figure 1.2. Principle of determination of spatial coordinates of a point P by stereophotogrammetric measurement. $O_L[X_{0L}, Y_{0L}, Z_{0L}]$ and $O_R[X_{0R}, Y_{0R}, Z_{0R}]$ are perspective centres of the left and right image.

Point measurement for DTM derivation from a stereopair of aerial images can be carried out manually, semi-automatically and fully automatically by means of image matching. The possibility of measurement exactly at positions of DTM grid points, mass points corresponding to significant terrain features (top of hills, lowest point of depressions, changes of slopes), measurement along breaklines and contour lines are the advantages of manual measurement. The main disadvantage is an economic aspect especially if a nationwide project is considered. Semi-automated measurement utilizes image matching algorithms and the role of an operator is to check and repeat the measurement at positions where an automated procedure failed or gave erroneous result. Photogrammetric software packages usually offer tools for navigating to DTM posts. Extreme points and breaklines must be measured by the operator.

1.2.1.2. Image matching

The goal of automated procedures is to find homologous points in two or more overlapping images. Area and feature based matching algorithms represent techniques that are often implemented in software packages for automated DSM (or DTM) generation.

Area based matching is based on a comparison of radiometric values of image patches selected from overlapping images. An image patch with an odd numbers of rows and columns is cut from one image and a corresponding patch is sought in the second image. In order to narrow the searching area, epipolar geometry is used. A normalized cross correlation coefficient is often calculated as a similarity measure between the image patches in photogrammetry. In computer vision other measures of similarity as mutual information, Euclidian (image) distance or a sum of absolute radiometric differences are used.

If g are radiometric values in images X and Y, then

correlation coefficient $$r = \frac{\sigma_{XY}}{\sigma_X \sigma_Y} = \frac{\sum_{r=1}^{M}\sum_{s=1}^{N}\left(g_{X_{r,s}} - \bar{g}_X\right)\left(g_{Y_{r,s}} - \bar{g}_Y\right)}{\sqrt{\sum_{r=1}^{M}\sum_{s=1}^{N}\left(g_{X_{r,s}} - \bar{g}_X\right)^2 \sum_{r=1}^{M}\sum_{s=1}^{N}\left(g_{Y_{r,s}} - \bar{g}_Y\right)^2}}$$

where M, N correspond to the number of rows and columns in the image patch, g is an average radiometric value in the image patch

σ_{XY} is a covariance and σ_X, σ_Y are standard deviations calculated from g values of the image patches.

Mutual information $M_{X,Y}=H_X+H_Y-H_{XY}$ is defined from the entropy H of images X and Y and their joint entropy H_{XY}. The entropies are calculated from the probability distribution of radiometric values in the images.

Image distance $$D_{X,Y} = \sqrt{\sum_{r=1}^{M}\sum_{s=1}^{N}\left(g_{X_{r,s}} - g_{Y_{r,s}}\right)^2}$$

The correlation coefficient is not sensitive to linear changes in scene illumination (a radiometric shift and gain) but it cannot cope with geometrical deformations in the scene due to steep slopes and different looking angle. Subpixel accuracy can be achieved by interpolation of the correlation coefficient values with a 2nd degree polynomial function and searching its maximum. In the same manner a maximum value if mutual information can be sought. Least squares matching (LSM) is a technique that allows for subpixel measurement and also for adapting the geometry of an image patch. A mathematical explanation can be found in (Grün, 1996) or (Kraus, 2007).

Semi-global matching is another and a rather new image matching method proposed by (Hirschmüller, 2005). It uses mutual information as a similarity measure. Moreover, it utilizes a condition of smoothness of disparities (x-parallaxes) in the point neighborhood. In a post processing step outliers are minimized by peak filtering of disparities. The method was successfully applied to both frame and pushbroom aerial images (Hirschmüller, 2008) as well as to very high resolution satellite images (Reinartz et al., 2010).

In order to select distinct points, which would be suitable for image matching, algorithms called interest operators were developed. For the given pixel and a size of an operator window, the algorithms calculate gradient of radiometric values in two (horizontal and vertical) or four (also diagonal) directions. One or more specific interest values (e.g. minimum of sums of squared differences calculated in four directions in case of the Moravec operator) are evaluated at each pixel of the image. If the interest values fulfill predefined conditions, a pixel is selected as a candidate for matching.

In feature based matching geometric primitives as points and lines are extracted first e.g. by means of interest operators or edge operators. A correspondence analysis is carried out afterwards based on feature attributes such as interest values or correlation coefficient. In case of known image orientation, candidate points are searched along epipolar lines. Moreover, topological relationships can be included. For large number of possible combinations of candidate features dynamic programming methods are applied.

The different types of image matching can be studied in e-learning programs LDIPInter and LDIPInter2. Their URLs are given under the references at the end of this chapter.

Example 1.1 The matching with subpixel accuracy in a profile can be calculated by means of the e-learning program LDIPInter, task 2.1.

Example 1.2 Practice feature based matching using the e-learning program LDIPInter2, task 2.1

1.2.1.3. DTM derivation by means of photogrammetry

In image matching, points corresponding to top of natural and manmade objects elevated above the earth surface are measured, i.e. DSM is created in the first step. The whole procedure of a DSM calculation runs in an iterative manner (compare Figure 1.3). First, image pyramids of the stereopair are created. DSM is calculated and improved with respect to resolution, accuracy and level of detail in each level of the image pyramid (starting from the top). Irregularly spaced elevations are derived by means of feature based matching. Regularly spaced grid is interpolated on each level and it is used as an approximation on the level with higher resolution. Least squares matching is applied in the images with original spatial resolution.

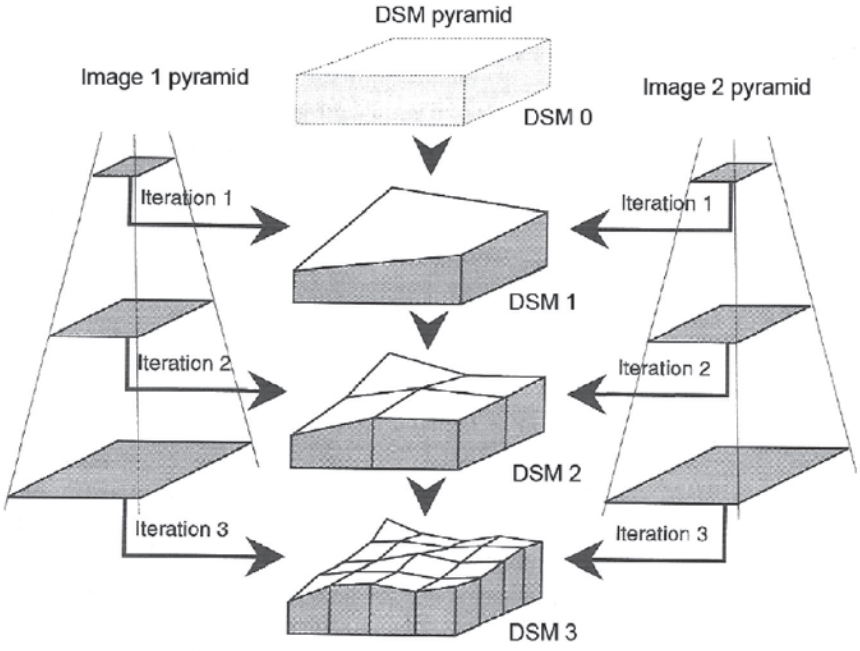

Figure 1.3. DSM derivation from a stereopair of aerial images. Source: Kraus, 1996.

Outliers can appear in DTMs automatically derived by image matching due to

- occlusions (a homologous point does not exist in the second image),
- low textures,
- repetitive object structures (several candidates for a selected image point exist).

In order to avoid the outliers, thresholds for similarity measures and precision of LSM as well as geometrical conditions e.g. differences in spatial coordinates of a point in case of matching from the left to the right image of a stereopair and vice versa can be applied.

Another approach that may help to avoid blunders and at the same time to reduce measurements on features elevated above bare earth is setting a so called parallax bound. It defines a value of maximal horizontal parallax in a given type of terrain (flat, hilly, mountainous). If a DSM is derived over a larger area covered by a block of images, multi-image matching in areas of overlap of four or six images can be applied in order to increase a reliability and accuracy of measured points.

Original DSM points are usually measured at the positions defined by interest operators. Theoretically, it would be possible to match each pixel. Another improvement can be done by extraction of edges and matching pixels on edges especially in built up areas (Zhang et al., 2007). Obtained DSM points are in general irregular and a DTM grid has to be derived by means of filtering and interpolation.

1.2.1.4. Accuracy of a DTM derived by photogrammetry

The accuracy of spatial coordinates σ_X, σ_Y, σ_Z of a point P determined by means of stereophotogrammetry is influenced by several factors as expressed by simplified formulas (exact formulas are given e.g. in Kraus, 2007):

$$\sigma_X^2 = \sigma_{X\_ori}^2 + \sigma_{X\_m}^2 \qquad \sigma_{X\_m} = m_b \sigma_{x'}$$
$$\sigma_Y^2 = \sigma_{Y\_ori}^2 + \sigma_{Y\_m}^2 \qquad \sigma_{Y\_m} = m_b \sigma_{y'}$$
$$\sigma_p^2 = \sigma_X^2 + \sigma_Y^2$$

$$\sigma_Z^2 = \sigma_{Z\_ori}^2 + \sigma_{Z\_m}^2 \qquad \sigma_{Z\_m} = m_b \frac{h}{b} \sigma_{px'}$$

where

$\sigma_{\_ori}$ accuracy of orientation of a stereopair
$\sigma_{\_m}$ accuracy of measurement in a stereopair

$\sigma_{x'}$, $\sigma_{y'}$ accuracy of measurement of image coordinates
$\sigma_{px'}$ accuracy of measurement of horizontal parallax
m_b image scale
h flying height above terrain
b length of base (in image $b' = b/m_b$)

Based on experience, accuracy of image coordinates $\sigma^2_{p'} = \sigma^2_{x'} + \sigma^2_{y'}$ and parallaxes $\sigma_{px'}$ corresponds to 1/3 of a pixel size in case of manual measurement. Accuracy of 1/5 to 1/10 of a pixel can be achieved by least squares matching provided an image of good contrast and texture is available (Kraus, 2007). Empirical results of (Höhle, 2011) showed that DTM mass points can be determined with $\sigma_{px'}$= 1/2 pixel only.

Base to height ratio is another parameter influencing height accuracy of DTMs. In contrary to analogue cameras with a standard format of 23 cm x 23 cm, images produced with modern digital cameras have a rectangular format. Keeping a forward overlap of 60 %, that is typical for mapping purposes, less favourable b/h values must be taken into consideration as shown in Table 1.2 (after Höhle, 2009 and Höhle, 2011a).

Table 1.2. Digital large-format cameras parameters having a direct influence on DTM accuracy

Camera name	Pixel size [μm]	Image size [mm]	Image base b' at 60% overlap [mm]	Camera constant c [mm]	b/h = b´/c
DMC	12	165.9 x 92.2	36.9	120	0.31
DMC II 250	5.6	96.4 x 82.1	32.8	112	0.29
UltraCam Xp WA	6	103.9 x 67.9	27.1	70	0.39
UltraCam Eagle	5.2	104.1x 68.0	27.2	80	0.34
DiMAC Wide+	6	78.0 x 53.4	21.4	70/120/210	0.31/0.18/0.10

DTM derivation from aerial images by means of stereophotogrammetry is a well established process, especially regarding manual measurements. Contemporary images gathered with digital cameras offer spatial resolution on a better level than digitized analogue photographs. Especially higher radiometric resolution gives a possibility for a better performance of automated measurements in the images. Improved spectral resolution extends the usage of images in different applications (agriculture, forestry or environment).

Automated procedures of DTM derivation seem to be more economic in the first view. Nevertheless, manual editing is necessary when high accuracy and models free of outliers are required. It is not possible to collect DTM data in areas without any texture (e.g. sand, asphalt) or in occlusions from buildings and vegetation. In comparison to other techniques, possibilities of deriving breaklines by manual measurements, re-using the images for other purposes (e.g. orthoimage production) and possibility to correct or repeat measurements after DTM derivation can be mentioned as main advantages of photogrammetry. The planimetric accuracy of photogrammetrically determined points is usually higher than the vertical accuracy. This is contrary to airborne laser scanning.

1.2.2 Airborne laser scanning

Airborne laser scanning (ALS), also called topographic LiDAR (Light Detection and Ranging), has developed into a broadly used technology for DTM data collection during the last fifteen years. As an active sensor it does not depend on illumination from the sun and the sun angle and the measurements are not influenced by sun shadows. Spatial coordinates of points (a point cloud) are the result of ALS measurement and data processing. ALS equipment consists of three parts: a scanning unit, a differential GNSS, and an inertial measurement unit (IMU). The principle of the measurement is demonstrated in Figure 1.4.

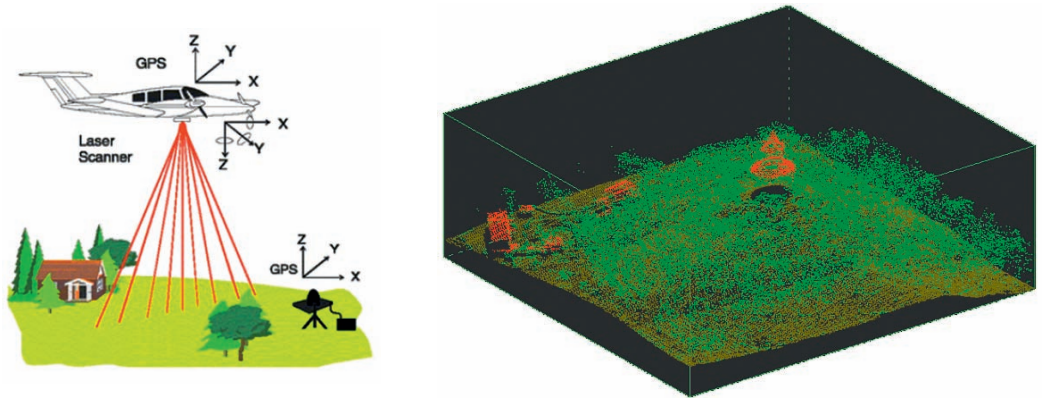

Figure 1.4. Principle of data collection with LiDAR and an example of a point cloud classified into three categories: roofs (red), high vegetation (green) and ground (green-yellow colour). Source: Southern Mapping Company (left), Czech Office for Mapping, Surveying and Cadastre (right).

A distance d between the sensor and a ground point is determined from the elapsed time t between transmission and reception of the pulse and the velocity *v* of the light pulse *(d=v·t/2)*. A pulse is sent in a known direction *α* with respect to the scanning unit. Rotating mirror or optic fibers are examples of technologies used for laser beam deflection. They determine the geometry of scanning pattern on ground (zig-zag, parallel lines). An example of parameters of a scanning unit can be found in Table 1.3.

If an object, which scatters back the pulse, does not cover the entire area of the laser beam footprint, the pulse propagates further and it is possible to record more than one pulse echo as it is shown in Figure 1.5. Recording several echoes is important for classification of point clouds to discriminate between vegetation, buildings and bare-earth points. Current laser scanners record first, last and several intermediate echoes. The newest development has brought full-waveform scanners. Analysis of the width of echo gives information of the vertical spread of the object surface and can be used for a point cloud classification (Figure 1.5, right image). An overview on full-waveform topographic LiDAR can be found e.g. in (Mallet & Bretar, 2009).

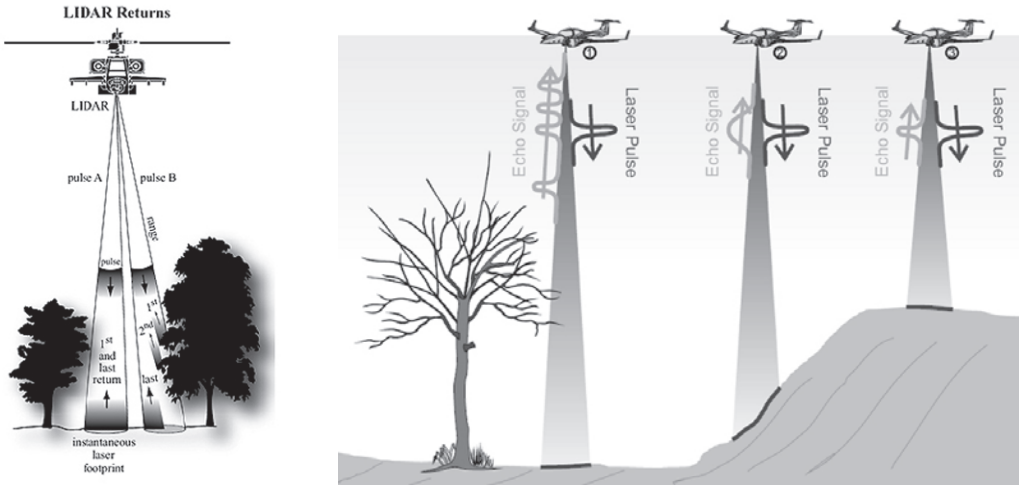

Figure 1.5. Principle of multiple LIDAR echo recording (left), full-waveform data recording (right). Source: Jensen, 2006 (left), Riegl® LMS-680i Data Sheet, 2010 (right).

Table 1.3. Typical parameters of commercial LIDAR systems

Parameter	Riegl LMS-Q560	TopoSys Falcon III	Leica ALS60
Field of view (total)	45°/60°	58°	75°
Effective measurement rate	up to 120 kHz /160 kHz	50 kHz - 125 kHz	up to 100 kHz
Laser beam divergence	≤ 0.5 mrad	≤ 0.7 mrad	0.2 mrad
Operating altitude	30 m - 1600 m	30 m - 2500 m	30 m - 5 000 m
Number of echoes recorded	full waveform	up to 9 per pulse	up to 4 per pulse
Intensity measurement	16 bit	12 bit	8 bit
Point vertical accuracy	< 0.15 m	< 0.10 m	0.08 - 0.24 m
Point horizontal accuracy*	< 0.25 m	< 0.20 m	< 0.64 m
Beam deflection system	rotating polygon mirror	fiber based	rotating mirror

* with respect to maximal operating altitude

Intensity of the returned pulse depends on material it is scattered from. Topographic LiDAR typically embodies an infrared laser (wavelength from 1060 nm to 1540 nm). Water, asphalt or synthetic rubber are examples of materials that show a high absorption in this interval of wavelengths. There is also a dependence on incidence angle. A returned signal is then too weak to be detected. In addition to the elapsed time, intensity of the returned signal is also recorded. The processing of this data results in a grey-tone image giving an overview about reflective properties of surfaces in the area of interest (Figure 1.6). Intensity can then be used as one of parameters in point cloud classification. Some materials (e.g. metals) are very smooth with respect to the used wavelength. Reflection from these materials is not diffusive but specular only and all energy reflects away from the sensor. On the other hand, some geometric constellation of objects, especially in built up areas, can cause a multipath effect that results in outliers, in this case "low points" under the ground.

Figure 1.6 Aerial image (left) and LIDAR intensity image (right) of a built-up area. Source: TopoSys.

Coordinates of a measured ground point $[X_P, Y_P, Z_P]^{\mathbf{mT}}$ in the reference coordinate system of the map projection *m* (the mapping frame) are determined by spatial transformation that can be described as (El-Sheimy, 2009):

$$\begin{bmatrix} X_P \\ Y_P \\ Z_P \end{bmatrix}^m = \begin{bmatrix} X \\ Y \\ Z \end{bmatrix}^m + \mathbf{R}_{\mathbf{b}}^{\mathbf{m}} \left[\mathbf{R}_{\mathbf{s}}^{\mathbf{b}} d \begin{pmatrix} -\sin\alpha \\ 0 \\ -\cos\alpha \end{pmatrix} + \begin{bmatrix} a_x \\ a_y \\ a_z \end{bmatrix}^b \right]$$

$[X, Y, Z]^{mT}$	coordinates of the IMU centre in the reference coordinate system
$\mathbf{R}_{\mathbf{b}}^{\mathbf{m}}$	rotation matrix from the IMU body frame to the reference coordinate system (navigation angles roll, pitch and yaw)
$\mathbf{R}_{\mathbf{S}}^{\mathbf{b}}$	rotation matrix expressing an angular misalignment between the scanner and IMU (boresight matrix)
$[a_x, a_y, a_z]^{bT}$	eccentricity between the IMU and laser scanner origin (leverarm)
d	calculated distance
α	angle of the laser beam in the scanning plane (usually measured from the vertical to both sides of scanning)

It is obvious from the above equation that accuracy of collected points depends on (Schär, 2010):

- Accuracy in absolute position ($\sigma_X, \sigma_Y, \sigma_Z$) and rotations ($\sigma_{roll}, \sigma_{pitch}, \sigma_{yaw}$) as determined from GNSS and IMU
- Accuracy of system calibration, i.e. determination of boresight angles and offsets between instruments
- Internal scanner errors – determination of distance d and angle α

To minimize these errors, sensor calibration, system mount calibration, careful flight planning and proper data processing must be carried out. Residual calibration errors or a change of GNSS accuracy within the flight will appear as differences in strip overlaps. Based on selected features – derived points, lines, and surfaces a strip adjustment is carried out. Transformation parameters (translations and sometimes rotations) describing a discrepancy between strips are calculated. The corrections are then applied directly to the strips or used for refining sensor parameters and reprocessing the entire point cloud.

In contrary to photogrammetry, the vertical accuracy of a DTM derived from laser scanning is less dependent on flying height but depends on point density. An empirically derived formula puts into a relation DTM height accuracy, point density and terrain slope (Kraus, 2007):

$$\sigma_h [cm] = \frac{6}{\sqrt{n}} + 120 \tan\alpha$$

where

n	point density per $1m^2$
$\tan\alpha$	ground slope

In general, vertical accuracy of points collected by airborne laser scanning is in the range of σ_h=10 cm to 15 cm but it can reach much higher values in areas of steep slopes as the formula above indicates. The horizontal accuracy depends on the flying altitude, the performance of the IMU, and the calibration. It is usually on the level of σ_p=30 cm to 50 cm (Höhle, 2011b). The point density is a function of scanning rate and flying height.

The obtained point cloud from first echo basically represents a DSM. If multiple echo recording is applied, also information below canopy is available and can be used for classification of vegetated areas. If a DTM is required, a filtering of original data must be carried out as described in chapter 1.3. An example is depicted in Figure 1.4 (right image). A simplified workflow of LiDAR data acquisition and processing is shown in Figure 1.7. LiDAR data are collected in a specific pattern that depends on the system for deflection of the laser beam. In some areas points might be missing due to absorption or specular reflection. A regularly spaced DTM is obtained by interpolation methods (see chapter 1.4).

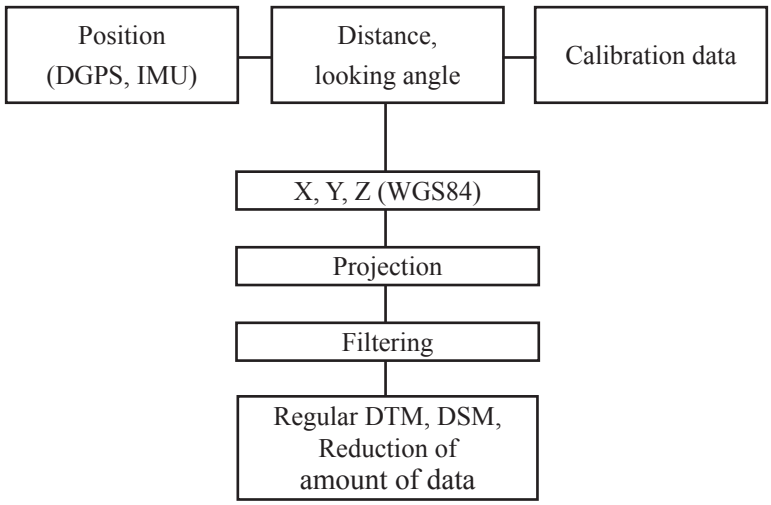

Figure 1.7. Workflow of processing steps of DTM generation from LIDAR data. After Wehr and Lohr, 1999.

1.2.3 Interferometric SAR

Synthetic aperture radar (SAR) is a technology of collecting image data in the microwave part of the spectrum (wavelengths approximately in the range from 1 cm to 1 m). In addition to the amplitude of the detected signal, its phase can also be recorded. From a difference of signal phases recorded with two antennas spatially separated in the cross-track direction, it is possible to derive an elevation of a point on a surface from where the signal was backscattered. The physical principle of this technique is based on interferometry and it is called interferometric SAR (InSAR or IfSAR). Explanation of physical principles is beyond the scope of this book but can be found in the literature (e.g. Maune, 2001, Richards, 2007).

Accuracy of a DTM derived with InSAR depends on sensor parameters and observation geometry (a wavelength, a length of a base line B, accuracy of determination of antenna positions, slant range distance R of the antenna to the target P, depression angle ψ) and ability to correctly generate a continuous elevation map from interferograms (compare Figure 1.8).

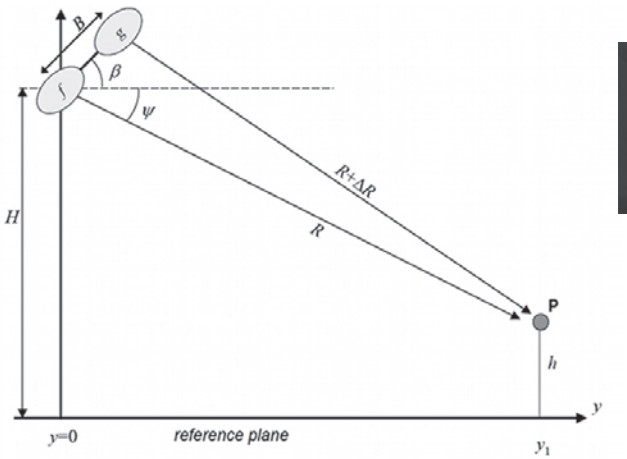

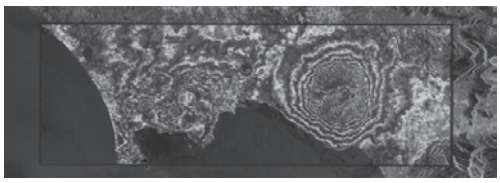

http://esamultimedia.esa.int/images/Earth-Observation/corv_257.jpg

Figure 1.8. InSAR geometry (source: Richards, 2007) and an interferogram superimposed on a radar intensity image (Vesuvius and its vicinity, source ESA)

In contrary to photogrammetry, InSAR systems as active sensors can operate under unfavourable atmospheric conditions (clouds, haze) and illumination (low sun angle, night). The accuracy of InSAR derived DEMs is lower than in case of photogrammetry or laser scanning but it is a cost-effective mapping technique in larger areas and in rapid mapping applications. The data processing is highly automated. It has problems in vegetated and urban areas as well as in mountainous terrains where some spots cannot be processed due to lack of data caused by radar shadows and layovers (effects of side-looking geometry). The last mentioned disadvantage can be compensated by combination of images from different viewing angles (in case of spaceborne sensors by combination of data acquired from ascending and descending orbits). It should be mentioned that the vertical and horizontal accuracy of DTM derived by InSAR is best in flat, open areas and it decreases with the steepness of slopes and vegetation coverage. Depending of the wavelength, the penetration depth with respect to vegetation also changes. While backscattering in X-band (wavelength about 3 cm) happens at the top of the canopy, data collected in P-band (wavelength between 30 and 100 cm) mostly correspond to bare earth.

In several European countries a nationwide DTM and DSM was derived by airborne InSAR within the NEXTMap project. According to the project specifications, an overall vertical accuracy of 1 m (RMSE) was required. In addition to the elevation models, orthorectified SAR images with 1.25 m resolution and a horizontal accuracy of 2 m (RMSE) were derived (NextMap, 2011).

Accuracy of DTM originating in spaceborne InSAR systems has been limited in the accuracy level of tens of meters to recent years. The latest development brought a new generation of SAR sensors utilizing a shorter wavelength (X-band) and allowing for higher spatial resolution (down to 1 m). TerraSAR-X and TanDEM-X can be named as examples. The configuration of these two satellites is designed for simultaneous acquisition of interferometric pairs of images. A DSM with a global coverage and absolute vertical accuracy of 10 m (relative 2 m) in a grid of 12 x 12 m^2 should be available in 2011 (Infoterra, 2011).

In addition to InSAR, a so called radargrammetry technique is also used for DTM derivation from SAR imagery. The principle is similar to photogrammetry. A DSM with 5 m absolute height accuracy at 10 m grid spacing was derived by this method from TerraSAR-X images (Infoterra, 2011).

1.2.4 Spaceborne imaging systems

During the last decade the number of very high resolution (VHR) sensors enabling acquisition of stereoimages (both with along and across track geometry) has increased considerably. Principles of DTM derivation from these sensors are similar to those used in digital photogrammetry and will not be discussed further. Commercial photogrammetric software packages usually offer modules for processing of that kind of data. Table 1.4 gives examples of VHR sensors and their parameters.

Table 1.4. Examples of VHR spaceborne sensors for stereoimage acquisition and their parameters (PAN – panchromatic channel, MS – multi spectral channel)

Sensor	Number of spectral bands	Resolution [m] PAN/MS	Operates from
WorldView-2	PAN/8 MS	0.5/1.84	2009
GeoEye-1	PAN/4 MS	0.5/2.0	2008
OrbView-3	PAN/4 MS	1.0/4.0	2003
QuickBird	PAN/4 MS	0.6/2.4	2001
IKONOS	PAN/4 MS	1.0/4.0	1999

Similarly to photogrammetry, image matching techniques can be used for automated derivation of DSMs. The latest studies showed that a vertical accuracy better than 2 meters can be achieved with a low number of control points (e.g. Capaldo et al., 2010). Integration of new image matching techniques as semi-global matching improves the level of detail and quality of derived DSM from satellite data (e.g. Reinartz et al. 2010). Information about the quality of DTMs derived from VHR sensors can be found e.g. in (Jacobsen & Buyuksalih, 2009). Quality assessment of such DTMs can be carried out in the same manner as discussed in the chapter 2.

1.2.5 Summary of methods for DTM data collection

All presented methods for data acquisition perform well in open terrain. They differ in accuracy but all of them are suitable for economic mapping over large areas. Problems appear in vegetated areas. Only laser scanning and InSAR (operating in L or P bands) are able to provide data under canopy. In areas of low and dense vegetation both photogrammetry and LiDAR produce points on vegetation surface that must be filtered out in following processing steps if only DTM is required. Laser scanning is also a suitable method for deriving DTMs in built-up areas. In contrary to photogrammetry smaller areas are obscured and the dataset can be used for automated modelling of single buildings.

Table 1.5. Comparison of performance of four methods for DTM data collection

DTM collection method	Vertical accuracy			Terrain type			
	<0.1 m	(0.1-1.0) m	> 1.0 m	Open terrain	Low vegetation	Forested	Built-up areas
PHM	+ *	+	+	+	-	-	+/-
ALS	+	+	+	+	+/- **	+	+
InSAR	-	-	+	+	-/+***	-/+***	+/-

* possible for low flying heights and small pixel size (GSD)
** depends on vegetation density *** depends on wavelength

DTM collection method	Strongly influenced by atmospheric effects	Holes in data	Large area (> 10 km^2)	Remark
PHM	+	+	+	
ALS	-	+	+	
InSAR	-	+	+	Fast, lower accuracy

ALS – airborne laser scanning, PHM – photogrammetry

1.3 Filtering of raw data

Airborne laser scanning, InSAR, and photogrammetry are, by their principle, methods for acquisition of DSMs. Recording not only first but also last and intermediate echoes in the case of laser scanning gives a better opportunity to collect measurements of bare earth e.g. in forest areas. Points on buildings, cars and dense vegetation remain in the data set and must be removed if a DTM is a final product that is required for a specific application. Utilizing a parallax bound for deriving DTMs from imagery reduces the number of points on off-terrain objects considerably but it may not work perfectly in dense built-up and vegetated areas. The goal of filtering is to separate points representing bare earth from points corresponding to measurements from objects rising above terrain. These objects can be stable such as buildings, trees or power lines but also dynamic as cars. Several filtering methods have been developed and can be divided into following categories (Pfeifer & Mandlburger, 2009):

- Progressive densification
- Surface-based filters
- Segmentation-based filters
- Morphological filters

In case of laser scanning, the last echo records are usually taken as a starting point of filtering. They do not always correspond to bare earth but to lower vegetation, to a top of dense crops but also to points under the surface that are a result of the multipath effect. Some filtering techniques combine point clouds with images. Spectral features are then analysed together with laser point distribution to identify vegetation and manmade structures.

1.3.1 Progressive densification

The first step of this method is based on finding a basic set of points belonging to bare earth. These points can be chosen as lowest points of grid cells overlaid over the area of interest (Axelsson, 2000), lower points of the convex hull of the point set or corner points of the evaluated dataset (Sohn&Dowman, 2002). The selected points are connected to triangles. The TIN is densified by adding other points fulfilling geometric criteria such as size of angles between the triangle face and the edges from the triangle vertices to the new point as shown in Figure 1.9 (Axelsson, 2000). Another possibility is a vertical distance d of the evaluated point to the reference triangle. The densification runs in two steps in the algorithm suggested by (Sohn & Dowman 2002). First, points below the current triangles are added (downward densification). During upward densification points belonging to bare earth above the triangles are included based on a set of geometrical conditions that a newly created tetraedons must fulfill. Progressive densification has been applied in the commercial product TerraScan of the TerraSolid company.

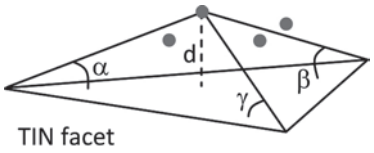

Figure 1.9. Geometric parameters for TIN densification. After Axelsson,2000.

1.3.2 Surface-based filters

This method suggested by (Kraus & Pfeifer, 1998) is also known as a robust interpolation. In the first step, the surface is approximated by a best fitting curve $z(x_i, y_i)$ by means of linear prediction or bivariate polynomials. Based on the residuals $r_i = z_i - z(x_i, y_i)$, points are weighted according to a specific weight function (Kraus, 2007, Pfeifer & Mandlburger, 2009):

where

$$w(r) = \begin{cases} r < g & 1 \\ g \le r \le g + h & \dfrac{1}{1 + (a(r-g))^b} \\ r > g + h & 0 \end{cases}$$

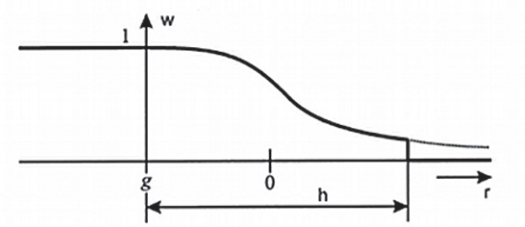

r residuals to the approximated surface
g defines the maximal residual with a weight equal to 1 (drop of the waiting function)
h gives the range of residuals with weight $0 < w(r) < 1$
a, b parameters controlling the shape of the weight function

In this way, points that are higher above the parameterized surface get lower weights or weights equal to zero if the residual $r > h+g$. The algorithm was originally developed for wooded areas. A hierarchical approach based on thinning of amount of data into several layers and applying a coarse to fine procedure

was further elaborated to handle large buildings and to reduce computational time (Pfeifer et al., 2001). The surface-based algorithm developed at TU Vienna has been implemented into the SCOP++ software package.

1.3.3 Segmentation-based filters

The idea of segmentation filters is to find homogeneous segments in point clouds and then to analyze the segments instead of individual points (Pfeifer & Mandlburger, 2009). Region growing algorithms based on different criteria of homogeneity such as a difference between adjacent normal vectors (Tovari & Pfeifer, 2005) or height differences (Nardinocchi et al., 2003) can be named as examples of segmentation based methods. Some tests have been also done with the eCognition software package that has been developed for object based image analysis.

1.3.4 Morphological filters

Morphological filters are based on the presumption that a large height difference between two nearby points will not be caused by a steep slope of terrain but it will more likely correspond to an object rising above the earth surface. For a given height difference the probability that the higher point is a ground point decreases if the distance between the points decreases. An acceptable height difference between two points is therefore defined as a function of distance between the points (cf. Figure 1.10). This function is used in the structure element in the morphological operation of erosion. The structure element is placed on each candidate point. In case that a height difference to one or more neighbouring points exceeds an acceptable value, the candidate point is classified as an off-terrain point (Vosselman, 2000, Pfeifer & Mandlburger, 2009). Several variants of this filter can be found in literature.

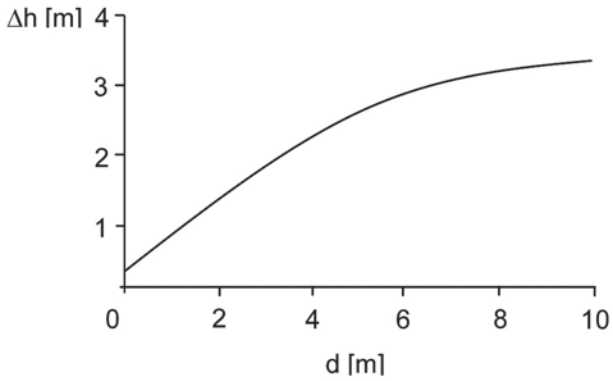

Figure 1.10. A function showing a relation between distance d and an acceptable height difference Δh between a candidate point and neighboring points in the structure element of the morphological filter. After Vosselman, 2000.

Sithole and Vosselman (2003) published results of a comparison of eight filtering algorithms applied on a dataset provided within a project "ISPRS comparison of filters". All filters mentioned above and their modifications were included in the test. Some of algorithms were based on an original point cloud and some

required an interpolation into a grid. Most of algorithms worked in an iterative manner. The filters were tested on eight datasets. They differed in point spacing (1 to 10 m) and type of terrain (rural and urban, different slopes, sizes of buildings and other features such as railways or river banks). Gaps in the dataset were present too. Regarding performance of the filters, all worked well in low complexity landscapes. Most problems were observed in a more complicated city structures as tier buildings or courtyards and in areas of bare earth discontinuities. Surface-based filters gave better results in the test but the authors encourage to carry out more investigations in segmentation and clustering algorithms. More research has to be carried out with respect to filters and point density. It is mentioned that full automation is not possible due to remaining errors; the filtered data sets must be checked and corrected. The eight data sets were collected within the EuroSDR project on laser scanning and are available on the internet.

1.4 Completion of DTMs by interpolation

Filtered data as well as original point clouds are usually represented by a set of irregularly spaced points. Moreover, gaps (holes) in collected data sets may occur. In case that a DTM is required in a form of regularly spaced points (grid, raster format), interpolation must be carried out to calculate elevation values in defined grid positions. Some filtering techniques work on raster bases. Interpolation is then performed on original data (e.g. last echo point cloud). Several interpolation algorithms exist. The following overview is based on (Maune, 2001, Mitas & Mitasova, 1999).

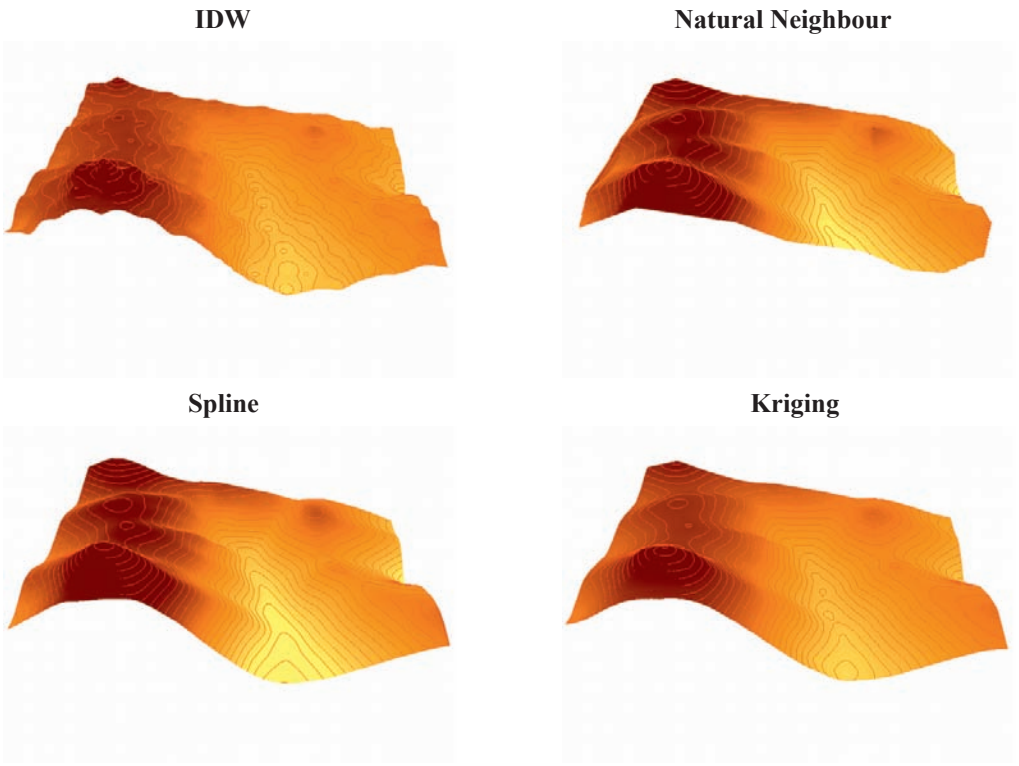

Figure 1.11. Interpolation methods applied on a dataset collected by terrestrial measurement for detailed mapping.

In the TIN model a linear approach where the elevation of a new point is calculated based on the plane given by vertices of a triangle the point belongs to represents a simple interpolation method. ***Inverse distance weighted interpolation*** (IDW) is not suitable for terrain data because a functional dependence of the interpolated elevation on the distance from the given position does not in general decrease. ***Natural neighbour*** interpolation uses weights based on areas of Thiessen polygons calculated with and without an interpolated point. The created surface is smooth except of the data point locations. In comparison to other interpolators (spline, kriging), natural neighbour interpolation does not create new peaks and depressions, only those existing in the original data set will appear in the interpolated model. In ***spline*** interpolation, a surface that minimizes the overall surface curvature is created. It is useful for areas with smoothly varying terrain. Sharp changes over short distances cause exaggeration of values in the neighbourhood. ***Kriging*** is a geostatistical interpolation method that creates a prediction model based on distance and correlation (covariance) among the measured points. Figure 1.11 shows an example of four mentioned interpolation methods applied on the same data. In photogrammetric software solutions for DTM generation a robust finite element interpolation method is often implemented (Inpho, Intergraph).

All processes from data collection to DTM interpolation are potential multiple sources of errors. Quality control of DTMs is necessary as it is discussed in detail in the chapter 2.

1.5 References

Axelsson, P., 2000. DEM Generation from Laser Scanner Data Using Adaptive TIN Models, IAPRS Vol. XXXIII, Part B4, Amsterdam http://www.isprs.org/proceedings/XXXIII/congress/part4/111_XXXIII-part4.pdf (last accessed October 2011)

Capaldo, P. et al., 2010. Geometric Potentiality of GeoEye-1 In-Track Stereo Pairs and Accuracy Assessment of Generated Digital Surface Models, In Proceedings of 30th EARSeL Conference, Paris, France

El-Scheimy, N., 2009. Georeferencing component of LiDAR systems, In: Shan, J., Toth, C. K. (Eds.): Topographic Laser Ranging and Scanning, CRC Press, ISBN 978-1-4200-5142-1

Grün, A., 1996. Least squares matching: a fundamental measurement algorithm, In: Atkinson (ed.): Close range photogrammetry and machine vision, Whittles Publishing, Caithness, UK, ISBN 1-870325-46-X

Jacobsen, K., Buyuksalih, G., 2010. Mapping with WorldView-1 Imagery, In: Imagin[e,g] Europe, Proceedings of 29th EARSeL Conference, Chania, Greece, pp. 190-200

Hirschmüller, H., 2005. Accurate and Efficient Stereo Processing by Semi-Global Matching and Mutual Information, Proc. IEEE Conf. Computer Vision and Pattern Recognition, vol. 2, pp. 807-814

Hirschmüller, H., 2008. Stereo Processing by Semi-Global Matching and Mutual Information, IEEE Transactions on Pattern Analysis and Machine Intelligence, vol. 30, pp. 328-341

Höhle, J., 2009. DEM Generation Using a Digital Large Format Frame Camera, Photogrammetric Engineering and Remote Sensing, Vol. 75, No. 1, pp. 87-93

Höhle, J., 2011a. DEM Generation by Means of New Digital Cameras, IAPRS, Vol. XXXVIII-3/W22, 6 p.

Höhle, J., 2011b. The assessment of the absolute planimetric accuracy of airborne laserscanning, proceedings of "Laser Scanning 2011", Calgary/Canada, 6 p.

Jensen, J. R., 2006. Remote Sensing of the Environment: An Earth Resource Perspective. 2nd ed., Prentice Hall, ISBN 978-0131889507

Kraus, K., 1996. Photogrammetry, Vol. 2., 4th edition, Dümmler Verlag, Bonn, ISBN 3-427-78694-3

Kraus, K., Pfeifer, N., 1998. Derivation of Digital Terrain Models in wooded areas, ISPRS Journal of Photogrammetry & Remote Sensing 53 (1998), pp. 193–203

Kraus, K., 2007. Photogrammetry: Geometry from Images and Laser Scans, 2nd edition, de Gruyter, 459 p., ISBN 978-3-11-019007-6

Maune, D. F. (Ed.), 2001. Digital elevation models Technologies and Applications: The DEM Users Manual, ASPRS, 539 p., ISBN: 1-57083-064-9

Mallet C., Bretar, F., 2009. Full-waveform topographic LiDAR: State-of-the-art, ISPRS Journal of Photogrammetry & Remote Sensing 64 (2009), pp. 1–16

Mitas, L., Mitasova, H., 1999. Spatial interpolation, in: Longley, P., Goodchild, M.F., Maguire, D.J., Rhind, D.W. (Eds.), Geographical Information Systems: Principles, Techniques, Management and Applications, Wiley. http://www.colorado.edu/geography/class_homepages/geog_4203_s08/readings/mitas_mitasova_1999_2005.pdf (last accessed October 2011)

Nardinocchi, C. Forlani, G., Zingaretti, P., 2003. Classification and Filtering of Laser Data, IAPRS Vol. XXXIV, PART 3/W13, Dresden http://www.isprs.org/proceedings/XXXIV/3-W13/papers/Nardinocchi_ALSDD2003.PDF (last accessed October 2011)

Pfeifer, N., Stadler, P., Briese, C., 2001. Derivation of Digital Terrain Models in the SCOP++ Environment, OEEPE Workshop on Airborne Laser scanning and Interferometric SAR for Digital Elevation Models, Stockholm http://www.ipf.tuwien.ac.at/cb/publications/np_stockholm.pdf (last accessed October 2011)

Pfeifer, N., Mandlburger, G., 2009. LiDAR Data Filtering and DTM Generation, In: Shan, J.,Toth, C. K. (Eds.): Topographic Laser Ranging and Scanning, CRC Press, ISBN 978-1-4200-5142-1

Reinartz et al., 2010. DSM Generation and Filtering from High Resolution Optical Stereo Satellite Data, In Proceedings of 30th EARSeL Conference, Paris, France

Richards, M. A., 2007. A Beginner's Guide to Interferometric SAR Concepts and Signal Processing, IEEE A&E SYSTEMS MAGAZINE Vol. 22, No. 9http://users.ece.gatech.edu/mrichard/AESS%20IFSAR%20Tutorial.pdf (last accessed October 2011)

Schär, P., 2010. In-Flight Duality Assessment and Data Processing of Airborne Laser Scanning, Ph.D. dissertation, EPA Lausanne

Sithole, G., Vosselman, G., 2003. ISPRS Comparison of Filters, ISPRS Report, Commission III, Working Group 3 http://www.itc.nl/isprswgIII-3/filtertest/MainDoc.htm (last accessed October 2011)

Sohn, G., Dowman, I., 2002. Terrain Surface Reconstruction by use of Tetrahedron Model with the MDL Criterion, IAPRS Vol. XXXIV, 3A, Gratz http://www.isprs.org/proceedings/XXXIV/part3/papers/paper137.pdf (last accessed October 2011)

Tovari, D., Pfeifer, N., 2005. Segmentation Based Robust Interpolation – a New Approach to Laser Data Filtering, ISPRS WG III/3, III/4, V/3 Workshop "Laser scanning 2005", Enschede http://www.isprs.org/proceedings/XXXVI/3-W19/papers/079.pdf (last accessed October 2011)

Vosselman, G., 2000. Slope based filtering of laser altimetry data, IAPRS Vol. XXXIII, Part B3, Amsterdam http://www.isprs.org/proceedings/XXXIII/congress/part3/935_XXXIII-part3.pdf (last accessed October 2011)

Wehr, A., Lohr, U., 1999. Airborne laser scanning - an introduction and overview, ISPRS Journal of Photogrammetry & Remote Sensing 54 (1999), pp. 68–82

Zhang, B., Miller, S., Walker, S., Devenecia, K., 2007. Next Generation Automatic Terrain Extraction Using Microsoft UltraCam Imagery, ASPRS 2007 Annual Conference Tampa, Florida http://www.socetset.com/docs/education/professional_papers-BAK/2007_asprs_ngate.pdf (last accessed October 2011)

URLs (last accessed October 2011):
Data acquisition
Intergraph [http://www.intergraph.com/photo/ia.aspx]
Leica Geossyems[http://www.leica-geosystems.com/en/Airborne-Sensors_57608.htm]
Microsoft Imaging [http://www.microsoft.com/ultracam/en-us/default.aspx]
Riegl [http://www.riegl.com]
TopoSys [http://toposys.de, http://www.trimble.com/geospatial/]
Infoterra [http://www.infoterra.de]
NextMap [http://www.intermap.com/nextmap-3d-mapping-program]

Software
eCognition [http://www.ecognition.com]
SCOP ++ [http://www.inpho.de]
TerraSolid [http://www.terrasolid.fi]

E-learning
LDIPInter [http://people.plan.aau.dk/~jh/LDIPInter1/ldipinter/]
LDIPInter2 [http://ldipinter2.plan.aau.dk/]

Data sets
ISPRS comparison of filters [http://www.itc.nl/isprswgIII-3/filtertest/DownloadSites.htm]

2. Methods of checking and improving the quality of DTMs

This chapter deals with the methods of checking and improving the quality of DTMs. First we define what is understood by quality of DTMs. The checking of the accuracy and completeness is then discussed. The improving of quality and completeness is dealt with thereafter. Relevant tools and literature are presented. A few examples will help to make the given formulae better understood. Finally, some programs, which solve statistical tasks, are presented.

2.1 What means DTM quality?

The quality of a DTM comprises accuracy, density, and completeness. The checking of the quality is necessary in order to fulfill the specifications and to carry out an application. The results of the checking by the producer as well as some other characteristics of the DTM are stored in the metadata of the DTM. The user of the data may wish to carry out an own quality control.

The DTM data can be available in different forms (point cloud, grid, and TIN). The application and the available programs will decide in which form the DTM has to be used. The forms of the DTM have their special features.

Point clouds are the original data. The points are irregular distributed in case of photogrammetric data acquisition. Laser scanners produce a pattern of points, which depends on the design of the scanner (fiber optics, oscillating or rotating mirror). There may be gaps in the data due to lack of return signals (at laser scanning) or lack of contrast and structure in the imagery (at automated photogrammetric procedures). Points are also on top of vegetation and buildings. Filtering is necessary in order to remove all points above the terrain. The original point clouds are not always distributed by the producer of the DTM data.

The **gridded DTM** has a regular arrangement of elevations. They are derived from the original point clouds by means of interpolation. The spacing between the individual points can be a few meters. Very dense DTMs result in large data volumes, which may give difficulties in handling the DTM data in application programs. Large spacing between elevations results in reduction of the accuracy of interpolated elevations or missing of objects like dykes and of other small structures in the terrain.

DTMs based on triangles (called Triangulated Irregular Network- or **TIN-DTMs**) adapt better to the terrain than gridded DTMs. Breaklines of the terrain are integrated in the triangle structure. Also the relation to neighboring triangles (topology) is part of the data structure. TIN based DTMs require more storage place.

The checking of the accuracy has to deal with these three forms of DTMs. The method of acquisition may also require different approaches. For example, the determination of the planimetric accuracy of the DTM is best done with the original point cloud.

2.2 Checking of the accuracy

In principle, the checking of DTM data is carried out by comparing the DTM data with reference values, which are more accurate than the DTM to be tested. This is done for a small sample only. Reference values can be determined in the field by geodetic methods (GNSS, leveling, etc.) with a very high accuracy but high efforts. Photogrammetric methods may allow higher numbers of checkpoints and better economy. Improving the DTM requires the measurement of many points in order to remove systematic errors and blunders for large areas.

2.2.1 Absolute and relative accuracy

The assessment of the quality is done with the final DTM, for example in the acceptance test. The producer of the data will make checks within the production process in order to ensure the demanded quality of the final product. Such internal checks are here not dealt with in detail. The user of DTM data is especially interested in the absolute accuracy, which is derived from comparison with reference data. The producer will assess the relative accuracy of the DTM data. For example, the data originating from two strips from laser scanning may have discrepancies in the overlap area. These discrepancies can be detected and reduced by very special methods.

2.2.2 DEM terrain types

The terrain may be very different. Some of the areas are covered with vegetation and buildings. In dense forests the laser beam, for example, cannot penetrate to the terrain. At black areas the laser beam is sometimes also absorbed and no measurements will occur. The final DTM is produced by classification and filtering. These automated processes are not error-free. In areas of no data the elevations must be determined by interpolation from nearby points. The accuracy in the DTM is therefore not equal. It is, therefore, useful to specify and assess the accuracy for different terrain types. In the FEMA[1] guidelines of the U.S.A, for example, the following terrain types are suggested:

- open terrain
- weeds and crops
- scrub and bushes
- forested
- built-up areas.

The achievable accuracy in open terrain is usually highest and can always be assessed. It is the fundamental accuracy. The assessment of the accuracy at the other terrain types is supplementary. It is named “Consolidated Accuracy” when all land cover categories will be combined. However, the highest user demands exist in the built-up areas and the assessment of the accuracy will often be specified separately.

[1]Federal Emergency Management Agency

2.2.3 Reference values for checking of the accuracy

The reference values must have a higher accuracy than the DTM to be tested. The factor between the two accuracies should be at least 3. It depends now on the quality of the DTM which accuracy the reference values should have. By means of land surveying methods accuracies of a few cm can be achieved. Photogrammetric measurements can be carried out when the DTM to be tested has an accuracy of a few decimeters (dm).

Besides new measurements of reference points also existing fix points or well-defined objects, of which co-ordinates are stored in databases, can be used for an assessment of the accuracy. In the following some details are given for these three possibilities.

2.2.3.1. Measuring by land surveying

Today the most applied surveying method is GNSS, which stands for Global Navigation Satellite Systems. The antenna of a GNSS receiver (mounted on a pole) is placed on the checkpoint. Pseudo-distances to four or more satellites are measured. The verticality of the pole has to be controlled by means of a level. The elevation of the antenna above the checkpoint is recorded together with other data (e.g. point number, pressure, temperature, thresholds for minimum angle to satellites and internal accuracy). In differential mode the GNSS receiver is connected by means of radio waves with a network of reference stations, which carry out simultaneously measurements and which are then transferred to the mobile GNSS receiver. All measurements are used to determine a 3D-position. The technique is called Real Time Kinematic (RTK). The availability of satellites around the horizon and with a minimum angle above horizon is important for accurate results. The internal accuracy can be observed by a displayed measure (PDOP value). The use of double measurements (with a time-interval of about one hour between measurements) is also good praxis. With careful use of the GNSS/RTK method an accuracy of 2cm can be obtained both horizontally and vertically.

In forests and built-up areas with tall objects (houses, trees, etc.) the measurement to satellites may be prevented. In such cases other surveying methods have to be applied (e.g. tacheometry or leveling). Also the combination of GNSS/RTK and other surveying method is used.

2.2.3.2. Measurement by aerial photogrammetry

The determination of many checkpoints can economically be determined by photogrammetry. An aerotriangulation will be carried out. In this process tie points, which connect the images, are automatically measured. A few ground control points are necessary to orient the block of images absolutely. The achievable accuracy of the checkpoints depends on the flying altitude from which the images are taken and from the quality of the camera. The taken images are characterized by the ground sampling distance (GSD). The accuracy of the check points are then about 0.75 GSD in planimetry and 0.53 GSD in elevation. For example, images with GSD=8cm of digital large format cameras enable accuracies of $RMSE_p$=6cm and $RMSE_Z$=4.3cm (Jacobsen et al., 2010).

2.2.3.3. Existing objects in topographic data bases

Checkpoints for the assessment of the horizontal and vertical accuracy can also be taken from existing databases. The 3D coordinates of well-defined objects like manhole covers, drain gratings, crossing of paths, buildings, etc. are stored in databases. If such objects are well defined, stable and of superior accuracy, then they qualify as checkpoints.

Checkpoints for the assessment of the horizontal accuracy can also be taken from existing orthoimages. Only well-defined points situated on the ground are suitable.

2.2.4 Accuracy measures

DTMs have to be checked for vertical as well as horizontal errors. If the position of the data points is in error, then additional vertical errors will occur in non-flat areas. In the following we deal first with the **assessment of the vertical accuracy**.

The reference points are determined in positions, which will not correspond to the position of the DTM point. Therefore, an interpolation is necessary. This interpolation may also be a reason for additional vertical errors. The distance to the surrounding DTM posts has to be small when differences in elevation exist.

The accuracy measures are derived from the differences between the DTM value and the reference value. The sign of the difference is important and should always be defined as an 'error' (DTM – reference). From the differences a Root Mean Square Error (RMSE) and a Mean Error (μ) are calculated. The Mean Error (also called Average Error) is an indication that the DTM is shifted regarding to the reference. Such a systematic error can be very problematic for volume determination required in construction work. The Standard Deviation (σ) is calculated from modified differences which do not include the systematic error (bias).

Gross errors may exist in the DTM and they should not influence the accuracy measures. They can be eliminated by means of a threshold if only very few check points have gross errors. The Table 2.1 displays the accuracy measures (including formula) to be applied at normal distribution of vertical errors. If many blunders exist and if the distribution of the errors is not normal, robust accuracy measures have to be applied. A histogram of the error distribution should be produced in order to find out about normality of the error distribution.

Figure 2.1 depicts a histogram of error distribution for photogrammetric measurements compared with checkpoints. In order to compare with normality, the figure contains a superimposed curve for a normal distribution (Gaussian bell curve) obtained by ordinary estimation of the Mean Error and Standard Deviation.

Because outliers are present in the data, the estimated curve does not match the data very well. The reasons are that the errors are not normally distributed, e.g. because the errors are not symmetric around the Mean Error (skew distribution) or because the distribution is more peaked around its mean than the normal distribution while having heavy tails. The latter effect is measured by the kurtosis of the distribution, which in this situation is bigger than zero.

Table 2.1. Accuracy measures for DTMs presenting a normal distribution of vertical errors

Number of checkpoints	n
Vertical error	$\Delta h = h_{DTM} - \text{reference height}$
Root Mean Square Error	$\hat{RMSE} = \sqrt{\frac{1}{n}\sum_{i=1}^{n}\Delta h_i^2}$
Mean error	$\hat{\mu} = \frac{1}{n}\sum_{i=1}^{n}\Delta h_i$
Standard deviation	$\hat{\sigma} = \sqrt{\frac{1}{(n-1)}\sum_{i=1}^{n}(\Delta h_i - \hat{\mu})^2}$
Threshold for outliers	$\lvert\Delta h\rvert \geq 3 \cdot \text{RMSE}$
Number of outliers	$N = n_{outliers}$

Example 2.1 Calculation of Δh_i, Root Mean Square Error (RMSE) and number of blunders ($n_{outliers}$) for the given sample.

#	X[m]	Y[m]	Z_ref [m]	Z_DTM[m]	Δh[m]
2866	-236325.00	283750.00	49.88	49.97	0.09
2944	-236300.00	283750.00	46.28	46.79	0.51
2945	-236275.00	283750.00	46.42	46.89	0.47
3024	-236250.00	283750.00	46.81	47.51	0.70
3025	-236225.00	283750.00	50.24	51.47	1.23
3106	-236200.00	283750.00	55.08	56.38	1.30
3107	-236175.00	283750.00	57.23	58.57	1.34
3188	-236150.00	283750.00	55.36	56.06	0.70
3189	-236125.00	283750.00	55.94	56.98	1.04
3270	-236100.00	283750.00	57.88	59.32	1.44
3271	-236075.00	283750.00	60.27	61.76	1.49
3351	-236050.00	283750.00	63.34	64.34	1.00
3352	-236025.00	283750.00	66.27	67.51	1.24
3432	-236000.00	283750.00	69.41	70.75	1.34
3433	-235975.00	283750.00	72.44	73.88	1.44
3509	-235950.00	283750.00	75.64	77.25	1.61
3510	-235925.00	283750.00	78.64	80.08	1.44
3586	-235900.00	283750.00	80.83	81.62	0.79
3587	-235875.00	283750.00	82.65	88.17	5.52
3665	-235850.00	283750.00	84.55	86.28	1.73

Result: Number of points: n = 20, RMSE = 1.69m, number of blunders $n_{outliers} = 1$

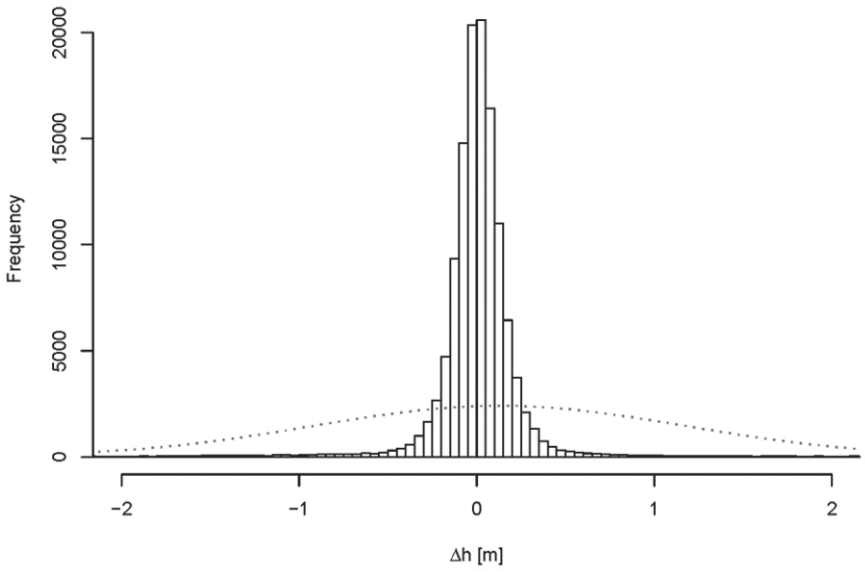

Figure 2.1. Histogram of the errors Δh. Superimposed on the histogram are the expected counts from a normal distribution with Mean and Standard Deviation estimated from the DTM data. For a better visualisation the histogram is truncated at -2m and 2m. The mismatch between data and estimated normal curve is due to heavy tails.

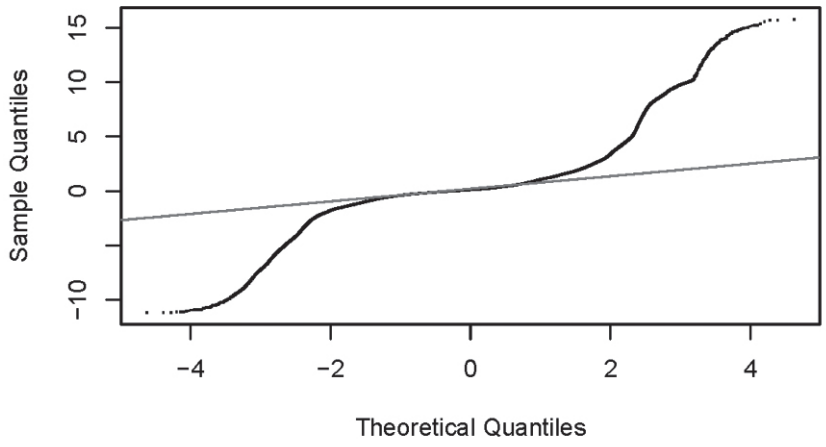

Figure 2.2. Normal Q-Q plot for the distribution of Δh.

A better diagnostic plot in order to detect a deviation from the normal distribution is the socalled quantile-quantile (Q-Q) plot. The quantiles of the empirical distribution function are plotted against the theoretical quantiles of the normal distribution. If the actual distribution is normal, the Q-Q plot should yield a straight line. Figure 2.2 shows the Q-Q plot for the distribution of Δh in the same example as in Figure 2.1. A strong deviation from a straight line is obvious, which indicates that the distribution of the Δh is not normal. The generation of a Q-Q plot is done by means of a program (cf. Table 2.7).

If the histogram of the errors (or the Q-Q plot) reveals non-normality, then **robust accuracy measures** should be applied. They are based on the Median of the distribution.

The Median is the middle value if all errors are put in an order, starting from the lowest value to the highest value. The median is named as the 50% quantile and denoted as Q(0.50) or $m_{\Delta h}$. It is a robust estimator for a systematic shift of the DTM. It is less sensitive to outliers in the data than the mean error and also provides a better distributional summary for skew distributions.

Another robust accuracy measure is the Normalized Median Absolute Deviation (NMAD). It estimates the scale of the Δh distribution and corresponds to the standard deviation when no outliers exist.

A robust and distribution-free description of the measurement accuracy is obtained by reporting quantiles of the distribution of the **absolute** errors, i.e. of |Δh|. For example, the 95% quantile of |Δh| literally means that 95% of the absolute errors have a magnitude within the interval [0, $Q_{|\Delta h|}(0.95)$]. The remaining 5% of the errors can be of any value making the measure robust against up to 5% blunders. Another important measure is the 68.3% quantile of the absolute errors, denoted as $Q_{|\Delta h|}(0.683)$. It indicates the value where all differences smaller than this value amount to 68.3% of all errors. This percentage is also used to define the standard deviation ($1 \cdot \sigma$) at normal error distribution.

The meaning of the robust accuracy measures can be explained by means of Figure 2.3 where the quantiles (Q) are plotted as function of the probability (p). Normal distribution of the errors is assumed and the unit of quantiles is the standard deviation (σ). $Q_{\Delta h}(0.50)$ or the 50% quantile is then the Median.

If absolute values of the errors are used, $Q_{|\Delta h|}(0.683)$ corresponds to $1 \cdot \sigma$ and $Q_{|\Delta h|}(0.95)$ to $1.96 \cdot \sigma$. The 50% quantile of the absolute values of the errors (solid red curve) equals to $0.67 \cdot \sigma$ and is named Median Absolute Deviation (MAD). Multiplication of MAD by the factor 1.4826 is then the Normalized Median Absolute Deviation (NMAD). At normal distribution the NMAD value corresponds to the standard deviation ($1 \cdot \sigma$).

When calculating the 68.3% and the 95% quantile the absolute errors (|Δh|) instead of the original errors (Δh) have to be used. In case of a skew distribution the calculated value is then not influenced and therefore more reliable. Table 2.2 displays the different accuracy measures and their notational expressions. The application of robust accuracy measures is necessary for areas with buildings and vegetation. In such areas occur very often blunders and non-normal error distribution. More details on the robust accuracy measures can be taken from the literature, e.g. (Höhle & Höhle, 2009).

The procedure for the checking of the geometric quality is depicted in Figure 2.4. Firstly we derive the differences between the DEM data and their reference values. A histogram or a Q-Q-plot will tell us whether a normal distribution of the differences (errors) is present. This visual approach can be replaced by numerical methods which will enable a more automated approach. If there are big deviations between the Mean and the Median or the Standard Deviation and the NMAD value, then the robust accuracy measures have to be used as quality measures.

Table 2.2 Robust accuracy measures for vertical errors of DTMs

accuracy measure	error type	notational expression
Median (50% quantile)	Δh	$\hat{Q}_{\Delta h}(0.50) = m_{\Delta h}$
Normalized Median Absolute Deviation	Δh	$NMAD = 1.4826 \cdot median_j(\lvert \Delta h_j - m_{\Delta h} \rvert)$
68.3% quantile	|Δh|	$\hat{Q}_{\lvert \Delta h \rvert}(0.683)$
95% quantile	|Δh|	$\hat{Q}_{\lvert \Delta h \rvert}(0.95)$

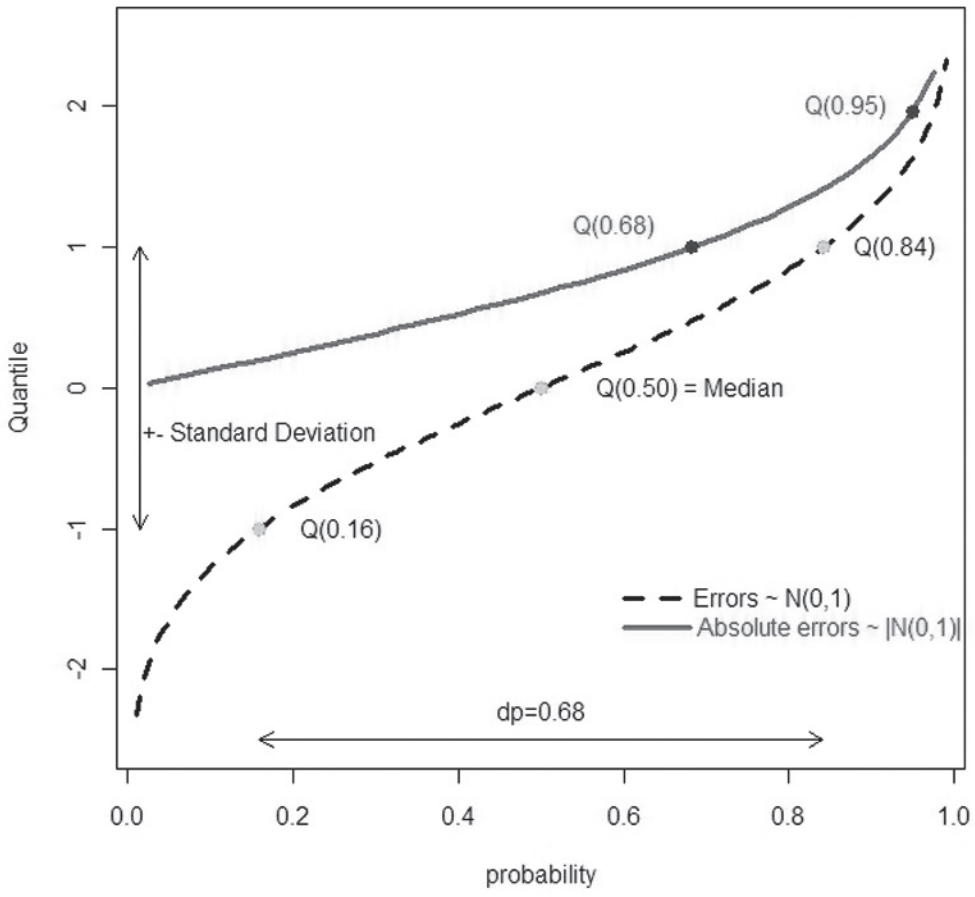

Figure 2.3. Meaning of the robust accuracy measures: Median or $Q_{\Delta h}(0.50)$, $Q_{|\Delta h|}(0.68)$, and $Q_{|\Delta h|}(0.95)$. The quantile function Q(p) for absolute errors (solid line) shows that $Q_{|\Delta h|}(0.68)$ corresponds to 1·σ in case of normal distribution. When original errors (Δh) are used (stippled line) then the difference dp=0.68 corresponds to the quantile range of ±1·Standard Deviation=±1·σ.

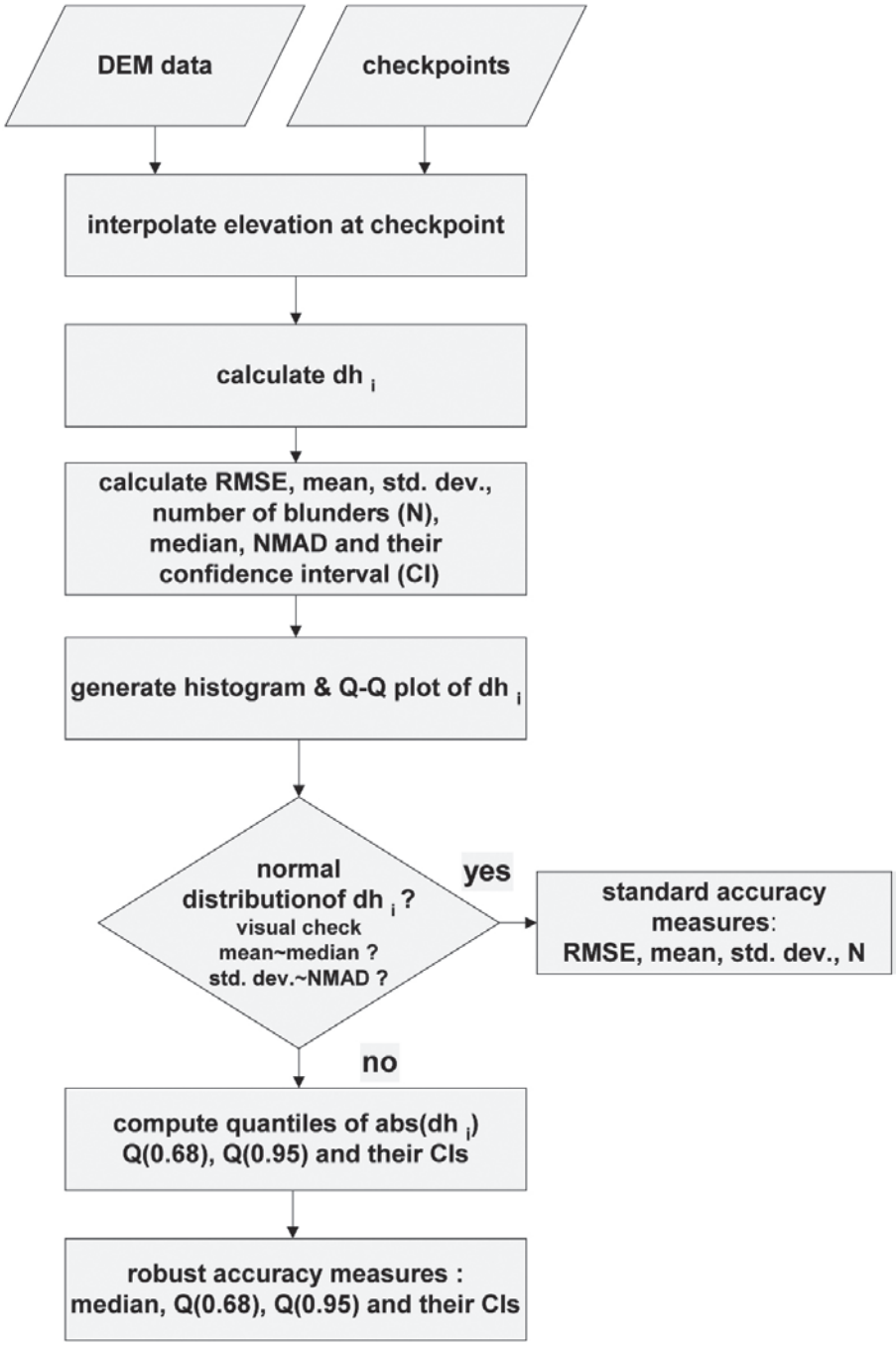

Figure 2.4. Test algorithm for the determination of DTM accuracy measures. It means: RMSE=Root mean square error, std. dev.=Standard deviation, N=number of outliers, NMAD=Normalized Median Absolute Deviation, Q=quantile, CI=confidence interval.

The assessment of the **horizontal (or planimetric) accuracy of DTMs** is more difficult than the assessment of the vertical accuracy. There are different approaches. Some of them are still under investigation.

Special targets can be placed on the ground before the flight. In the case of airborne laser scanning (ALS) the targets have to be of special reflecting materials, with differences in elevation and relatively large in size. This approach is not very practical and also time consuming and thereby expensive. The problem of ALS is that single laser points cannot be recognized in the nature.

Artificial checkpoints can, however, be derived by intersecting planes. Planes can be found on roofs of houses and their mathematical definition is possible by means of several laser points. There are several types of roofs. Some of them are suitable for deriving points from planes (cf. Figure 2.5).

Optimally are so-called hip roofs, where three planes of different slope and exposition exist (cf. Figure 2.6). Three planes intersect to a point. These points can also be measured by manual photogrammetry with superior accuracy. Their coordinates will serve as reference values. More details on this method can be found in (Höhle & Pedersen, 2009).

If such hip roofs do not exist in the area then other houses with a gable roof or cross gable can be used. Manual measurements will then determine lines, their intersection can be computed and the coordinates of the intersected points are used as reference values. The lines can also be derived from the ALS data by intersecting planes. The intersection of the lines can be computed with the same procedure as before.

Instead of manual photogrammetric measurements, the automatic photogrammetric generation of roof points can also be used. The derivation of planes, intersecting of planes and derivation of reference values are carried out with the same procedure as with the laser points. Both co-ordinates are then compared and differences at several houses will lead to the planimetric errors. This approach is relative inexpensive when aerial images with orientation data exist.

The terrestrial derivation of roof planes by means of a few points is then an alternative.

There are some *other approaches* to check the planimetric accuracy of DTM data:

-The manual measurement of house corners in the final DSM or normalized DSM (nDSM) and comparison of the coordinates with accurate map data is a rather simple and fast approach.

-The intensity image, which is at ALS created together with the spatial data, can display paint stripes on asphalt. Their position can be compared with the position derived by ground measurements.

Type of roof	3D graph
gable roof	
hip roof	
cross gable roof	

Figure 2.5. Roof types usable for the derivation of planimetric errors

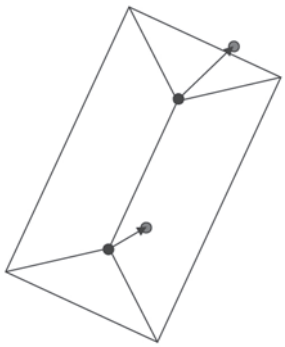

Figure 2.6. Planimetric errors at roof points of hip houses.

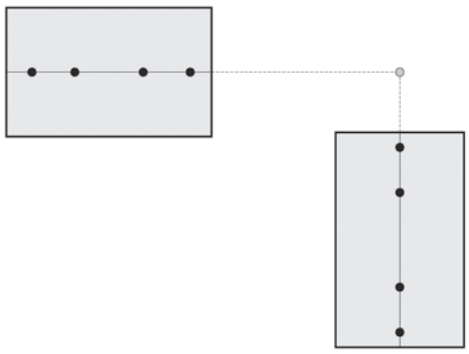

Figure 2.7. Intersecting roof lines (ridges) of two houses. The reference lines are derived from manual photogrammetric measurements (black dots). The ALS data are used to derive the same lines by means of intersection of planes. The intersected point (gray circle) is determined twice. The deviations between the two determinations are a measure of the planimetric accuracy.

Reliable results for the planimetric error with these two methods can only be obtained when the spacing between elevations is smaller than about three times the (manual) measurement error. For example, when measuring points in a DTM/DSM with spacing of 2m, the error of the manual measurements is already 0.67m.

The accuracy of ALS data may also be determined by means of geo-referenced scans of a terrestrial laser scanner. An investigation in this regard has recently been published in (Fowler & Kadatskiy, 2011).

The assessment of the horizontal accuracy has to be carried out by means of a sufficient number of check points of superior accuracy (see details in chapter 2.2.5). They should be distributed over the whole DTM area. The calculation of the accuracy measures (cf. Tables 2.3 and 2.4) is similar as before. The single co-ordinate errors are used to derive point errors (r_i). A plot will show if there are systematic errors present (cf. Figure 2.8).

Table 2.3. Horizontal accuracy measures for DTMs at normal distribution of errors

Number of checkpoints n	
Horizontal error	$\Delta E = E_{DTM} - E_{reference}$ $\Delta N = N_{DTM} - N_{reference}$ $r_i = \sqrt{\Delta E_i^2 + \Delta N_i^2}$
Root Mean Square Error	$\hat{RMSE}_P = \sqrt{\frac{1}{n}\sum_{i=1}^{n} r_i^2}$
Mean error	$\hat{\mu}_E = \frac{1}{n}\sum_{i=1}^{n} \Delta E_i$ $\hat{\mu}_N = \frac{1}{n}\sum_{i=1}^{n} \Delta N_i$
Standard deviation	$\hat{\sigma}_E = \sqrt{\frac{1}{(n-1)}\sum_{i=1}^{n} (\Delta E_i - \hat{\mu}_E)^2}$ $\hat{\sigma}_N = \sqrt{\frac{1}{(n-1)}\sum_{i=1}^{n} (\Delta N_i - \hat{\mu}_N)^2}$
Threshold for outliers	$\lvert r_i \rvert \geq 3 \cdot \hat{RMSE}$
Number of outliers	$n_{outliers}$

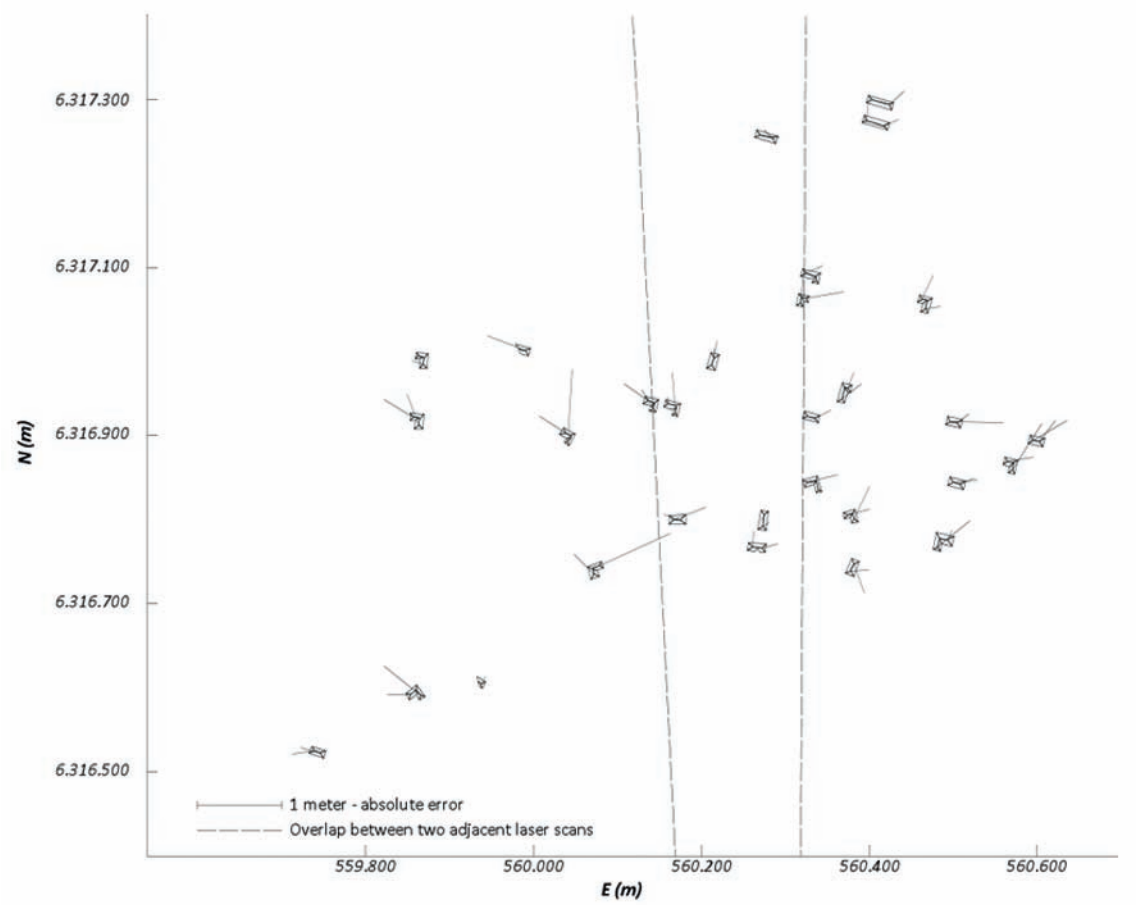

Figure 2.8. Plot of the absolute horizontal errors of an ALS point cloud

The definition of the planimetric error is according:

$$\hat{\sigma}_P \approx \sqrt{\hat{\sigma}_E^2 + \hat{\sigma}_N^2} \qquad (1)$$

This error is named Mean Square Positional Error (MSPE). Other definitions are also used, e.g.

the circular standard error (Circ):

$\sigma_c \approx 0.5 \cdot (\sigma_E + \sigma_N)$ (2)

and the Circular Error Probable (CEP):

$CEP \approx 0.589 \cdot (\sigma_E + \sigma_N)$ (3)

The probability that radial errors (r_i) occur less than σ_p depend on the ratio σ_N / σ_E. If $\sigma_E = \sigma_N$ then the probability is 0.632 or 63.2% (Mikhail & Ackermann, 1976).

The Figure 2.9 shows the different definitions of planimetric errors. The definitions are based on the probability of a bivariate distribution.

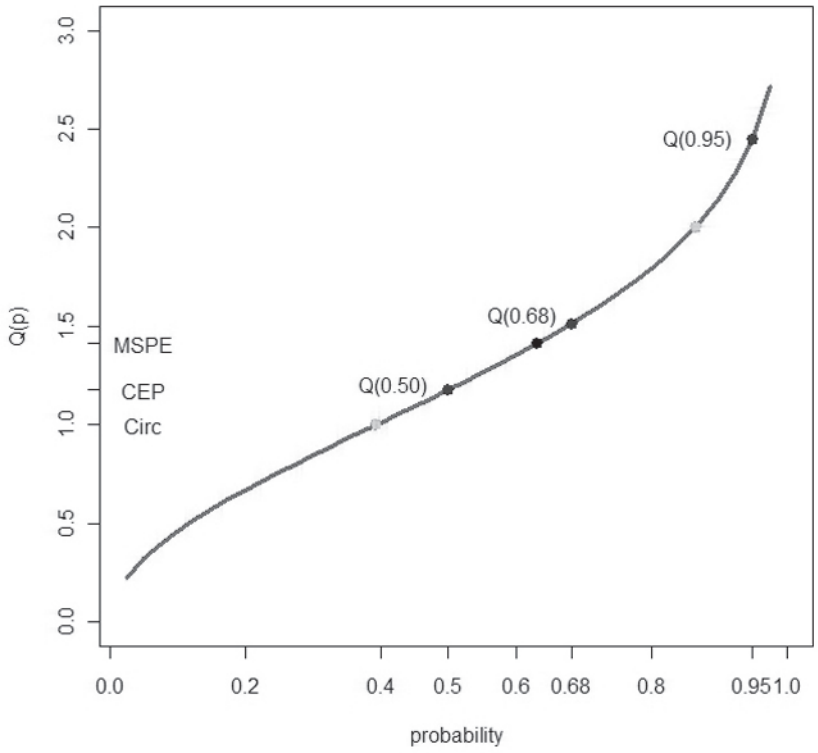

Figure 2.9. Definition of planimetric errors by means of their probability of a bivariate distribution. It means: Circ=Circular Standard Error (σ_c), CEP=Circular Error Probable and MSPE=Mean Square Positional Error (σ_p).

The probabilities depend on the ratio between σ_E and σ_N. The formulae (1)-(3) are therefore approximations. After US standards the approximations can be used if the ratio σ_{min} /σ_{max} is not smaller than 0.2.

Another way to monitor the planimetric accuracy is to plot ellipses of constant probability (cf. Figure 2.10)

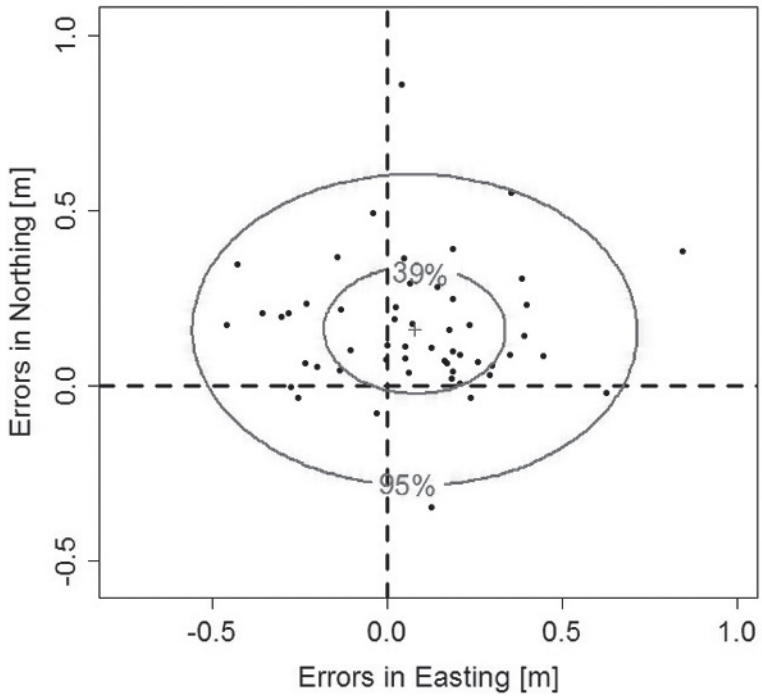

Figure 2.10. Planimetric errors together with the 95% confidence ellipse
The probability is based on bivariate normal distribution were both coordinate errors are considered to be independent and occur jointly.

The histogram or Q-Q plot of the error distribution can also be supplemented. If normal distribution does not exist and big systematic errors are present, then robust accuracy measures have to be applied (cf. Table 2.4).

Table 2.4. Robust accuracy measures for a variable x

Median (50% quantile)	$\hat{Q}_x(0.50) = m_x$
Normalized Median Absolute Deviation	$NMAD=1.4826 \cdot median_i(\lvert x_i - m_x \rvert)$
68.3% quantile	$\hat{Q}_{\lvert x \rvert}(0.683)$
95% quantile	$\hat{Q}_{\lvert x \rvert}(0.95)$

The Median, NMAD, Q(0.683), and Q(0.95) are calculated for each coordinate and the unbiased radius (r_i'). This radius is derived for each point by:

$$r_i' = \sqrt{(\Delta E_i - \mu_E)^2 + (\Delta N_i - \mu_N)^2}$$

The NMAD value for the radii (r and r' respectively) is calculated for a bivariate distribution.

$NMAD_r = 0.8496 \cdot median_i(|r_i - m_r|)$

$NMAD_r$ is based on a probability of p=0.393 only (Höhle 2011).

2.2.5 Some details

Some important details have to be supplemented in order carry out the assessment of the DTM accuracy. These are the required accuracy of the reference values, the number of the checkpoints and the confidence interval of the accuracy measures.

The **accuracy of the reference values** (checkpoints) should be more accurate than the DTM elevations being evaluated. By using the formula for error propagation the influence on the DTM accuracy can be estimated:

$$\sigma^2_{DTM-REF} = \sigma^2_{DTM} + \sigma^2_{REF} \qquad (2.1)$$

If the total DTM accuracy ($\sigma_{DTM\text{-}REF}$) may be incorrect by 5%, the accuracy of the reference should be $\sigma_{REF} \approx \frac{1}{3} \cdot \sigma_{DTM}$. For example, if the accuracy of a DTM is specified with σ=10cm then the checkpoints should have an accuracy of $\sigma \leq 3.3$cm.

An important issue is the spatial distribution of the checkpoints: They should be distributed randomly. If checkpoints are positioned along break lines, at steep slopes, at positions of sudden slope change, close to buildings, etc., large errors may be found.

The **number of checkpoints** (also known as sample size) should be sufficiently large in order to obtain reliable accuracy measures.

For the normal distribution a statistical test can be used in order to derive the sample size. The result of the test for a DTM specification with σ_{spec} = 10cm is depicted in Figure 2.11 from which the required sample size can be taken. More explanations are given in (Höhle & Höhle, 2010).

At non-normal error distribution the number of checkpoints should be higher. An approximate formula for the sample size is given in (Desu & Raghavarao, 1990). With a comparable formulation as used in the normal setting, one obtains a sample size of n=110 to prove that the 68.3% quantile of the error distribution is below 10cm.

The American Society of Photogrammetry and Remote Sensing (ASPRS) recommends a minimum of 20 checkpoints in each of the major land cover categories. In the case of three landcover classes (e.g. open terrain, forested areas, and urban areas) a minimum of n=60 checkpoints are required.

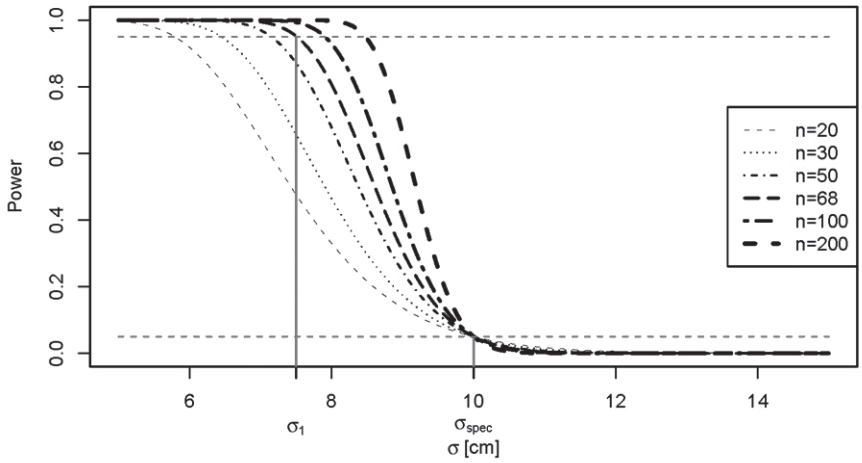

Figure 2.11. Required sample size (n) that a specified standard deviation (σ_{spec}) is not exceeded. A probability (Power) of 95% is achieved when the calculated standard deviation σ_1=7.5cm is determined by means of n=68 checkpoints. In order to reject the null hypothesis, H_o: $\sigma = \sigma_{spec}$, at higher values of σ than 7.5cm and the same probability, a higher number of checkpoints has to be measured.

In a statistical context all estimates should be supplied by measures quantifying the uncertainty of the estimator due to estimation from a finite sample. One way to achieve this is to supply with each point estimator a **confidence interval** (CI) with a certain coverage probability. For example, a 95% CI [c_1, c_2] for the sample Mean says that in 95% of the cases the interval [c_1, c_2] contains the true but unknown Mean of the error distribution.

In the standard literature of the error theory, e.g. (Mikhail & Ackermann, 1976), we can find the formulae for the 95% CI for the parameters "Mean" and "Variance". It requires statistical tables for the "Student t Density Function" and the "Chi-Square Function" respectively.

$$p\left\{\bar{x} - t_{\alpha/2,n-1}\cdot\frac{s}{\sqrt{n}} < \mu < \bar{x} + t_{\alpha/2,n-1}\cdot\frac{s}{\sqrt{n}}\right\} = (1-\alpha) \qquad (2.2)$$

$$p\left\{\frac{ms^2}{\chi^2_{\alpha/2,n-1}} < \sigma^2 < \frac{ms^2}{\chi^2_{1-\alpha/2,n-1}}\right\} = (1-\alpha)$$

where: p=probability, μ=Mean of population, x=Mean of sample, (1-α)=confidence level, $t_{\alpha 2,\,n-1}$=Student *t* Density Function, s=standard deviation of sample, n=number of checkpoints, σ^2=variance of population, s^2=variance of sample, $\chi^2_{\alpha 2,m}$=Chi-Square Function, m=(n-1)=degrees of freedom

The CI for the standard deviation (σ) is obtained by taking the square root of each site on the interval of the variance.

Example 2.2. For the given data the confidence intervals for the Mean and for the Standard Deviation are the following:

Data:
0.09, 0.51, 0.47, 0.70, 1.23, 1.30, 1.34, 0.70, 1.04, 1.44, 1.49, 1.00, 1.24,
1.34, 1.44, 1.61, 1.44, 0.79, 5.52, 1.73

CI for the Mean:
n=20, $\bar{x}$ =1.32, s=1.08, α=0.05:
$t_{\alpha/2,\ n-1}$=2.09 (taken from the table for the Student t Density Function*)
P[1.32-2.09·1.08/√20<μ<1.32+2.09·1.08/√20]=0.95
95%CI [0.81, 1.83]

CI for the Standard Deviation.
m=19, s=1.08, α=0.05
$\chi^2_{\alpha/2,\ n-1}$=32.85, $\chi^2_{1-\alpha/2,m}$=8.91 (taken from the table for the Chi-Square Function*)
p[19·1.082/32.85<σ2<19·1.082/8.91]=0.95
p[0.67<σ^2<2.49]=0.95
p[0.82<σ<1.58]=0.95
95%CI [0.82, 1.58]

The sample has a blunder (Δh_{19}=5.52m), which should be detected (by means of a threshold) and removed. The confidence intervals are then much smaller:

CI for the Mean:
n=19, $\bar{x}$=1.10, s=0.44, α=0.05:
$t_{\alpha/2,\ n-1}$ =2.10
p[1.10-2.10·0.44/√19<μ<1.10+2.10·0.44/√19]=0.95
95%CI [0.89, 1.31]

CI for the Standard Deviation.
m=18, s=0.44, α=0.05
$\chi^2_{\alpha/2,m}$=31.53, $\chi^2_{1-\alpha/2,m}$=8.23
p[18·0.442/31.53<σ2<18·0.442/8.23]=0.95
p[0.11<σ^2<0.42]=0.95
p[0.33<σ<0.65]=0.95
95%CI [0.33, 0.66]

The solution can also be found by means of a program. An R-program is given in Table 2.6.

*Such tables are contained in the standard books of statistics, e.g. in (Fahrmeir et al., 2007), (Mikhail & Ackermann, 1976).

The confidence interval can also be used to estimate the required number of checkpoints (n). For example, the CI for the Mean

$$\bar{x} \pm d$$
$$d = z \cdot (1 - \alpha / 2) \cdot \frac{s}{\sqrt{n}}$$
$$n = (z \cdot (1 - \alpha / 2))^2 \cdot s^2 / d^2$$

where

z=quantile of the probability range dp=1-α/2, d=confidence interval, $\bar{x}$ =Mean, s=standard deviation.

If d=0,2· $\bar{x}$ and α=0.05

$$n = (1.96)^2 \cdot s^2 / (0.2 \cdot \bar{x})^2$$

Example 2.3

For $\bar{x}$ =1.10m, s=0.44m, and α=0.05 (values from above):

In order to achieve at the 95% probability level a confidence interval of 20% of the Mean $\bar{x}$ =(1.10 ± 0.22)m, the sample should comprise n=16 checkpoints.

These calculations of the confidence interval require that the distribution of errors is normal. In the case of non-normal distribution of errors we may use the bootstrap approach to assess the uncertainty of the sample quantiles as estimators of the true quantiles of the underlying distribution. Here one draws a sample of size n with replacement from the available data $\{x_1,...,x_n\}$ and then uses this new sample to compute the desired Q(p). This procedure is repeated a sufficiently large number of m times, for example m=999. A bootstrap based 95% confidence interval of Q(p) can then be obtained as the interval from the 2.5% to the 97.5% sample quantiles of the 1000 available values $\{Q(p), Q_1(p), ..., Q_{999}(p)\}$. The calculation of the confidence intervals for robust accuracy measures is carried out by means of a program. An example is given in Table 2.8.

The vertical DTM errors are influenced by the horizontal error in **areas with slope**. In airborne laser scanning, for example, the planimetric errors can be relatively high. The resulting elevation error is estimated by equation (2.3).

$$\Delta h = \Delta p \cdot \tan\alpha \qquad (2.3)$$

In an area with 30° slope and a horizontal error of Δp=1m, for example, the elevation error amounts to $\Delta h = 1.0m \cdot \frac{\sqrt{3}}{3} = 0.58m$. Small planimetric errors are, therefore, necessary in order to have a high vertical accuracy.

Characteristics of checkpoints

The checkpoints (CPs) have to be distributed randomly in each class of terrain. They should not be placed on break lines of the terrain and in the very neighborhood of buildings. There are big differences to expect when the DTM has planimetric errors.

If airborne laser scanning is used as data acquisition method, the characteristics of the CPs (material, height) are also defined. In the US FEMA guidelines, for example, the testing in "open terrain" will be performed using CPs on sand, rock and/or short vegetation up to 15cm in height. Testing in "built-up areas" will be performed on asphalt or concrete surfaces. The testing in "forests" should occur with trees taller than 1.8m. In data acquisition by photogrammetry, the CPs should be independent, i.e. not be used as observations in the bundle adjustment.

Probability level 95%

The Root Mean Square Error (RMSE) and the standard deviation (σ) are used in Europe as accuracy measures. They are based on 68.3% probability at normal distribution of errors. In some specifications, e.g. the National Standard for Spatial Data Accuracy (NSSDA) of the USA, the 95% probability level is used for the derivation of accuracy measures. Then, only 5% of the errors may be bigger than this value. In order to convert from 68.3% probability to the 95% probability a factor has to be applied. The new value is then called "Accuracy".

$$Accuracy_Z = 1.9600 \cdot RMSE_Z$$

$$Accuracy_r = 1.7308 \cdot RMSE_r$$

The same factors are used for the standard deviation. A 95% probability level means that a single elevation error would be within the interval [Mean error-1.96·σ, Mean error+1.96·σ]. The definition of the horizontal error (σ_p) as in Table 2.3 requires that $\sigma_x \approx \sigma_y$. If there are differences between the two values, then the probability will differ and with it the factor (1.7308).

2.2.6 Completeness of the DTM

The DTM should have a complete regular grid. The data acquisition may have gaps and elevations are removed in the filtering process. Such areas are filled by interpolation using surrounding points. A maximum 'gap distance' is specified (e.g. 3 times the grid width). If this threshold is exceeded then void areas will exist in the DTM. The areas of these data-free zones can be determined. The percentage of the sum of all areas is a measure of the completeness.

If the user has access to the original data then **other quality parameters** can be determined.

The *density* of the original data is such a quality measure. An average figure can be derived. Of interest is also a density plot (cf. Figure 2.12).

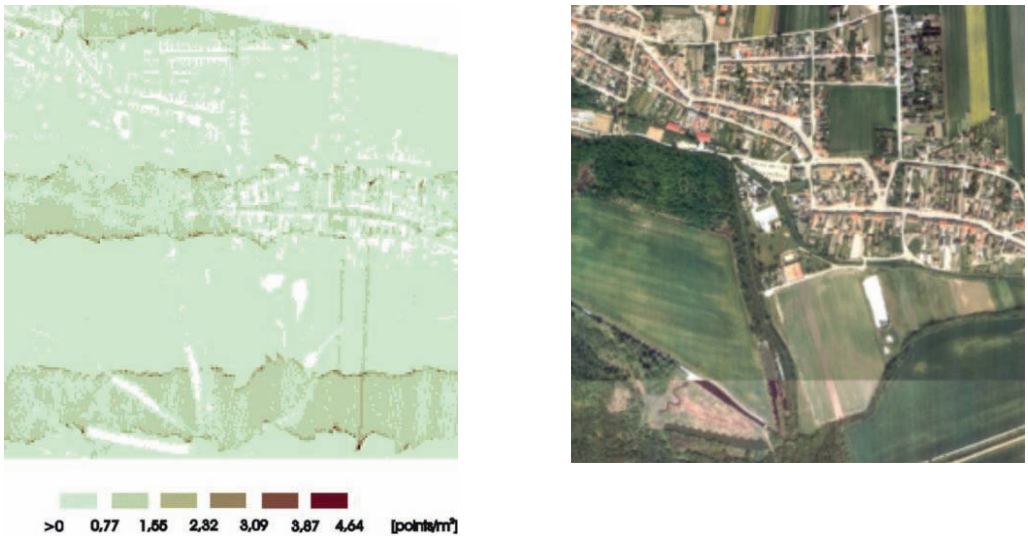

Figure 2.12. Density plot of ALS data (left) together with an orthophoto (right) of the same area. Source: Karel & Kraus, 2006.

The distance between each grid point of the DTM and the terrain point next to it is another quality parameter. If a certain threshold is exceeded, the elevation of the grid point is not very useful.

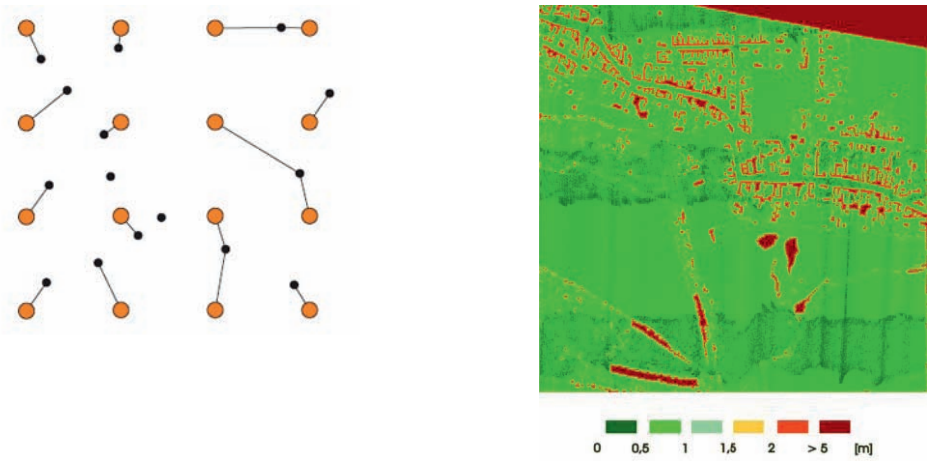

Figure 2.13. Distances between grid points and terrain points. A plot can be generated, which shows areas of different classes in distance. The dark areas are very likely the areas with inaccurate elevations. Source: Karel & Kraus, 2006

2.2.7 Metadata

Metadata describe the dataset and include information on the DTM quality. General information and how to use the data correctly is, for example:

- date of the acquisition (date and time)flight lines
- horizontal datum and projection
- vertical datum
- units
- post spacing (resolution)
- extension of the data (tile size)

Information on the quality of the data is, for example:

- accuracy of the data (horizontal and vertical)
- information on the error distribution (histogram, Q-Q plot)
- number of outliers
- percentage of the areas without data

Besides the metadata other information can be found in the "Deliverables" when the work is outsourced and a written contract is available. The National mapping agency has then the task to carry out the checking of the delivery and to manage the quality assurance. Steps are then taken to check and to improve the quality of the delivered DTM data. Such improvement of the quality of the delivered data is described in the next chapter. It may require additional data (point cloud data, intensity images of ALS, photogrammetric images), which a DTM user normally has no access to it. For special applications the DTM data may also have to be supplemented or reduced in order to be "fit for the purpose". This work is briefly described in the next chapter.

2.3 Improving the quality of DTMs

2.3.1 Improvement of the accuracy

In the overlap areas of the ALS strips differences can be observed and adjusted. The relative accuracy of the DTM can then be improved. Because only smooth surfaces are suitable, a 'roughness mask' is used at each strip. From the remaining data several tilted planes are derived which will be used to connect the strips. The strip adjustment can include also ground control planes, which then improves the absolute accuracy of the DTM derived by ALS. Figure 2.14 depicts the differences in the overlap area between to strips before and after the strip adjustment.

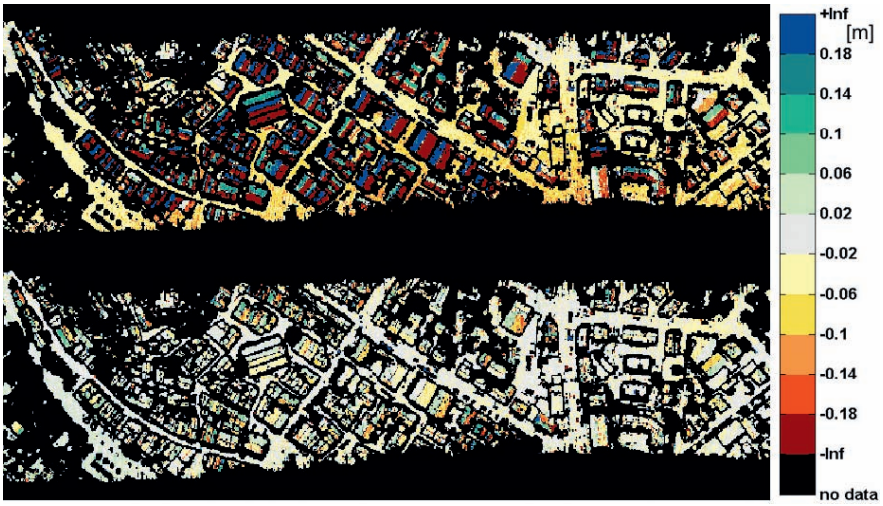

Figure 2.14. Example of a colour-coded strip difference for the original (top) and for the improved georeferencing after strip adjustment (bottom). Right: Legend of colour coding. Black is used for the area outside the overlap of two neighbouring strips, but also for the parts covered by the 'roughness mask'. Taken from (Haala et al., 2010).

The use of topographic maps can help to detect errors and blunders in the dataset. All elevations inside lakes have to have the same elevation equal to the water level. The elevations on the shoreline of creeks and rivers should decrease. Elevations inside buildings should be removed because they do not represent the terrain (cf. Figure 2.15).

Figure 2.15. Result of the filtering and removing of points within the outlines of buildings.
It means: Remaining elevation points (gray), check points (black), buildings and roads (black lines).

If the quality of the DTM is of superior quality, then it can serve as a reference for the checking of DTMs at **all** DTM posts. The derived errors may be used as corrections and an improved DTM can be generated. It may be done by combining both DTMs or just by replacing the outdated part with the new one. This updating of existing DTMs will be further discussed in chapter 3.

2.3.2 Improvement of the completeness

The DTM should cover the whole area with valid elevations. Missing areas (e.g. without return signal or correlation, gaps in the flying, etc.) can be detected by means of topographic maps and/or orthophotos. Interpolation with the remaining points can close smaller gaps if the gap distance does not exceed a threshold (e.g. 3 times the grid spacing). In such a case, new data acquisition has to be carried out to fill the gaps. Other data collection methods, e.g. stereo-photogrammetry, ground surveying, may be considered.

Other data have to be supplemented in order to adapt the DTM to a special application. This can also be a thinning of the DTM.

2.4 Visualization of the quality

The quality of the DTM is best presented graphically. In this text some of the quality features were already visualized (error distribution, absolute horizontal errors, point density, differences between adjacent ALS strips, and result of filtering on top of a topographic map). Other possibilities for visualizing problem areas in the DTM are:

- 2D plot of color coded elevations
- contour lines on top of an orthophoto (cf. Figure 2.16)
- perspective view with color coding of the elevations (cf. Figure 2.17)
- profiles with color coding of the DTM elevations (cf. Figure 2.18)

A very good possibility to detect errors within the DTM is stereo viewing. The DTM can be overlaid on top of stereo-pairs and differences between the stereo model and the DTM can be recognized by an operator.

With all of the mentioned visualizations a visual control can be carried out. Errors, gaps and artifacts can easily be detected. The editing of the data requires special tools. Commercial hardware and software have recently been developed and will be mentioned in the next chapter.

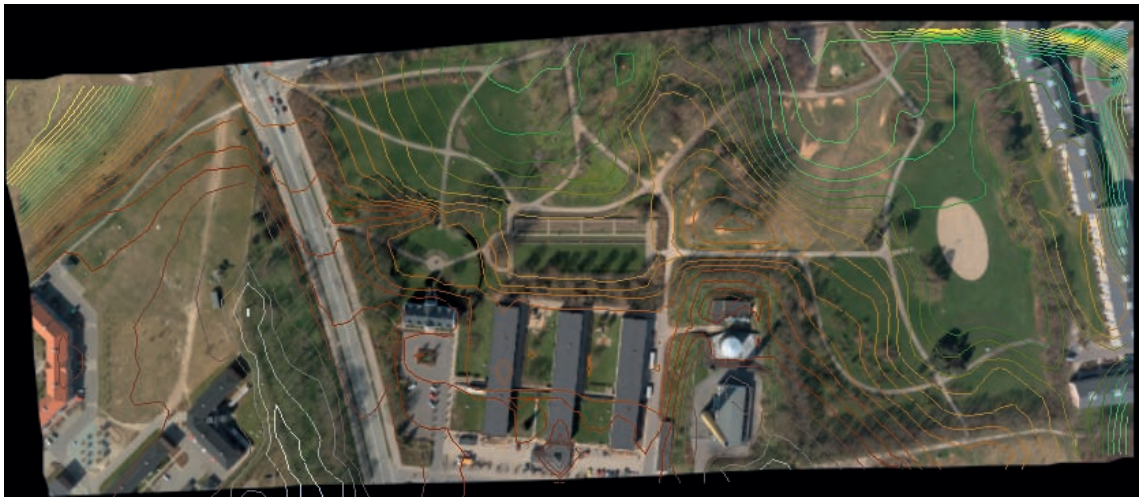

Figure 2.16. Contour lines on top of orthophoto

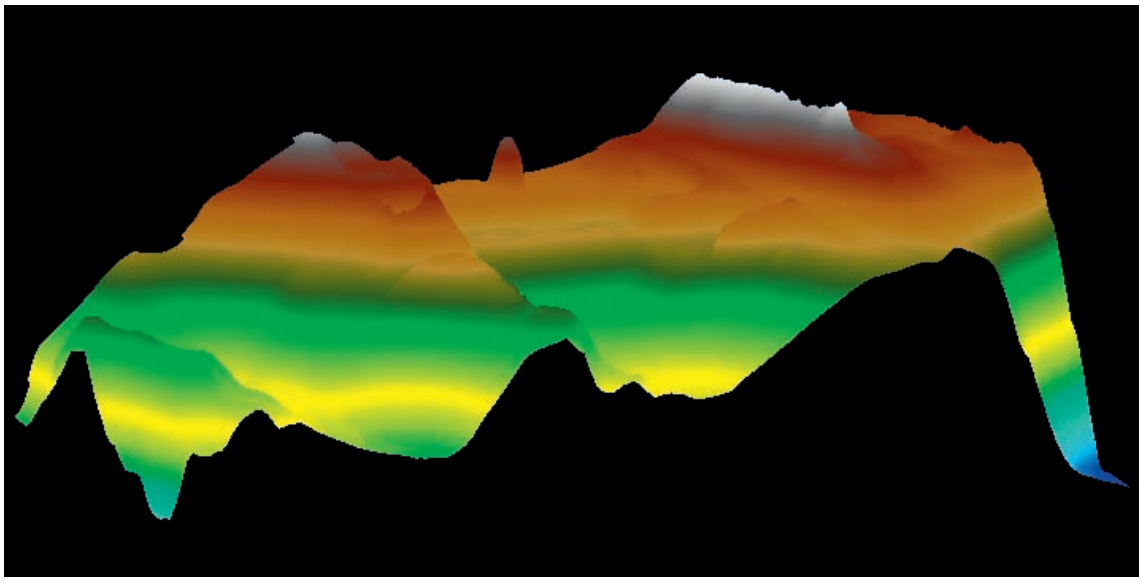

Figure 2.17. Perspective view of DEM (color-coded)

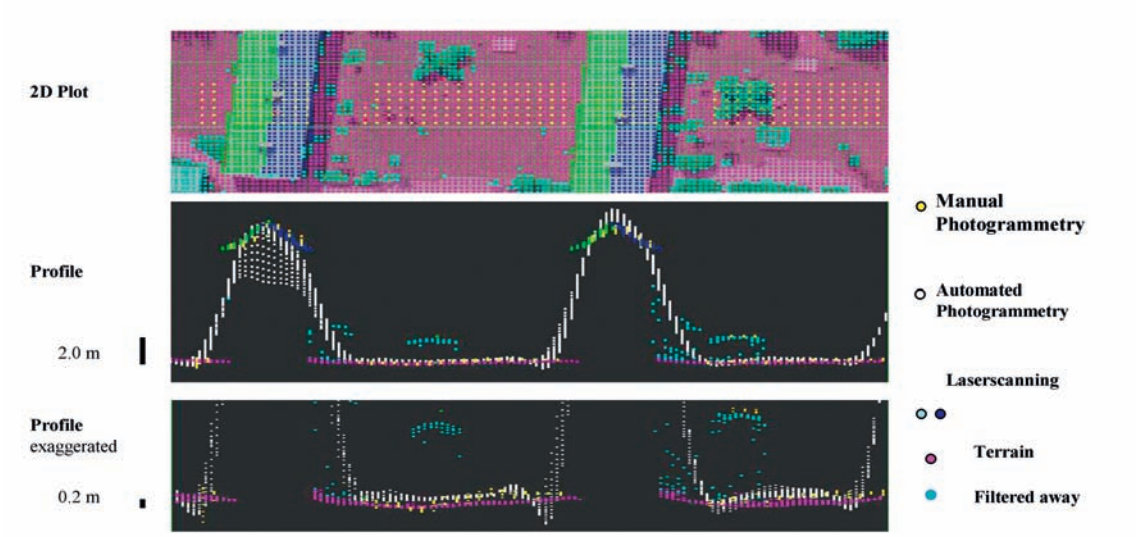

Figure 2.18. Profiles of elevation data from different acquisition systems

Figure 2.19. Editing of DTM data by means of a photogrammetric workstation with stereo display

2.5 Tools for the checking, completion and visualization

The checking, completion and visualization of DTMs require various tools which fulfill the required tasks correctly and economically. These tools comprise photogrammetric stereo workstations, editing stations and software packages.

2.5.1 Photogrammetric stereo workstations

Photogrammetric workstations enable stereo-vision. Intergraphs “Image Station”, for example, includes software packages for stereo display, 3D mapping, aerotriangulation, and DTM data collection. Break lines and shore lines can be added using the 3D mouse (cf. Figure 2.19). The DTM data, e.g. represented as contour lines, can be superimposed onto the stereo-model.

2.5.2 Editing stations

Editing stations are used for the display, correction and supplementing of DTMs. Other data (maps, orthophotos) can be imported and used together with DTM data.

An example of such a DTM editor is DTMaster program of Inpho GmbH, Germany. There are two versions of the program, DTMaster Stereo and DTMaster for monoscopic measurements. The use of the stereo vision enables efficient editing of the DTMs as well as 3D data collection. The program integrates photogrammetry, handling of DTMs and map/orthophoto data for the tasks of editing, supplementing and quality control. A DTM toolkit allows for merging, splitting and format change. The program ApplicationsMaster is used for in- and output and for control of various programs.

2.5.3 Software packages

There exist numerous software packages. In the following examples of companies, research institutes and state organizations will be characterized.

Programs of Terrasolid Ltd., Finland

The suite of programs of Terrasolid (TerraModeller, TerraScan, TerraPhoto, TerraMatch, TerraScan Viewer) enable the processing of raw laser **and** image data. The combination with images enables accurate and reliable results. For example, the validating of the planimetric position of laser points can be seen at high intensity paint markings on asphalt. Such objects will show up as linear features in the laser data and can be matched to field measurements. Discrepancies between field measurements and laser data will be visible in images (cf. Figure 2.20) and can then be removed. Vertical accuracy measures (Mean and standard deviation) are automatically determined and if systematic errors are present, the laser data will be corrected.

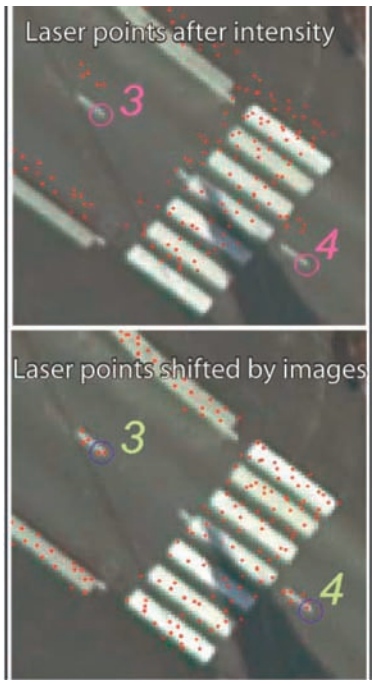

Figure 2.20.
Checking of planimetric accuracy
by means of high intensity road markings.

Source: Terrasolid Ltd.

Programs of the Institute of Photogrammetry and Remote Sensing, TU Vienna

An extensive program system for computation and utilization of DTMs is SCOP. It can handle large projects and can derive elevations by a variety of interpolation methods. It generates contour lines of high cartographic quality, orthoimages, slope and visibility maps. The architecture of the SCOP++ is shown in Figure 2.21. All programs can be controlled by means of simple commands or via menus. Generation of the DTM by means of surface-based filters (cf. chapter 1.3.2) is also part of the program package.

Programs of the National Mapping Agency, Denmark

-PINGPONG

The program derives from the original point cloud a grid of elevations and the distance between the grid point and the nearest point of the point cloud. Also the density of the original point cloud is determined. (The graphic representation of the results corresponds to Figure 2.13 and Figure 2.12 respectively). Details can be found in (Knudsen, 2008).

-DETECTION OF HORIZONTAL OFFSETS

The program determines from point clouds and a dense net of reference points the parameters of a 3D transformation. Also the Mean Absolute Error and the RMS error of the elevations are determined. The reference data should have enough features to distinguish the area from the surrounding terrain. Such features are edges, ridges and pointy hills. Plots of the histograms and graphs depicting the position of reference data within the DTM can be generated.

Both programs are announced as free and open source.

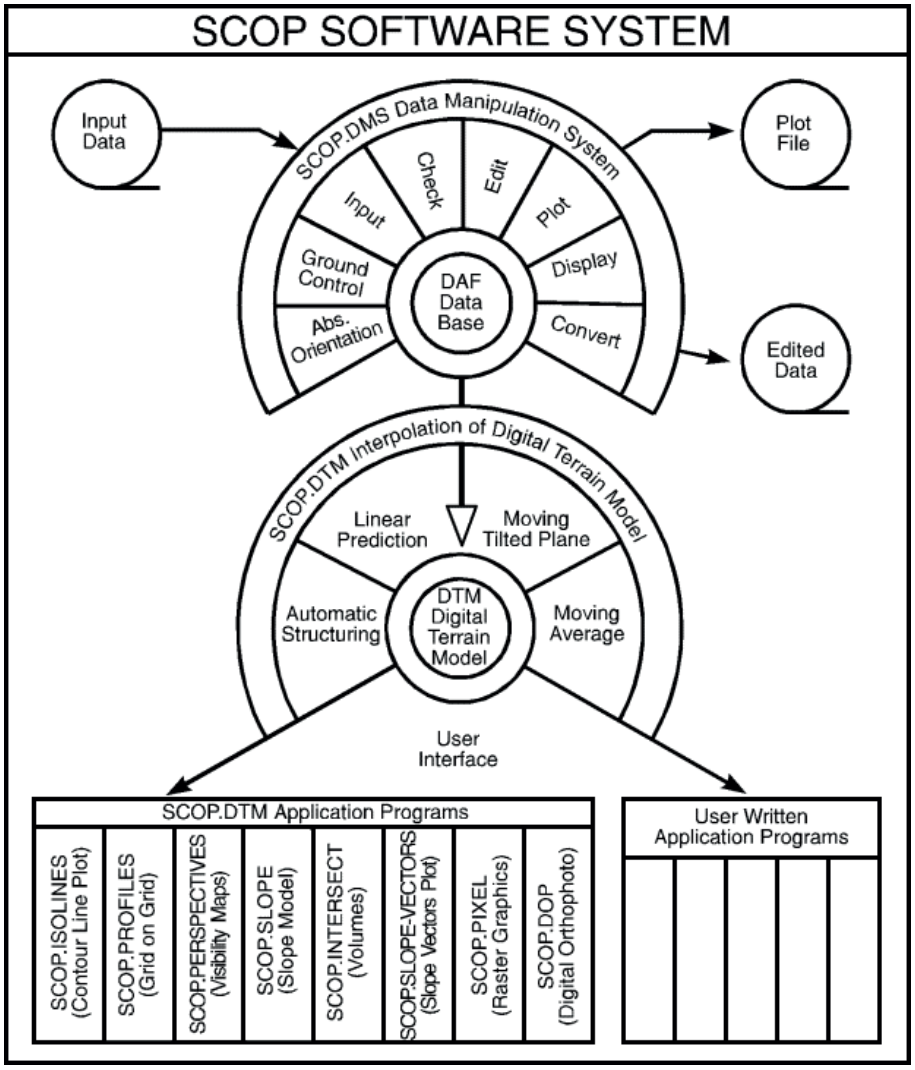

Figure 2.21 Main modules of the 'SCOP++' DTM software system
Source: Institute of Photogrammetry and Remote Sensing, TU Vienna)

2.6 Tools for the calculation accuracy measures

2.6.1 Use of statistical functions in MS EXCEL

The calculation of accuracy measures of samples can be carried out by means of table programs such as MS EXCEL. For a set of data the tool 'Data Analysis' can be started and accuracy measures such as Mean, Standard Deviation, Median and Confidence Interval can be computed. Also a histogram can be created. The result of the function 'Descriptive Statistics' is displayed in Table 2.4.*

*The data are the same as in example 2.1. The blunder (Δh_{19}), however, has been removed from the sample).

Table 2.4. Result of data analysis in MS EXCEL (2003)

Mean	1,10
Standard Error	0,10
Median	1,24
Mode	1,44
Standard Deviation	0,44
Sample Variance	0,20
Kurtosis	-0,21
Skewness	-0,74
Range	1,64
Minimum	0,09
Maximum	1,73
Sum	20,90
Count	19
ConfidenceLevel(95%)	0,21

The 95% confidence interval for the Mean of the population is calculated with $\mu=1.10\pm0.21$m. In contrast to the formula (2.2) the standard normal density function is applied instead of the student density function. This is an approximation, which is justified when the number of deviations (count) is higher than 30.

2.6.2 Use of the statistical computing environment "R"

Statistical computing may be carried out by programs. The language "R", for example, became popular because it is 'open source' and thus available as free software. Furthermore, there are many statistical and graphical functions available. Densities such as the normal or the student density are easily available and a large number of extension packages provide functionality for almost every sort of statistical analysis. Detailed information can be found at (R Development Core Team, 2008).

An editor for R-language can also be used, e.g. Tinn-R (see at: http://www.sciviews.org/). Examples are given in Table 2.6, 2.7, and 2.8. The plots in Figures 2.3, 2.9 and 2.10 are also produced by means of a program in "R".

Table 2.6. Calculation of the 95% confidence interval (CI) for "Mean" and "Std.Dev."

R-program
x<- c(0.09, 0.51, 0.47, 0.70, 1.23, 1.30, 1.34, 0.70, 1.04, 1.44, 1.49, 1.00, 1.24, 1.34, 1.44, 1.61, 1.44, 0.79, 1.73) alpha<-0.05 n<-length(x) xm<-mean(x) s<-sd(x) lower_limit= (xm-qt(1-alpha/2,n-1)*s/sqrt(n)) upper_limit =(xm+qt(1-alpha/2,n-1)*s/sqrt(n)) confidence_interval<-c(lower_limit, upper_limit) upper_limit_s=sqrt((n-1)*s^2/(qchisq(0.025, df=18))) lower_limit_s=sqrt((n-1)*s^2/(qchisq(0.975, df=18))) confidence_interval_s<-c(lower_limit_s, upper_limit_s) cat("Mean=",xm,"95% CI=","[",confidence_interval,"]",sep=" ", "\n") cat("Std.Dev.=",s,"95% CI=","[",confidence_interval_s,"]",sep=" ", "\n")
Result
Mean= 1.10, 95% CI= [0.89, 1.31] Std.Dev.= 0.44, 95% CI= [0.34, 0.66]

Table 2.7. Generation of a QQ-plot

R-program

#data
de<-c(0, 0.064, 0.186, -0.2, 0.39, 0.126, 0.208, 0.187, 0.398, 0.163, 0.291, 0.127, 0.625, 0.184, 0.142, 0.206,
0.135, -0.283, 0.061, -0.032, 0.299, 0.354, 0.049, -0.43, -0.276,
-0.105, 0.237, 0.17, 0.024, 0.175, 0.07, 0.235, -0.461, 0.042, -0.302, 0.187, 0.019, 0.843,
-0.231, -0.237, -0.255, -0.136, -0.142, -0.359, 0.446, 0.048, 0.349, 0.188, 0.259, 0.049, 0.384, -0.042, -0.003)
#qq-plot
qqnorm(de, main="Normal Q-Q plot"); qqline(de)

Result: 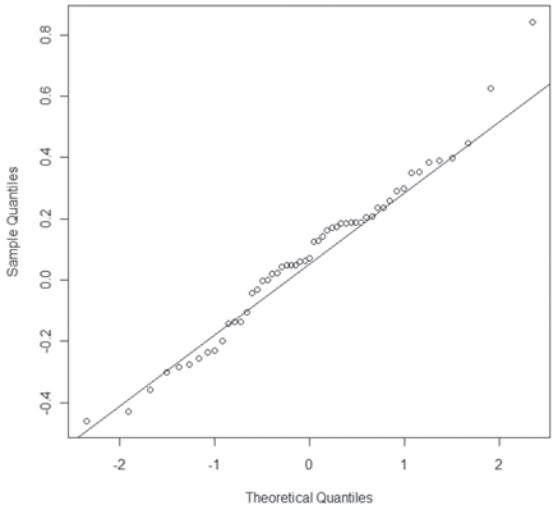   Figure 2.22. Q-Q plot

Table 2.8 Calculation of robust accuracy measures with their confidence intervals

R-program

```
# Bootstrap function (written by M. Höhle)
myboot <- function(f,val,R=999) {
   #Prepare
   t0 <- t(as.matrix( f(rep(val[,1], times=val[,2]))))
   t <- matrix(NA,nrow=R,ncol=ncol(t0))
   #Boot it
   for (i in 1:nrow(t)) {
      t[i,] <- f(sample(val[,1], size=nrow(val), replace=TRUE, prob=val[,2]))
   }
   ci <- apply( rbind(t,t0), MARGIN=2, quantile, p=c(0.025, 0.975))
   dimnames(ci) <- list(c("lower","upper"), colnames(t0))
   colnames(t) <- colnames(t0)
   return(list(t0=t0,t=t,perc.ci=ci))
}
#input of data
 points<-read.table("data_dz.txt", col.names="dz")
 print(points$dz)
 print(sprintf("========== Robust accuracy measures ============\n"))
#Standard errors of the sample quantiles
 dz.table <- table(points$dz)
 weights <- as.numeric(dz.table)
 val <- cbind(as.numeric(names(dz.table)), weights)
#Bootstrap
 f <-function(x) {
    c(Median=median(x),NMAD=mad(x),quantile(abs(x), p=c(pnorm(1)-pnorm(-1), 0.95)))
 }
 qboot <- myboot(f,val,R=999)
 print(qboot$t0)
 print(qboot$perc.ci)
```

Input data ("data_dz.txt")

```
  [1] 0.167 0.141 0.191 0.027 0.171 0.161 0.084 0.569 -0.073 -0.059 0.562 0.262 0.024
 [14] 0.143 0.433 0.230 -0.012 0.326 0.028 0.199 0.264 0.253 -0.087 0.243 0.166 0.303
 [27] 0.269 0.318 0.033 0.271 0.042 0.092 0.198 0.188 0.078 0.252 0.327 0.174 0.104
 [40] 0.138 0.042 0.023 0.224 0.216 0.130 0.290 0.098 0.018 0.105 0.133 -0.001 0.479
 [53] 0.524 0.346 0.167 0.027 0.141 0.165 0.064 0.380 -0.171 0.020 0.334 0.085 0.087
 [66] 0.236 0.166 0.053 0.089 0.193 0.271 0.346 0.208 0.217 0.178 0.296 0.099 0.307
 [79] 0.347 0.584 0.050 -0.093 0.100 0.057 0.205 0.048 0.077 0.016 0.172 0.155 -0.058
 [92] 0.239 0.240 0.590 0.310 -0.091 0.281 0.350 0.178 0.360 0.337 0.236 0.224 -0.095
[105] 0.138 0.234 0.281 0.133 0.059 0.181 -0.016 0.126 0.146 0.226 0.460 0.205 0.271
[118] 0.439 0.406 0.383 0.287 0.032 0.159 0.050 0.025 0.071 0.128 0.196 0.257 0.021
[131] 0.069 0.170 0.143 0.233 0.124 -0.118 0.194 0.133 0.014 0.040 0.377 0.361 -0.069
[144] 0.308
```

Result

	Median	NMAD	68.3%	95%
[1,]	0.1685	0.1504839	0.236	0.4381
lower	0.141	0.1193493	0.2010171	0.350
upper	0.197	0.1794131	0.2710000	0.562

2.7 References

Bayer, N., Potuckova, M., Höhle, J., 2009. Automated checking methods of the Digital Terrain Models based on TIN, Proceedings of 29th conference on geometry and computer graphics (JCMF 2009), Doubice/CR, pp. 69-81, ISBN 80-86195-61-9

Desu, M., M., Raghavarao, D., 1990. Sample size methodology. Academic Press, Inc.

Fahrmeir, L., Künstler, R., Piegeot, I., Tutz, G., 2007. Statistik, ISBN 978-4-540-69713-8, Springer, 610p.

Fowler, A., Kadatskiy, V., 2011. Accuracy and Error Assessment of Terrestrial, Mobile and Airborne Lidar, proceedings of "ILMF 2011", New Orleans/USA, 10p.

Haala, N., Hastedt, H., Wolf, K., Ressl, C., Baltrusch, S., 2010. Digital Photogrammetric Camera Evaluation – Generation of Digital Elevation Models, Photogrammetrie, Fernerkundung, Geoinformation (PFG), nr. 2, pp. 99-116

Höhle, J., Potuckova, M., 2005. Automated Quality Control for Orthoimages and DEMs, Photogrammetric Engineering and Remote Sensing, Vol. 7, no. 1, pp. 81-87

Höhle, J., 2009. DEM generation using a digital large format frame camera, Photogrammetric Engineering & Remote Sensing, vol. 75, no. 1, pp. 87-93

Höhle, J., Höhle, M., 2009. Accuracy assessment of digital elevation models by means of robust statistical methods, ISPRS Journal of Photogrammetry and Remote Sensing, vol. 64, issue 4, pp. 398-406

Höhle, J., Pedersen, C., Ø., 2009. A new method for checking the planimetric accuracy of Digital Elevation Models derived by Airborne Laser Scanning, proceedings of "Accuracy 2010, Leicester/UK, pp. 253-256

Höhle, J., 2011. The assessment of the absolute planimetric accuracy of airborne laserscanning, proceedings of "Laser Scanning 2011", Calgary/Canada, 6 p.

Jacobsen, K., Cramer, M., Ladstätter, R., Ressl, C., Spreckels, V., 2010. DGPF Project: Evaluation of Photogrammetric Camera Systems – Geometric Performance, Photogrammetrie, Fernerkundung, Geoinformation (PFG), nr. 2, pp. 83-97

Karel, W., Kraus, K., 2006. Quality Parameters of Digital Terrain Models, In: "The EuroSDR Test 'Checking and Improving of Digital Terrain Models' "

Knudsen, T., PINGPONG: a program for height model gridding and quality control, Proceedings of the 2nd NKG workshop on national DEMs, Copenhagen, November 11-13, 2008, ftp://ftp.kms.dk/download/Technical_Reports/KMS_Technical_Report_4.pdf (last accessed October 2011)

Kokkendorff, S. L., 2008. A procedure for detection of horizontal offsets in point cloud laser data, Proceedings of the 2nd NKG workshop on national DEMs, Copenhagen, November 11-13, 2008, ftp://ftp.kms.dk/download/Technical_Reports/KMS_Technical_Report_4.pdf

Mikhail, E.M., Ackermann, F., 1976. Observations and Least Squares, ISBN 0-7002-2481-5, IEP, New York

R Development Core Team, 2008, R: A Language and Environment for Statistical Computing, R Foundation for Statistical Computing, Vienna, Austria, ISBN 3-900051-07-0, http://www.R-project.org (last accessed October 2011)

3. Photogrammetric methods for automated DTM checking

Several photogrammetric methods with a different level of automation were investigated in the EuroSDR test "Checking and improving of Digital Terrain Models". Principles of two of them, namely the method of two overlapping orthoimages and the back-projection method, will be explained with more details in the following. A discussion of advantages and drawbacks of DTM checking methods based on photogrammetry concludes this chapter.

3.1 Method of two overlapping orthoimages

The main idea of this method is that the position of corresponding points in two overlapping orthoimages should be identical. If this condition is not fulfilled then errors in orientation or in the DTM used for orthoimage derivation exist. Accuracy of image orientation is verified by measurement of check points in a stereomodel or in a block of images. Only errors originating in the DTM are considered in the following text.

The positions P_1 and P_2 of an evaluated point P are found in two overlapping orthoimages. Due to an erroneous DTM the points are shifted from their correct position. An approximate formula relating the shift in position dX along the direction of the baseline b and the error in the DTM elevation dh can be expressed as dh = dX*h/b. The exact formula can be derived from Figure 3.1. The influence of the second term dh_2 is negligible (e.g. for flying height h = 500 m and dh_1 = 2.00 m, dh_2 =0.01 m). Because the correction of the DTM is calculated, the method is suitable both for checking and improving of the model. The improvement is achieved in an iterative process. This approach was published by (Norvelle, 1994).

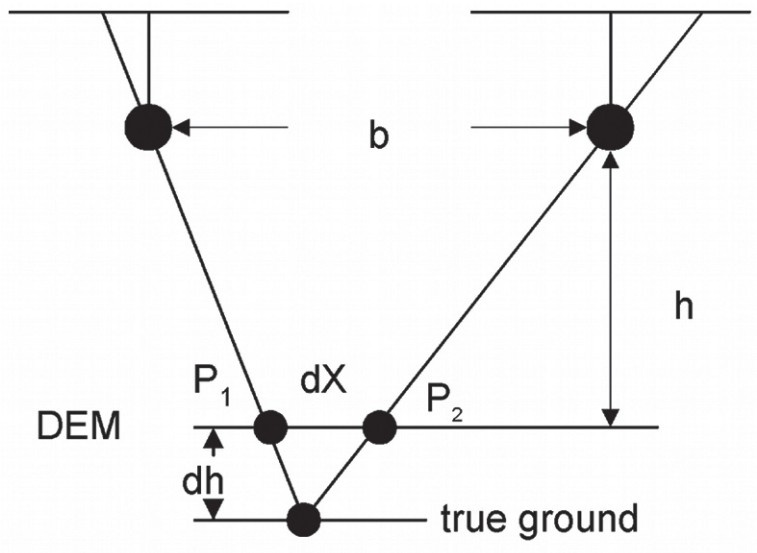

$$dh = dX\frac{h+dh}{b}$$

$$dh \approx dX\frac{h}{b} + \left(dX\frac{h}{b}\right)^2 \frac{1}{h}$$

$$dh \approx dh_1 + dh_2 = dh_1 + \frac{{dh_1}^2}{h}$$

dh	*height correction*
dX	*ground difference (shift)*
h	*flying height*
b	*length of base*

Figure 3.1. Principle of the method for checking and correcting DEMs (DTMs/DSMs) based on two overlapping orthoimages.

Example 3.1 Calculation of the total correction in elevation $dh = dh_1+dh_2$ by means of the method of two overlapping orthoimages. The measured parallax dX = 1.70 m, flying height h = 1820 m, camera constant c = 120 mm, forward overlap p = 60%, and image format 165.9 mm x 92.2 mm (s'_H x s'_W).

image scale $m_b = h/c = 15\ 167$
length of base $b=(1-p)/100*s'_W*m_b = 559$ m (overlap calculated along a shorter side of the image format)
Correction in elevation:
$dh_1 = 5.53$ m
$dh_2 = 0.02$ m
Total correction in elevation $dh=dh_1+dh_2$ is 5.55 m.

Searching for corresponding points can be done automatically, e.g. by means of area based matching. Utilization of least squares matching allows for subpixel accuracy. Corresponding points can be matched either directly on DTM positions or points suitable for correlation can first be found using interest operators. Matching itself is not free of errors. Therefore methods for eliminating mismatches should be applied in order to check and improve the DTM without introducing additional errors.

The described approach was further investigated by two research groups that later on participated in the EuroSDR project on DTM checking. Detail of the used methodology can be found in (Potuckova, 2004 & 2006) and (Skarlatos & Georgopoulos, 2006).

In the approach of Potuckova, the DTM corrections are calculated directly on DTM points. A local maximum of the normalized cross-correlation coefficient is searched in order to find the corresponding points. The position is then improved by least squares matching. To minimize the number of errors, thresholds for the correlation coefficient and for the standard deviation of shift parameters derived in least squares matching were applied. Moreover, two other procedures were developed and tested:

- searching corresponding points along epipolar lines, setting thresholds for differences between matching from the left orthoimage (template) to the right one (search area) and vice versa (L/R method),
- calculation of corrections in the surrounding of the DTM points and statistical evaluation of these corrections (histogram method).

A comparison with reference data indicated that the histogram method combined with epipolar geometry, thresholds for the correlation coefficient and the accuracy of least squares matching gives the best results. Built-up and forest areas were in advance excluded based on a topographic database. As a result of the proposed method, the input DTM points are divided in two groups. The first one comprises points where the criteria for matching are fulfilled and corrections in elevations are calculated. The second group represents points where the tested method failed the required criteria and it is not applied. Superimposition of these two groups of points in different colors on an orthoimage gives a quick overview where the DTM was checked and possibly improved and where the checking method was not successful (cf. Figure 3.2).

In the EuroSDR project an improvement of DTMs derived by means of photogrammetry (Test A, 25 m grid, image scale 1:25 000, h = 3 800 m, GSD = 0.525 m) and by means of contour lines (Test B, 10 m grid, 5 m interval of the original contour lines) was achieved by application of the histogram method. Colored images at the scale of 25 000 with GSD of 0.525 m were used for checking of the DTMs. The corrections

were calculated on 2 033 and 10 390 reference points in the case of the Test A and B, respectively. 86 % of the checked points fulfilled the criteria of the histogram method and the corrections were applied. 14 % of points were left for visual inspection. The results are summarized in Table 3.1. The number of outliers in the corrected part of the data sets was only 1 %. The expected accuracy of the corrected DTMs was 0.47 m.

Table 3.1. Results of the application of the histogram method on the datasets of the EuroSDR test on DTM checking.

	Test A		Test B	
	Before correction	After correction	Before correction	After correction
Number of points*	1729 (86 % of all tested points)		8973 (86 % of all tested points)	
RMSE [m]	0.7	0.5	1.4	0.4
Mean [m]	0.2	0.1	0.3	0.1
σ [m]	0.7	0.5	1.4	0.4
Max |Δh| [m]	4.9	4.6	10.9	6.0

* Number of points where the criteria of the correction method were fulfilled

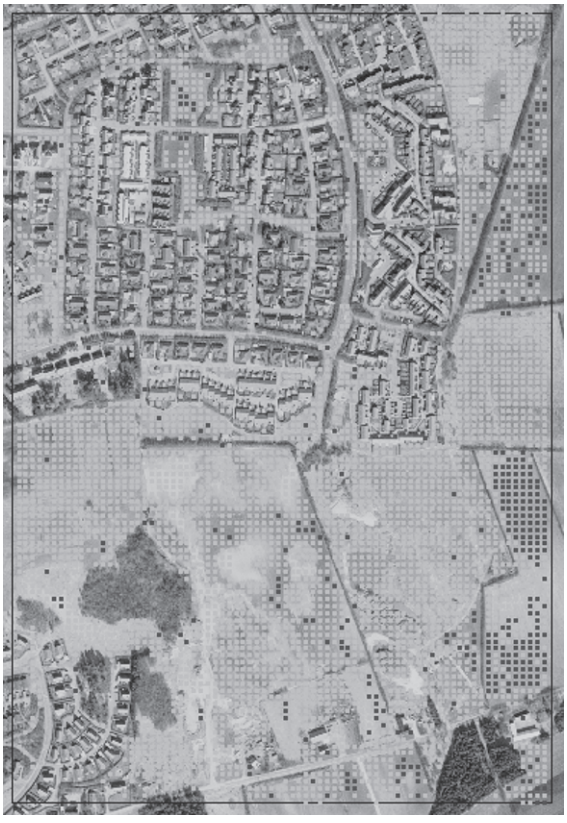

Figure 3.2. Division of the tested DTMs (derived from scanned stereoimages at the scale of 1:25 000, c = 15 cm, GSD = 0.525 m) into two categories. Bright points fulfilled all set criteria and comprise a minimum of outliers; dark points must be checked by other methods. The distance between points is 10 m.

Skarlatos and Georgopoulos extended the geometrical solution of the discussed method. In addition to corrections in elevations shifts in position from the DTM points are also calculated (compare Figure 3.3). A subpixel matching technique using elliptical templates was developed (Skarlatos & Georgopoulos, 2004). Moreover, the 50% level of confidence test is applied on derived corrections in elevation to avoid errors

due to image matching. Elevation corrections are calculated with a higher density than an original DTM grid. Because of positional shifts from original DTM points, a TIN of corrections or corrected elevations are delivered as a result.

Figure 3.3 Concept of the method for DTM checking and correcting based on two overlapping orthoimages proposed by Skarlatos and Georgopoulos. Source: Skarlatos & Georgopoulos, 2006.

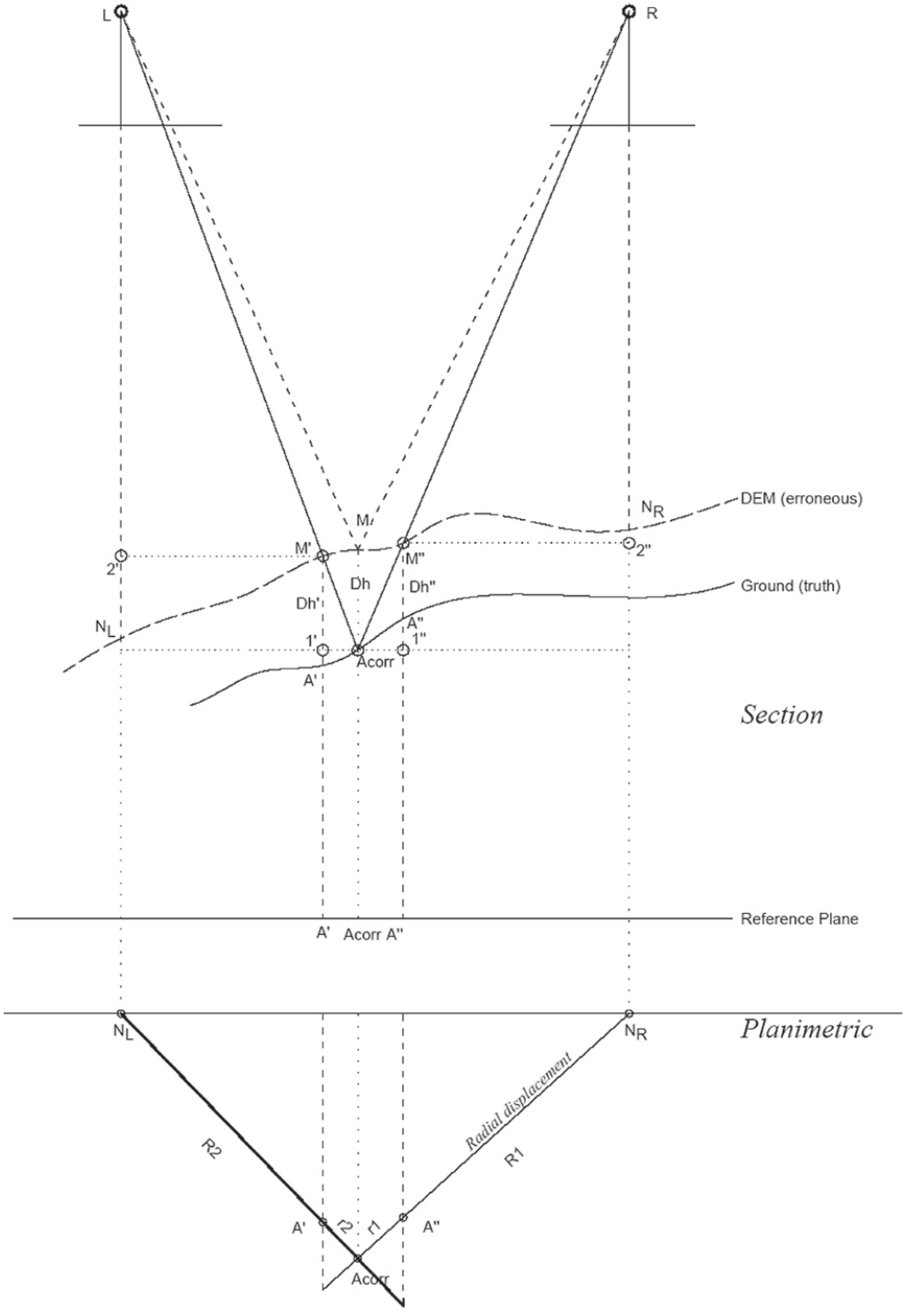

3.2 Method of back-projection

Interpolation that is a part of the orthoimage derivation process causes a lower radiometric quality of ortho-images in comparison to original images. This is a disadvantage of the approaches discussed in the previous chapter. A DTM checking method using image matching in original images was suggested by Schenk et al. (2001) and Jancso and Zavoti (2006). Having a stereopair of aerial images and parameters of their inner and exterior orientation, a selected point from the left image (L´=A´) can be projected on an evaluated DTM and from there to the second image (L´´) as depicted in Figure 3.4 (left image). Image matching along an epipolar line is carried out in the neighborhood of the point L´´. The goal is to find a position of the best fit to the point L´=A´ in the right image (A´´). If the distance between positions of the points L´´ and A´´ (dp´) exceeds a given threshold, a correction of the DTM is calculated based on the parallax equation. Instead of searching a homologues pair along an epipolar line, a point can be shifted along a vertical line at the grid position. The corrected DTM elevation will correspond to the most favorable score of a matching function calculated for points Li projected to the left and right images (cf. Figure 3.4, right image).

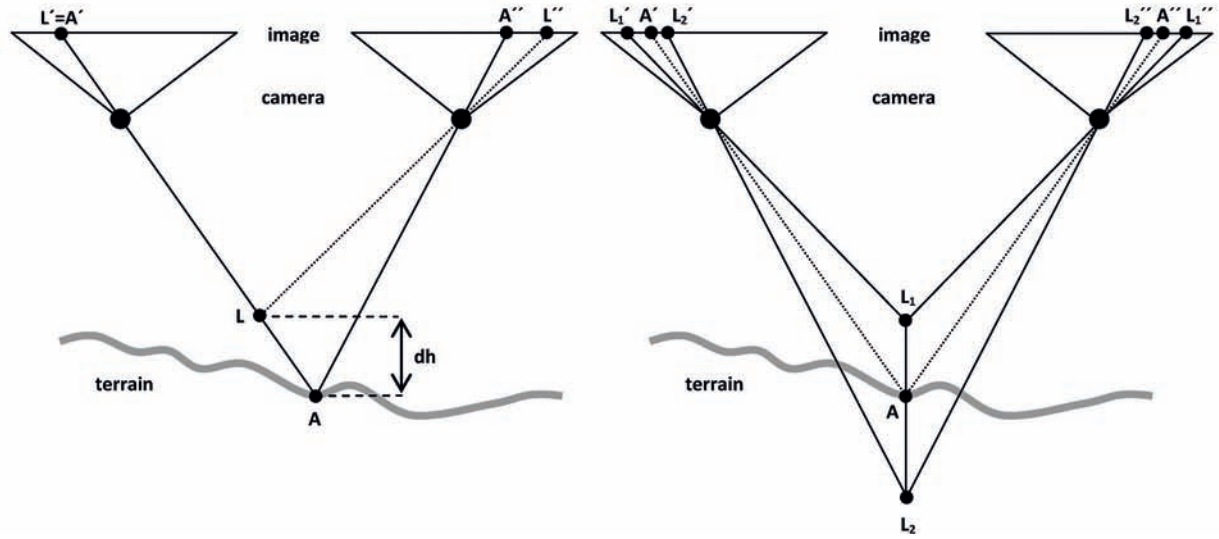

Figure 3.4. Back-projection method for checking and improving of a DTM. To left - the approach based on matching along an epipolar line, to right - matching along a vertical line at a DTM point. After Jancso & Zavoti, 2006.

Example 3.2 Using the back-projection method and vertical line locus, the following values of the shift from the original DTM elevation dh and correlation coefficient r were calculated:

dh [m]	-1.20	-0.80	-0.40	0.00	**0.40**	0.80	1.20
r	0.21	0.43	0.36	0.56	**0.85**	0.66	0.39

The original DTM elevation was 75.15 m

We search the dh-value corresponding to the highest correlation coefficient.
The corrected elevation of the terrain at the given DTM position is 75.15 + 0.40 = 75.55 m.

3.3 Other DTM checking methods in the EuroSDR test

Jancso and Zavoti (2006) applied the back-projection method and investigated possibilities of improvement of area based matching using different combinations of R, G, B bands, such as:

- Cross Correlation (RGB): maximum of three correlation coefficients r_R, r_G, r_B calculated for each band is used, $r = \max\{r_R, r_G, r_B\}$
- Cross Correlation (RGB - weighted): the correlation coefficient is calculated as a weighted mean of r_R, r_G, r_B. A texture coefficient is used as a weight and it is calculated for each band.
- Cross Correlation (Gray): Correlation is calculated in a gray level image that represents and average of all three bands.
- Cross Correlation (RGB – H, V): The correlation is carried out in images with a reduced resolution with a factor of two in horizontal (H) and vertical (V) directions. $r = \max\{r_H, r_V\}$ is taken as a final value.

According to the authors, RGB-HV and RGB algorithms showed to perform best.

Three other methods of DTM checking were presented in the EuroSDR test. One of them is based on a derivation of elevations at the positions of DTM points by means of area based matching in an oriented stereopair of aerial images. The derived DTM and the original one are compared and a hypothesis of equality of their mean difference (error) is tested (Paszotta & Szumilo, 2006). The second method is based on manual measurements in a stereomodel. A statistical comparison of a TIN corresponding to an evaluated DTM and a reference TIN originating from manual measurement follows (Fiala & Sima, 2006). The last method searches for outliers in the tested DTM by comparison of a difference of an elevation at the DTM point with an average elevation of its neighborhood (Kim & Shan, 2006).

Some tasks connected to photogrammetric methods connected to checking of DTMs can be studied by means of the e-learning program “DTM Checking”. Its URLs can be found under the references at the end of this chapter.

3.4 Discussion on methods for DTM checking and improving based on images

DTM checking based on two overlapping images as well as the back-projection method allow for a full automated processing. Theoretically, no reference data are needed. The number of check points is not limited in general but they can be found only in areas suitable for image matching. Performance of the image matching algorithm is extremely important. Both solutions of the orthoimage method also incorporate statistical tests on calculated corrections of elevations and principles of redundancy to decrease the number of outliers caused by erroneous results of image matching. Skarlatos and Georgopoulos (2006) also suggest smoothing of the final surface of corrections in elevations.

Nowadays, it is a standard to use color images in most photogrammetric applications including derivation of DTMs and orthoimages. Nevertheless, image matching is usually performed in a single band only. The potential of the full range of spectral information for image matching is still under investigation although some research has been carried out as mentioned in the previous chapter.

What is an advantage of using a method based on image matching for checking a DTM that was in many cases derived by the same procedure? Why to use orthoimages instead of original images? These are two questions often asked in connection with the presented methods of DTM checking. The answers are very clearly given by Skarlatos and Georgopoulos (2006):

1. Initial approximations, which is the main problem of least squares image matching and often the basic reason of outliers, are almost eliminated in the orthoimages used.

2. The affine transformation, which in real photographs might be inadequate due to strong slopes, are almost eliminated in orthoimages and therefore matching is faster and more reliable.

3. Any two overlapping orthoimages can be used, not only the two images which formed the original stereopair.

4. Using image matching in orthoimages for DTM checking provides a very strong and redundant system. Since the main scope of the described application is checking and there is no need for complete coverage of the area of interest, a loss of a large number of matched points (e.g. 50%) can be tolerated, in order to increase reliability of the rest. The remaining thousands of points are still plenty for DTM checking.

5. Maps or other georeferenced datasets can be overlaid on orthoimages and used to monitor results.

Both presented methods allow for a fast and automated checking of DTMs in large areas and they are not limited to small samples of data as in the case of check points collected by terrestrial methods. Moreover, they give a possibility for a simple updating of DTMs and improvement of quality if parameters of aerial images (and orthoimages) are sufficient for determination of elevations of higher accuracy than an original DTM. In the EuroSDR test, these methods worked well especially for checking and improving DTMs of lower accuracy such as those derived by digitizing contour lines from topographic maps. Their performance was poor with respect to DTMs originated in laser scanning. On the other hand, photographs used in the test for checking such high quality DTMs were acquired with an analogue camera and scanned with resolution of 15 μm. New investigations will be carried out based on images taken with modern digital photogrammetric cameras that perform better in image matching due to higher spatial and radiometric resolution.

3.5 References

Fiala, R., Sima, J., 2006. The Czech Method of DTM Checking. . In: The EuroSDR Test “Checking and Improving of Digital Terrain Models”, EuroSDR Official Publication No. 51, pp. 87-94

Jancso, T., Zavoti, J., 2006. Quality control of digital terrain models using different autocorrelation techniques. In: The EuroSDR Test “Checking and Improving of Digital Terrain Models”, EuroSDR Official Publication No. 51, pp. 95-112

Kim., J. S., Shan, J., 2006. A Statistical Approach to DTM Quality Evaluation, . In: The EuroSDR Test “Checking and Improving of Digital Terrain Models”, EuroSDR Official Publication No. 51, pp. 113-123

Norvelle, F. R., 1996. Using iterative orthophoto refinements to generate and correct digital elevation models (DEM’s), In: Digital Photogrammetry: An Addendum to the Manual of Photogrammetry, American Society for Photogrammetry and Remote Sensing, ISBN 1-57083-037-1

Paszotta, Z., Szumilo, M., 2006. Application of a statistical Test of Hypothesis to Check DTM Accuracy over the Internet, . In: The EuroSDR Test “Checking and Improving of Digital Terrain Models”, EuroSDR Official Publication No. 51, pp. 79-86

Potuckova, M., 2004. Image Matching and its Applications in Photogrammetry, Ph.D. thesis, Czech Technical University in Prague, 132 pages

Potuckova, M., 2006. Checking and Improvements of DTMs in the EuroSDR Test, In: The EuroSDR Test “Checking and Improving of Digital Terrain Models”, EuroSDR Official Publication No. 51, pp. 69-78

Schenk, T., Suyoung, S., Csathó, B., 2001. Accuracy Study of Airborne Laser Scanning Data with Photogrammetry, IAPRS XXXIV-3/W4, Annapolis http://www.isprs.org/proceedings/XXXIV/3-W4/pdf/Schenk.pdf (last accessed October 2011)

Skarlatos, D., Geogopoulos, A., 2004. Automating the Checking and Correcting of DEMs without Reference Data, IAPRS XXXIV, Istanbul http://www.isprs.org/proceedings/XXXV/congress/comm2/papers/190.pdf (last accessed October 2011)

Skarlatos, D., Geogopoulos, A., 2006. The Method of Two Overlapping Orthoimages for Checking the Produced DTM, In: The EuroSDR Test “Checking and Improving of Digital Terrain Models”, EuroSDR Official Publication No. 51, pp. 59-68

E-learning program “DTM Checking” http://web.natur.cuni.cz/gis/dtmchecking/index.php (last accessed October 2011)

4. Existing specifications, standards, and recent DEM projects

In the following a few existing specifications and standards of DEMs are discussed with respect to the assessment of quality. Furthermore, it is dealt with the assessment of quality in some recent projects.

4.1 Specifications and standards

4.1.1 Specification of the Danish National Survey and Cadastre (KMS)

For the production of the country-wide DEM of Denmark the National Survey and Cadastre (KMS) came up with specifications for four products (point cloud, DTM grid, DSM grid, and contour lines). They specified density, accuracy, and reliability in classification. Regarding the vertical accuracy the maximum values for Mean (μ), Standard Deviation (σ), and the maximum difference in elevation ($|\Delta h_{Max}|$) were specified (cf. Table 4.1). Two private companies carried out data acquisition by ALS and delivered the requested DEMs. Quality control took then place at KMS and the products were improved and adapted to different applications.

Table 4.1 Specification of the Danish National Survey and cadastre for DEM production density horizontal

	density	**horizontal accuracy true error** ε_E, ε_N [cm]	**vertical accuracy**			**classification**
			μ_{Max} [cm]	σ_{Max} [cm]	$\lvert\Delta h_{Max}\rvert$ [cm]	maximum number of outliers
point cloud	1 footprint/ cell	<100	10	10	40	1 per1000 ha
DTM grid	ΔE, ΔN<2m	<100	10	10	40	1 object per1000 ha
DSM grid	ΔE, ΔN<2m	<100	20	20	100	1 per1000 ha (high vegetation)
contour lines (CL)	ΔH=0.5 m	<100	15	10	40	object code for each CL, with correct topology and of cartographic quality

The way how the updating of the new DEM will be carried out is not decided yet. A study whether the aerial imagery for orthoimage production and updating of topographic maps can be used for the DEM updates has been carried out. It revealed that accuracy and density of the elevations is nearly the same as with laser scanning. The planimetric (horizontal) accuracy is, however, better at the photogrammetric method.

A third private company produced another DEM also covering the whole territory of Denmark. They used ALS for acquisition as well, but produced after slightly different specifications. More information on both DEMs is given in the chapter “Results of projects”.

National standards for DEMs do not exist in Denmark at present. The Danish organization "Geoforum" has published guidelines for DEMs. These guidelines explain the production and applications of DEMs to users (Geoforum 2011).

4.1.2 German Standards

The requirements for photogrammetric and other products are written by "Deutsches Institut für Normung" and are available as DIN books or DIN sheets. DIN 18740-3, for example, deals with the requirements for orthoimages. The required DEM accuracy is there specified with $\sigma_Z = 2 \cdot \sigma_{E,N}$, that means twice the standard deviation of the coordinates of the orthophoto which is produced from wide angle photographs.

The requirements for all DEMs will be in DIN 18740-6, which is, however, not yet available.

4.1.3 European standards, directives, and guidelines

European Standards regarding the quality of DEMs do not exist yet. It is expected that the **CEN/TC287** (Comité Européen de Normalisation/Technical Committee Geographic Information) will deal with it and produce a European Standard (EN). Besides the European Standard (EN), CEN produces also Technical Specification (CEN/TS), Technical Reports (CEN/TR), and CEN Guides.

The **INSPIRE** (Infrastructure for Spatial Information in Europe) **directive** aims to create spatial data infrastructure for the European Union. It will enable the sharing of environmental spatial information among public sector organizations and facilitate public access to spatial information across Europe. One step in this directive is to use metadata for all geographic data. The Guidelines on INSPIRE Metadata are based on ISO 19115 and ISO 19119 (cf. chapter 4.1.5).

JRC guidelines for best practice and quality checking of orthoimagery are produced by the Joint Research Centre of the European Commission in Ispra/Italy. They include demands on DEMs to be used in the production of orthophotos derived from aerial and satellite imagery. Regarding the vertical accuracy of the DEM it requires 2 x planimetric 1-D RMSE. The grid spacing of the DEM should be 5 to 20 times of the orthophoto pixel size. The DEM should be of sufficient detail, complete, continuous, and without any gross anomalies.

The quality control should confirm that the DEM is correctly geo-referenced and elevations have not been corrupted or accidentally re-scaled during reformatting and preparation. Attention should be paid to datum references (mean sea level vs. ellipsoidal heights, for example). Vertical accuracy of the DEM must be checked by comparison against independent control. The use of histograms and 3D views is recommended in order to check for spikes and holes. The completeness in the project zone and continuity along tile boundaries should also be checked. More details are published in (EUR 23638 EN 2008).

4.1.4 Standards in USA

The US Standards for DEMs and maps have a long history. Their standards are based on the probability levels of 90% or 95% (instead of 68% as in Europe). There exist several standards and only the new ones and DEM relevant standards will be mentioned in the following.

National Standards for Spatial Data Accuracy (NSSDA)

Accuracy measures are RMSE, Mean and Standard Deviation. The standards for vertical errors are:

Root Mean Square Error (RMSE): $RMSE = \sqrt{\sum_i^n (e_i)^2 / n}$

Mean: $\overline{X} = \sum_i^n e_i / n$

Standard deviation: $S = \sqrt{\sum_i^n (e_i - \overline{X})^2 / (n-1)}$

The dispersal interval of true errors (e_i) around the Mean (X) is based on the 95% probability level and is calculated by

$\overline{X} \pm 1.96 \cdot RMSE$

The value $1.96 \cdot RMSE$ is named as "NSSDA Vertical Accuracy". Furthermore, NSSDA recommends that a minimum of 20 independent checkpoints (ICPs) should evenly be distributed over the geographic area of interest.

ASPRS guidelines for reporting vertical accuracy of LIDAR data

Accuracy assessment has to be carried out for five different land cover classes (open terrain, tall weeds and crops, brush lands and low trees, forested areas fully covered by trees, and urban areas with dense human-made structures).

Three different accuracy measures depending on ground cover are determined:

1. Fundamental vertical accuracy (computed from samples measured in open terrain and after the definition of NSSDA).

2. Supplementary vertical accuracy (all areas with ground cover) using the "95th percentile error"*. 95% of the sampled errors will be less than this value.

3. Consolidated vertical accuracy (combination of the samples from both open terrain and other ground cover classes) using the "95th percentile error".*

*The 95% percentile corresponds to the 95% quantile ($Q_{\Delta h}(0.95)$). Note that the errors are the original errors (Δh) and not the absolute errors ($|\Delta h|$) as used in Table 2.2.

US Federal Geographic Data Committee

A Geographic Information Framework Data Content Standard on elevation data is produced by the US Federal Geographic Data Committee. It describes the content of geospatial elevation data models to support the exchange of elevation information. Regarding the quality of elevation data FGDC requires that the accuracy shall be reported according to NSSDA. Detailed information is published in (FGDC 2008).

4.1.5 International standards

International standards are necessary in the times of globalization. Official standards are developed by the International Organization for Standardization (ISO) and the Open Geospatial Consortium (OGC). In the following a short overview on standards regarding the field of Geographic Information and Geomatics are given. The basics of standards, description of ISO standards (up to 2004) and their application in industry and national standards are published in (Kresse & Fadaie, 2004).

ISO (International Organization for Standardization)

ISO publishes international standards which are produced in the technical committees (TCs). The TC 211, for example, deals with Geographic Information and Geomatics. The completed standards are "ISO/TS 19101-2" (reference model for imagery), "ISO 19115-2" (metadata for imagery), "ISO/TS 19130" (geo-referencing of imagery, and "ISO/TS 19129" (framework).

"ISO/TS 19130-2 will contain the sensor models for geo-positioning when using sensors like SAR, InSAR, LIDAR, and SONAR. ISO 19139:2007 deals with XML for ISO 19115. The "ISO/TS 19159" is in preparation and will deal with calibration and validation of remote sensing imagery sensors and data. The sensors include digital aerial cameras, airborne laser scanners and sonar equipment used for bathymetric measurements. Calibration procedures for geometry and radiometry will be addressed.

Beside the mentioned standards, more general standards regarding quality exist:

ISO 19157: Geographic information — Data quality
ISO 9000: Quality management systems — Fundamentals and vocabulary.

The ISO standards are updated and they may change to other names or being dropped. Usually the year of publication is added in the title.

OGC (Open Geospatial Consortium)

The Open Geospatial Consortium, Inc. is an international industry consortium of companies, government agencies, and universities. Beside other activities it has published three standards which are related to the 3D GeoWeb. These are:

- A revised version of the Web 3D Service (W3DS),
- the Web View Service (WVS),
- an extension profile of the Symbology Encoding Specification for 3D (SE 3D).

These standards establish a new family of 3D portrayal services focusing on virtual 3D maps, interactive virtual environments, and 3D cartographic visualization. Details of the many activities of the Open GIS Consortium can be found on the OGC homepage (http://www.opengis.org).

Regarding digital elevation models international standards are lacking. The current efforts of the German Institute for Standardization with DIN 18740-6 may lead to a first DEM standard.

4.2 Assessment of quality in recent projects

Some examples are given how quality of DEMs is assessed in projects. The examples are from Europe only.

4.2.1 Danish DEMs

The National Survey and Cadastre of Denmark (KMS)

KMS carried out an extensive quality control of the new country-wide DEM derived by laserscanning. Internal checks regarded the point density, the differences in the overlap between adjacent strips and the completeness of the data. The assessment of the absolute vertical accuracy used 162 control patches of approximate 100 points within an area of 20m x 20m each (cf. Figure 4.1). The individual points of the patches were measured by means of GNSS/RTK and accuracy measures (Mean, RMSE, Std. Dev., Median) were derived from the differences. A histogram displayed the distribution of errors.

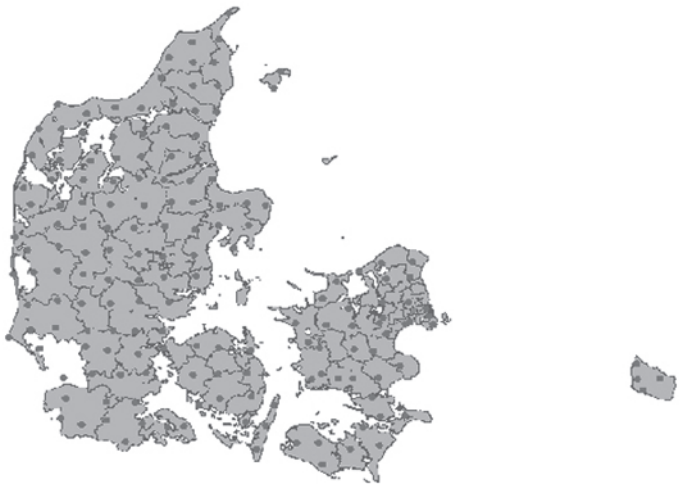

Figure 4.1. Reference measurements of the Danish DEM. Source: (KMS, 2009)

Regarding the planimetric (horizontal) accuracy the corners of 142 buildings in four different test sites were visually identified in a normalized DSM*. The obtained coordinates were compared against coordinates taken from existing digital maps. The differences between the two coordinate sets were used to derive (relative) accuracy measures (RMSE, Mean, Std. Dev.). Details are published in (Hawa et al., 2010).

COWI A/S

Details from information material of the COWI company on quality of its Digital Height model of Denmark (DDH®) include the geometric accuracy and metadata information. The vertical accuracy is specified for well-defined areas with σ_Z=10cm; the planimetric accuracy with $\sigma_{E,N}$=80cm for well-defined areas. Check points and 'check houses' are used for the assessment of DDH's geometric quality.

The metadata of the DDH contain point density, geometric accuracy, and time of data acquisition. The point density is documented by means of a plot where the number of collected points is visualized for 10m x 10m cells. (cf. Figure 4.2).

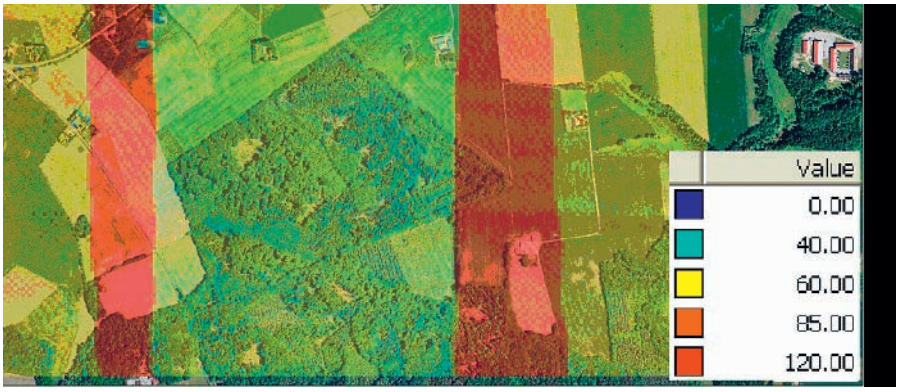

Figure 4.2 Point density of DDH. The number of points in 10m x 10m cells is color coded. Source: COWI A/S

The COWI Company uses the term DEM for the difference model (DSM-DTM). In this paper, as in the Anglo-American literature, the term DEM is used as the collective name for all elevation models, e.g. Digital Terrain Model (DTM), Digital Surface Model (DSM), Canopy Height Model (CHM), etc.

More dense and more accurate DEMs are produced from lower altitudes and often by one flight line (**corridor projects**). Special targets (placed on ground before flight) and airborne system calibration are required (cf. Figure 4.3). The checking of the accuracy can be carried out by means of special targets and natural objects.

Figure 4.3 Ground control and checking in corridor projects using ALS. Targets with elevation difference to the ground and special reflecting material (left) can precisely be identified in the dense point cloud (right). Source: Flatman 2009

* The normalized DSM (nDSM) is the difference between the Digital Surface Model and the Digital Terrain Model (nDSM=DSM-DTM)

4.2.2 EuroSDR project “Automated checking and improving of DEMs”

The research project of the European Organization of Spatial Data Research (EuroSDR) compared different methods of automated checking and improving of DEMs. The investigated three DEMs were of different quality. Reference values were determined from images of low flying heights or by GNSS (cf. Figure 4.4).

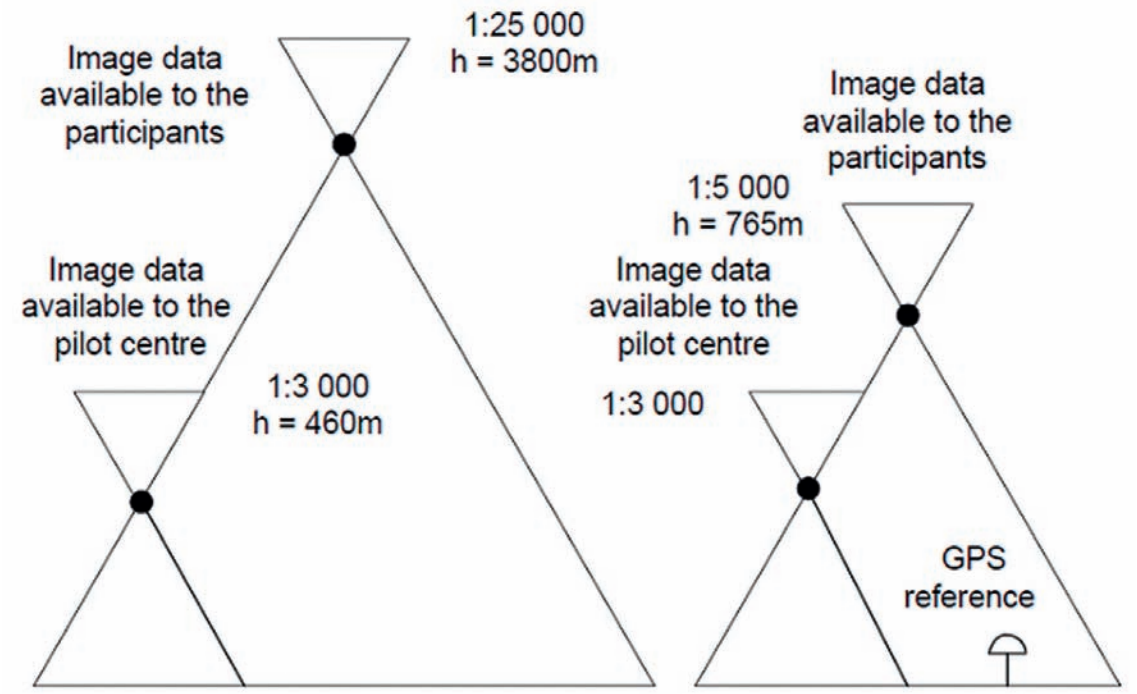

Figure 4.4. Methods for the assessment of the accuracy of DEMs. The left configuration is used for DEMs derived by digital photogrammetry and by scanning of contour lines, the right one for DEMs derived by laserscanning.

The tested methods of checking and improving DEMs applied mainly photogrammetry. Errors in the DEM can be found by matching patches of two overlapping orthoimages (cf. chapter 3).

The DEM assessment used the same accuracy measures as in Table 2.1 of chapter 2. Blunders were removed from the data set when the difference (Δh) to the true value exceeded the threshold ($3 \cdot$ RMSE). The number of blunders were recorded and compared in the test.

The photogrammetric methods of checking and improving DEMs have a high potential for automation. Highly accurate DEMs have to be checked by ground surveying.

4.2.3 Tests of the German Society of Photogrammetry and Remote Sensing (DGPF Test)

Different DEMs derived by digital photogrammetry using up-to-date digital cameras and software packages were tested by different research groups (Haala et al., 2010). Absolute vertical errors (RMSE, Mean, ΔMax/ΔMin) were derived after elimination of blunders using the 3·RMSE threshold (cf. Table 4.2). Reference was a LIDAR point cloud as well as targets measured by GNSS.

	Sensor	RMS [cm] (without gross errors)	Mean [cm]	ΔMax/Min [cm]		# points
LIDAR	ALS 50	3.3	0.4	9.4	-6.7	59
Photogrammetry	DMC	3.3	0.9	9.5	-6.9	60
	UltraCam-X	4.8	0.6	11.7	-10.0	60
GSD=8cm Raster=0.2m	DigiCAM	6.0	-1.7	15.5	-15.7	61
	RMK	4.6	2.4	8.2	-11.5	61

Table 4.2. Absolute vertical errors derived from ALS and various large frame digital cameras using signalized check points. Source: Haala et al. 2010.

A relative accuracy was determined from the elevation differences in the overlap zone of ALS 50 strips. A robust accuracy measure, the Normalized Median Absolute Deviation (NMAD) was used, in order to avoid the influence of blunders. Suitable DEM points should belong to a smooth surface. By means of a 'roughness mask' such points were extracted. The produced density of Leica ALS 50 airborne laserscanner (taken from 500 m altitude) and automated photogrammetry with GSD= 8cm is compared. Figure 4.5 depicts the DSMs of a built-up area.

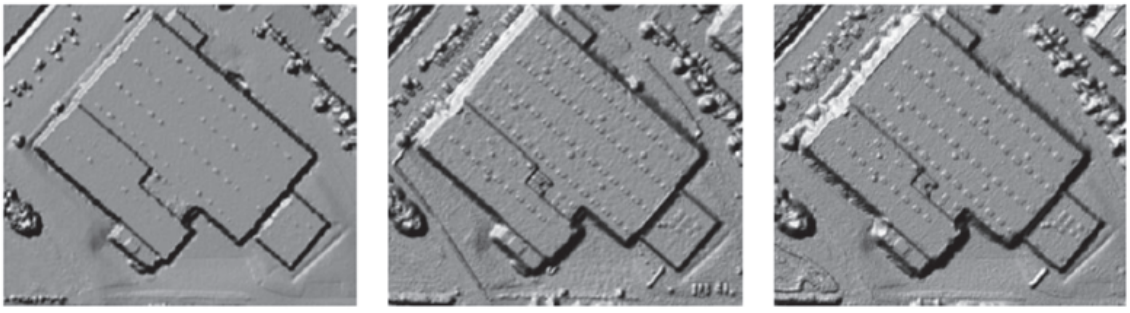

Figure 4.5. DSMs derived from ALS data (left) and digital large format cameras DMC (middle) and UltraCam-X (right image). Source: (Haala et al., 2010).

In addition the accuracy of **manual photogrammetry** has been tested. In comparison to accurate ground control the measured points in a stereo-workstation revealed high accuracy for all three coordinates (cf. Table 4.3).

Table 4.3 Accuracy of manually measured Ground Control Points (GCPs)
Source: (Spreckels et al., 2010).

Camera	No. of GCPs	σ_X [cm]	σ_Y [cm]	σ_Z [cm]
DMC	58	1.8	2.8	3.4
UltraCam-X	58	1.2	2.1	4.8
RMK	60	2.4	3.5	7.5

The signalized points were measured three times. The orientation data of the images were determined in an aerotriangulation and then transferred to the stereo-workstation. The measurement of natural points is less accurate. The obtainable accuracy will depend on the structure and contrast of the surroundings.

In (Spreckels 2011) standard deviations for mass points were determined with σ_Z=6-9cm for images with GSD=10cm. Such accuracy is necessary for high precision DTMs, e.g. in areas of mining activities where ground movements have to be determined accurately and reliably.

Instead of manual measurements semi-automatic measurements can be carried out. The operator places the points on areas with structure and contrast and the measurement uses correlation (matching).

4.2.4 Elevation Model of the Netherlands (AHN-2)

AHN-2 is the second nationwide DEM of the Netherlands. The work started in 2007 and is supposed to be finished in 2012. The specification requires a high point density (10 points/m^2), a very high absolute vertical accuracy ($\mu_Z = \sigma_Z$=5cm), and an identification of all objects larger than 2m x 2m with a maximum horizontal accuracy of $\mu_X = \mu_Y \leq$50cm (absolute deviation). Only one classification error should be present in an area of 10km2. The quality control includes point density check, the point distribution and the quality of the strip adjustment. It is carried out by a third party. The data acquisition of the first subareas has been carried out by different companies using ALS. In order to fulfill the high requirements in classification of objects aerial imagery has been taken in addition (Hofmann, 2011).

4.2.5 Elevation Model of Sweden

A new elevation model has been started in 2009. The 450 000 km^2 area with 65% forest is surveyed by means of ALS. The specification requires a density of 0.5 points/m^2 in single scans, 200m overlap between adjacent scanning areas, accuracies of σ_Z<20cm at distinct areas (elevation) and σ_p<60cm (planimetry). Results of the checking of the first areas by means of ground surveying revealed higher accuracies ($RMSE_Z$<5cm and $RMSE_p$<25cm). The huge project is supposed to be finished in 2013 (Petersen & Burman Rost, 2011).

4.2.6 EuroDEM

The association of the National Mapping Agencies in Europe (EuroGeographics) establishes a European elevation model. The specification requires a vertical accuracy of σ = 8-10m and a spacing of 2 seconds of arc (about 60m). The data of 33 countries were collected by different methods (digitizing of existing contours, photogrammetry, and radar). Data of the Shuttle Radar Topography Mission (SRTM) were used for areas where better data were not available. The accuracy, spacing, reference system, differ in the provided data and had, therefore, to be harmonized. A working group of EuroGeographics collects the comments from the use of EuroDEM and will specify a new version (EuroDEM30). This new DEM will have a spacing of 30m and an accuracy of σ=5m. The DEM data will be in the reference systems ETRS89 (geographic coordinates) and EVRS (elevation).

There are many **other projects** to mention. Nearly each day new DEM projects become known in journals and proceedings of conferences. A summary of several projects dealing with the generation and application of DEMs was recently published in (Höhle, 2010).

4.3 References

EUR 23638 EN 2008 – Joint Research Centre – Institute for the Protection and Security of the Citizen, Title: Guidelines for Best Practice and Quality Checking of Ortho Imagery Author(s): Dimitrios Kapnias, Pavel Milenov and Simon Kay Luxembourg: Office for Official Publications of the European Communities 2008 – 40 pp., EUR – Scientific and Technical Research series – ISSN 1018-5593 ISBN 978-92-79-10969-0, DOI 10.2788/36028

FGDC 2008. Geographic Information Framework Data Content Standard. Part 3: Elevation, FGDC-STD-014.3-2008. Available: http://www.fgdc.gov/standards/projects/FGDC-standards-projects/framework-data-standard/GI_FrameworkDataStandard_Part3_Elevation.pdf (last accessed October 2011)

Flatman, A., 2009. Korridor-kortlægning med LiDAR (Corridor Mapping by means of LIDAR), præsentation at ”Kortdage 2009”

Geoforum, 2011. Geoforums Højdemodelvejledning (Geoforum’s guidance to elevation model), 59 p.

Haala, N., Hastedt, H., Wolf, K., Ressl, C., Baltrusch, S., 2010. Digital photogrammetric camera evaluation - generation of digital elevation models, published in PFG, nr. 2 http://www.ifp.uni-stuttgart.de/dgpf/PDF/03-PFG-02-2010-Höhenmodelle-FinalVersion-20100112.pdf (last accessed October 2011)

Hawa, M. N., Knudsen, Kokkendorff, S.L., Olsen, B.P., Rosenkranz, B.C., 2010. Horizontal Accuracy of Digital Elevation Models, Technical Report no. 10, National Survey of Cadastre, 19p. ftp://ftp.kms.dk/download/Technical_Reports/KMS_Technical_Report_10.pdf (last accessed October 2011)

Hofmann, A., 2011. Qualitätsmanagement für ALS-Projekte am Beispiel “AHN Niederlande”, Lecture at the DIN workshop, January 2011, Berlin

Höhle, J., 2007. The EuroSDR Project ‘Automated Checking and Improving of Digital Terrain Models’, Proceedings of the Annual Conference of the American Society of Photogrammetry and Remote Sensing, Tampa, Florida, 12 p.

Höhle, J., 2009. DEM Generation Using a Digital Large Format Frame Camera, Photogrammetric Engineering & Remote Sensing, Vol. 75, no. 1, pp. 87-937

Höhle, J., 2010. Generation and Application of Digital Elevation Models, Aalborg University, 69p., http://people.plan.aau.dk/~jh/Articles/Hoehle_D_final.pdf (last accessed October 2011)

Höhle, J., Pedersen, C. Ø., 2010. A new method for checking the planimetric accuracy of Digital Elevation Models data derived by airborne laser scanning, Proceedings of the 9th International Symposium on Spatial Accuracy Assessment in Natural Resources and Environmental Sciences ("Accuracy 2010"), pp. 253-256

Jancso, T., Zavoti, J., 2006. Quality control of digital terrain models using different autocorrelation techniques. In: The EuroSDR Test "Checking and Improving of Digital Terrain Models", EuroSDR Official Publication No. 51, pp. 95-112

Kresse, W., Fadaie, K., 2004. ISO Standards for Geographic Information, Springer-Verlag, ISBN 3-540-20130-0

Mikhail, M., Ackermann, F., 1976. Observations and Least Squares, IEP, New York, ISBN 0-7002-2481-5

Petersen, Y.M., Burman Rost, H., 2011. Swedish Lidar Project, GIM International, February 2011, pp. 20-23

Rosenkranz, B., 2009. DHM Danmarks Højdemodel (DHM Denmarks Elevation Model), presentation at "Kortdage 2009".

Spreckels, V., Syrek, L., and Schlienkamp, A., 2011, DGPF Project: Evaluating of Digital Photogrammetric Camera Systems – Stereoplotting

Spreckels, V. 2011, Anforderung an digitale Geländemodelle zur Bodenbewegungsüberwachung, Lecture at the DIN workshop, Berlin, January 2011

5. Summary and outlook

The assessment of the quality of Digital Terrain Models is an important task for mapping organizations. In Europe recently several countries produced a DTM based on laser scanning. Beside the production of new DTMs also the updating of the DTM has to be carried out. Other methods of acquisition and tools for processing may then be necessary. The applications of DTMs are multiple. Each application has its own requirement. The landscape is very different regarding the amount and type of vegetation and buildings. The checking of the quality of DTMs is therefore a complex task and needs some guidance. This book provides the basic information for the different tasks in quality control of DTMs. It is divided in four chapters.

In the first chapter an overview on methods of deriving DTMs is given. The acquisition by means of different sensors as well as the processing of the data is dealt with. Emphasis is given to the methods of high accuracy and resolution. These are laser scanning and digital photogrammetry.

The second chapter defines first DTM quality. The checking of a DTM is usually done by means of samples where reference data of superior accuracy are collected and compared with the DTM data. The equations for standard accuracy measures for horizontal and vertical accuracy are given. Often elevation errors are not normally distributed. Other accuracy measures have then to be applied. The background for robust accuracy measures is given. The reliability of the derived accuracy measures is also discussed and formulae and algorithms for confidence intervals for the derived accuracy measures are provided.

The third chapter deals with the checking of extended areas. It is based on a EuroSDR project where several research groups participated in a contest to solve the checking and improvement of DTMs automatically by means of photogrammetric methods. Different approaches are described and the results of them are presented.

The fourth chapter deals with existing specifications, standards and recent DEM projects. The assessment of quality in recent projects is monitored. The variety of tasks and solutions will show the complexity of tasks for assessment of the quality of DTMs. New DTM projects with new requirements will come every day. There is a need for guidelines and standards for the assessment of the quality of DTMs.

A list of relevant references is added to each chapter. Furthermore, figures and examples for the calculation of accuracy measures, and some programs are added to the text. Internet-based learning programs will make the complex topics better understood. The four e-learning courses held by the authors on this subject helped to improve the first version of the text.

Development on this topic is going on. New large format aerial cameras and new laser scanners are announced. Matching of imagery has very much improved recently and EuroSDR is currently carrying out a project on “Image Matching for DSM”. New filtering and extraction methods give hope that the generation of DTMs will improve in future with respect to density and accuracy. Also the derivation of DTMs for continents and the whole world can be done by means of new satellites and sensors. The generation of new DTMs as well as the updating and the monitoring of changes in the landscape will be future challenges for the mapping community.

LIST OF OEEPE/EuroSDR OFFICIAL PUBLICATIONS

State – December 2011

1 *Trombetti, C.*: „Activité de la Commission A de l'OEEPE de 1960 à 1964" – *Cunietti, M.*: „Activité de la Commission B de l'OEEPE pendant la période septembre 1960 – janvier 1964" – *Förstner*, R.: „Rapport sur les travaux et les résultats de la Commission C de l'OEEPE (1960-1964)" – *Neumaier, K.*: „Rapport de la Commission E pour Lisbonne" – *Weele, A. J. v. d.*: „Report of Commission F." – Frankfurt a. M. 1964, 50 pages with 7 tables and 9 annexes.

2 *Neumaier, K.*: „Essais d'interprétation de »Bedford« et de »Waterbury«. Rapport commun établi par les Centres de la Commission E de l'OEEPE ayant participé aux tests" – „The Interpretation Tests of »Bedford« and »Waterbury«. Common Report Established by all Participating Centres of Commission E of OEEPE" – „Essais de restitution »Bloc Suisse«. Rapport commun établi par les Centres de la Commission E de l'OEEPE ayant participé aux tests" – „Test »Schweizer Block«. Joint Report of all Centres of Commission E of OEEPE." – Frankfurt a. M. 1966, 60 pages with 44 annexes.

3 *Cunietti, M.*: „Emploi des blocs de bandes pour la cartographie à grande échelle – Résultats des recherches expérimentales organisées par la Commission B de l'O.E.E.P.E. au cours de la période 1959–1966" – „Use of Strips Connected to Blocks for Large Scale Mapping – Results of Experimental Research Organized by Commission B of the O.E.E.P.E. from 1959 through 1966." – Frankfurt a. M. 1968, 157 pages with 50 figures and 24 tables.

4 *Förstner, R.*: „Sur la précision de mesures photogrammétriques de coordonnées en terrain montagneux. Rapport sur les résultats de l'essai de Reichenbach de la Commission C de l'OEEPE" – „The Accuracy of Photogrammetric Co-ordinate Measurements in Mountainous Terrain. Report on the Results of the Reichenbach Test Commission C of the OEEPE." – Frankfurt a. M. 1968, Part I: 145 pages with 9 figures; Part II: 23 pages with 65 tables.

5 *Trombetti, C.*: „Les recherches expérimentales exécutées sur de longues bandes par la Commission A de l'OEEPE." – Frankfurt a. M. 1972, 41 pages with 1 figure, 2 tables, 96 annexes and 19 plates.

6 *Neumaier, K.*: „Essai d'interprétation. Rapports des Centres de la Commission E de l'OEEPE." – Frankfurt a. M. 1972, 38 pages with 12 tables and 5 annexes.

7 *Wiser, P.*: „Etude expérimentale de l'aérotriangulation semi-analytique. Rapport sur l'essai »Gramastetten«." – Frankfurt a. M. 1972, 36 pages with 6 figures and 8 tables.

8 „Proceedings of the OEEPE Symposium on Experimental Research on Accuracy of Aerial Triangulation (Results of Oberschwaben Tests)" *Ackermann, F.*: „On Statistical Investigation into the Accuracy of Aerial Triangulation. The Test Project Oberschwaben" – „Recherches statistiques sur la précision de l'aérotriangulation. Le champ d'essai Oberschwaben"– *Belzner, H.*: „The Planning. Establishing and Flying of the Test Field Oberschwaben" – *Stark, E.*: Testblock Oberschwaben, Programme I. Results of Strip Adjustments" – *Ackermann, F.*: „Testblock Oberschwaben, Program I. Results of Block-Adjustment by Independent Models" – *Ebner, H.*: Comparison of Different Methods of Block Adjustment" – *Wiser, P.*: „Propositions pour le traitement des erreurs non-acci dentelles"– *Camps, F.*: „Résultats obtenus dans le cadre du project Oberschwaben 2A" –

Cunietti,M.; Vanossi, A.: „Etude statistique expérimentale des erreurs d'enchaînement des photogram mes"–*Kupfer, G.*: „Image Geometry as Obtained from Rheidt Test Area Photography" – *Förstner, R.*: „The Signal-Field of Baustetten. A Short Report" – *Visser, J.; Leberl, F.; Kure, J.:* „OEEPE Oberschwaben Reseau Investigations" – *Bauer, H.*: „Compensation of Systematic Errors by Ana lytical Block Adjustment with Common Image Deformation Parameters." – Frankfurt a. M. 1973, 350 pages with 119 figures, 68 tables and 1 annex.

9 *Beck, W.*: „The Production of Topographic Maps at 1 : 10,000 by Photogrammetric Methods. – With statistical evaluations, reproductions, style sheet and sample fragments by Landesvermessungsamt Baden-Württemberg Stuttgart." – Frankfurt a. M. 1976, 89 pages with 10 figures, 20 tables and 20 annexes.

10 „Résultats complémentaires de l'essai d'«Oberriet» of the Commission C de l'OEEPE – Further Results of the Photogrammetric Tests of «Oberriet» of the Commission C of the OEEPE"*Hárry, H.*: „Mesure de points de terrain non signalisés dans le champ d'essai d'«Oberriet» – Measurements of Non-Signalized Points in the Test Field «Oberriet» (Abstract)" – *Stickler, A.; Waldhäusl, P.*: „Restitution graphique des points et des lignes non signalisés et leur comparaison avec des résultats de mesures sur le terrain dans le champ d'essai d'«Oberriet» – Graphical Plotting of Non-Signalized Points and Lines, and Comparison with Terrestrial Surveys in the Test Field «Oberriet»" – *Förstner, R.*: „Résultats complémentaires des transformations de coordonnées de l'essai d'«Oberriet» de la Commission C de l'OEEPE – Further Results from Co-ordinate Transformations of the Test «Oberriet» of Commission C of the OEEPE" – *Schürer, K.*: „Comparaison des distances d'«Oberriet» – Comparison of Distances of «Oberriet» (Abstract)." – Frankfurt a. M. 1975, 158 pages with 22 figures and 26 tables.

11 „25 années de l'OEEPE" *Verlaine, R.*: „25 années d'activité de l'OEEPE" – „25 Years of OEEPE (Summary)" – *Baarda, W.*: „Mathematical Models." – Frankfurt a. M. 1979, 104 pages with 22 figures.

12 *Spiess, E.*: „Revision of 1 : 25,000 Topographic Maps by Photogrammetric Methods." – Frankfurt a. M. 1985, 228 pages with 102 figures and 30 tables.

13 *Timmerman, J.; Roos, P. A.; Schürer, K.; Förstner, R.*: On the Accuracy of Photogrammetric Measu rements of Buildings – Report on the Results of the Test "Dordrecht", Carried out by Commission C of the OEEPE. – Frankfurt a. M. 982, 144 pages with 14 figures and 36 tables.

14 *Thompson C. N.*: Test of Digitising Methods. – Frankfurt a. M. 1984, 120 pages with 38 figures and 18 tables.

15 *Jaakkola, M.; Brindöpke, W.; Kölbl, O.; Noukka, P.*: Optimal Emulsions for Large-Scale Mapping – Test of "Steinwedel" – Commission C of the OEEPE 1981–84. – Frankfurt a. M. 1985, 102 pages with 53 figures.

16 *Waldhäusl, P.*: Results of the Vienna Test of OEEPE Commission C. – *Kölbl, O.*: Photogrammetric Versus Terrestrial Town Survey. – Frankfurt a. M. 1986, 57 pages with 16 figures, 10 tables and 7 annexes.

17 *Commission E of the OEEPE:* Influences of Reproduction Techniques on the Identification of Topographic Details on Orthophotomaps. – Frankfurt a. M. 1986, 138 pages with 51 figures, 25 tables and 6 appendices.

18 *Förstner, W.*: Final Report on the Joint Test on Gross Error Detection of OEEPE and ISP WG III/1. – Frankfurt a. M. 1986, 97 pages with 27 tables and 20 figures.

19 *Dowman, I. J.; Ducher, G.*: Spacelab Metric Camera Experiment – Test of Image Accuracy. – Frankfurt a. M. 1987, 112 pages with 13 figures, 25 tables and 7 appendices.

20 *Eichhorn, G.*: Summary of Replies to Questionnaire on Land Information Systems – Commission V – Land Information Systems. – Frankfurt a. M. 1988, 129 pages with 49 tables and 1 annex.

21 *Kölbl, O.*: Proceedings of the Workshop on Cadastral Renovation – Ecole poly-technique fédérale, Lausanne, 9–11 September, 1987. – Frankfurt a. M. 1988, 337 pages with figures, tables and appendices.

22 *Rollin, J.; Dowman, I. J.*: Map Compilation and Revision in Developing Areas – Test of Large Format Camera Imagery. – Frankfurt a. M. 1988, 35 pages with 3 figures, 9 tables and 3 appendices.

23 *Drummond, J. (ed.)*: Automatic Digitizing – A Report Submitted by a Working Group of Commission D (Photogrammetry and Cartography). – Frankfurt a. M. 1990, 224 pages with 85 figures, 6 tables and 6 appendices.

24 *Ahokas, E.; Jaakkola, J.; Sotkas, P.*: Interpretability of SPOT data for General Mapping. – Frankfurt a. M. 1990, 120 pages with 11 figures, 7 tables and 10 appendices.

25 *Ducher, G.*: Test on Orthophoto and Stereo-Orthophoto Accuracy. – Frankfurt a. M. 1991, 227 pages with 16 figures and 44 tables.

26 *Dowman, I. J. (ed.)*: Test of Triangulation of SPOT Data – Frankfurt a. M. 1991, 206 pages with 67 figures, 52 tables and 3 appendices.

27 *Newby, P. R. T.; Thompson, C. N. (ed.)*: Proceedings of the ISPRS and OEEPE Joint Workshop on Updating Digital Data by Photogrammetric Methods. – Frankfurt a. M. 1992, 278 pages with 79 figures, 10 tables and 2 appendices.

28 *Koen, L. A.; Kölbl, O. (ed.)*: Proceedings of the OEEPE-Workshop on Data Quality in Land Information Systems, Apeldoorn, Netherlands, 4–6 September 1991. – Frankfurt a. M. 1992, 243 pages with 62 figures, 14 tables and 2 appendices.

29 *Burman, H.; Torlegård, K.*: Empirical Results of GPS – Supported Block Triangulation. – Frankfurt a. M. 1994, 86 pages with 5 figures, 3 tables and 8 appendices.

30 *Gray, S. (ed.)*: Updating of Complex Topographic Databases. – Frankfurt a. M. 1995, 133 pages with 2 figures and 12 appendices.

31 *Jaakkola, J.; Sarjakoski, T.*: Experimental Test on Digital Aerial Triangulation. – Frankfurt a. M. 1996, 155 pages with 24 figures, 7 tables and 2 appendices.

32 *Dowman, I. J.*: The OEEPE GEOSAR Test of Geocoding ERS-1 SAR Data. – Frankfurt a. M. 1996, 126 pages with 5 figures, 2 tables and 2 appendices.

33 *Kölbl, O.*: Proceedings of the OEEPE-Workshop on Application of Digital Photogrammetric Workstations. – Frankfurt a. M. 1996, 453 pages with numerous figures and tables.

34 *Blau, E.; Boochs, F.; Schulz, B.-S.*: Digital Landscape Model for Europe (DLME). – Frankfurt a. M. 1997, 72 pages with 21 figures, 9 tables, 4 diagrams and 15 appendices.

35 *Fuchs, C.; Gülch, E.; Förstner, W.*: OEEPE Survey on 3D-City Models. *Heipke, C.; Eder, K.*: Performance of Tie-Point Extraction in Automatic Aerial Triangulation. – Frankfurt a. M. 1998, 185 pages with 42 figures, 27 tables and 15 appendices.

36 *Kirby, R. P.:* Revision Measurement of Large Scale Topographic Data. *Höhle, J.*: Automatic Orientation of Aerial Images on Database Information. *Dequal, S.; Koen, L. A.; Rinaudo, F.*: Comparison of National Guidelines for Technical and Cadastral Mapping in Europe ("Ferrara Test") – Frankfurt a. M. 1999, 273 pages with 26 figures, 42 tables, 7 special contributions and 9 appendices.

37 *Koelbl, O. (ed.)*: Proceedings of the OEEPE – Workshop on Automation in Digital Photogrammetric Production. – Frankfurt a. M. 1999, 475 pages with numerous figures and tables.

38 *Gower, R.*: Workshop on National Mapping Agencies and the Internet. *Flotron, A.; Koelbl, O.*: Precision Terrain Model for Civil Engineering. – Frankfurt a. M. 2000, 140 pages with numerous figures, tables and a CD.

39 *Ruas, A.*: Automatic Generalisation Project: Learning Process from Interactive Generalisation. – Frankfurt a. M. 2001, 98 pages with 43 figures, 46 tables and 1 appendix.

40 *Torlegård, K.; Jonas, N.*: OEEPE workshop on Airborne Laserscanning and Interferometric SAR for Detailed Digital Elevation Models. – Frankfurt a. M. 2001, CD: 299 pages with 132 figures, 26 tables, 5 presentations and 2 videos.

41 *Radwan, M.; Onchaga, R.; Morales, J.*: A Structural Approach to the Management and Optimization of Geoinformation Processes. – Frankfurt a. M. 2001, 174 pages with 74 figures, 63 tables and 1 CD.

42 *Heipke, C.; Sester, M.; Willrich, F. (eds.)*: Joint OEEPE/ISPRS Workshop – From 2D to 3D – Establishment and maintenance of national core geospatial databases. Woodsford, P. (ed.): OEEPE Commission 5 Workshop: Use of XML/GML. – Frankfurt a. M. 2002, CD.

43 *Heipke, C.; Jacobsen, K.; Wegmann, H.*: Integrated Sensor Orientation – Test Report and Workshop Proceedings. – Frankfurt a. M. 2002, 302 pages with 215 figures, 139 tables and 2 appendices.

44 *Holland, D.; Guilford, B.; Murray, K.*: Topographic Mapping from High Resolution Space Sensors. – Frankfurt a. M. 2002, 155 pages with numerous figures, tables and 7 appendices.

45 *Murray, K. (ed.)*: OEEPE Workshop on Next Generation Spatial Database – 2005. *Altan, M. O.; Tastan, H. (eds.)*: OEEPE/ISPRS Joint Workshop on Spatial Data Quality Management. 2003, CD.

46 *Heipke, C.; Kuittinen, R.; Nagel, G. (eds.)*: From OEEPE to EuroSDR: 50 years of European Spatial Data Research and beyond – Seminar of Honour. 2003, 103 pages and CD.

47 *Woodsford, P.; Kraak, M.; Murray, K.*; Chapman, D. (eds.): Visualisation and Rendering – Proceedings EuroSDR Commission 5 Workshop. 2003, CD.

48 *Woodsford, P. (ed.)*: Ontologies & Schema Translation – 2004. Bray, C. (ed.): Positional Accuracy Improvement – 2004. Woodsford, P. (ed.): E-delivery – 2005. Workshops. 2005, CD.

49 *Bray, C.; Rönsdorf, C. (eds.)*: Achieving Geometric Interoperability of Spatial Data, Workshop – 2005. *Kolbe, T. H.; Gröger, G. (eds.)*: International Workshop on Next Generation 3D City Models – 2005. *Woodsford, P. (ed.)*: Workshop on Feature/Object Data Models. 2006, CD.

50 *Kaartinen, H.; Hyyppä J.*: Evaluation of Building Extraction. *Steinnocher, K.; Kressler, F.*: Change Detection. *Bellmann, A.; Hellwich, O.*: Sensor and Data Fusion Contest: Information for Mapping from Airborne SAR and Optical Imagery (Phase I). *Mayer, H.; Baltsavias, E.; Bacher, U.*: Automated Extraction, Refinement, and Update of Road Databases from Imagery and Other Data. 2006, 280 pages.

51 *Höhle, J.; Potuckova J.*: The EuroSDR Test "Checking and Improving of Digital Terrain Models". *Skaloud, J.*: Reliability of Direct Georeferencing, Phase 1: An Overview of the Current Approaches and Possibilities. *Legat, K.; Skaloud, J.; Schmidt, R.*: Reliability of Direct Georeferencing, Phase 2: A Case Study on Practical Problems and Solutions. 2006, 184 pages.

52 *Murray, K. (ed.)*: Proceedings of the International Workshop on Land and Marine Information Integration. 2007, CD.

53 *Kaartinen, H.; Hyyppä, J.*: Tree Extraction. 2008, 56 pages.

54 *Patrucco, R.; Murray, K. (eds.)*: Production Partnership Management Workshop – 2007. *Ismael Colomina, I.; Hernández, E. (eds.)*: International Calibration and Orientation Workshop, EuroCOW 2008. *Heipke, C.; Sester, M. (eds.)*: Geosensor Networks Workshop. *Kolbe, T. H. (ed.)*: Final Report on the EuroSDR CityGML Project. 2008, CD.

55 *Cramer, M.*: Digital Camera Calibration. 2009, 257 pages.

56 *Champion, N.*: Detection of Unregistered Buildings for Updating 2D Databases. *Everaerts, J.*: NEWPLATFORMS – Unconventional Platforms (Unmanned Aircraft Systems) for Remote Sensing. 2009, 98 pages.

57 *Streilein, A.; Kellenberger, T. (eds.)*: Crowd Sourcing for Updating National Databases. *Colomina, I.; Jan Skaloud, J.; Cramer, M. (eds.)*: International Calibration and Orientation Workshop EuroCOW 2010. *Nebiker, S.; Bleisch, S.; Gülch, E.*: Final Report on EuroSDR Project Virtual Globes. 2010, CD.

58 *Stoter, J.*: State-of-the-Art of Automated Generalisation in Commercial Software. *Grenzdörffer, G.*: Medium Format Cameras. 2010, 266 pages and CD.

59 *Rönnholm, P.*: Registration Quality – Towards Integration of Laser Scanning and Photogrammetry. *Vanden Berghe, I.; Crompvoets, J.; de Vries, W.; Stoter, J.*: Atlas of INSPIRE Implementation Methods. 2011, 292 pages and CD.

The publications can be ordered using the electronic order form of the EuroSDR website

www.eurosdr.net